A humanized yeast model for studying TRAPP complex mutations

Erta Zykaj

A Thesis

In the

Department Of

Biology

Presented in Partial Fulfillment of the

Requirements for the Degree of Master of

Science (Biology) at Concordia University

Montréal, Quebec, Canada

May 2023

CONCORDIA UNIVERSITY

School of Graduate Studies

This is to certify that the thesis

Prepared by: Erta Zykaj

Entitled: A humanized yeast model for studying TRAPP complex mutations

and submitted in partial fulfillment of the requirements for the degree of
Master of Science (Biology)

complies with the regulations of the University and meets the accepted standards with respect to originality and quality.

Signed by the final Examining Committee:

_____ Chair

Chair's Name

_____ Examiner

Dr. Aashiq Kachroo

_____ Examiner

Dr. William Zerges

_____ External Examiner

Dr. Steve Shih

_____ Supervisor

Dr. Michael Sacher

Approved by

_____

Dr. Robert Weladji, Graduate Program Director

_____

Dr. Pascale Sicotte, Dean of the Faculty of Arts and Sciences

_____2023

Abstract

A humanized yeast model for studying TRAPP complex mutations

Erta Zykaj, MSc

Rare diseases affect 3.5–5.9% of the global population and mutations in membrane trafficking proteins are known to cause rare disorders with severe symptoms. The highly conserved transport protein particle (TRAPP) complexes are key membrane trafficking regulators that are also involved in autophagy. Pathogenic variants in specific TRAPP subunits are linked to neurological disorders, muscular dystrophies, and skeletal dysplasias. Characterizing these mutations and their phenotypes is important for understanding general and specialized roles of TRAPP subunits. Patient-derived cells are not always available, which poses a limitation for the study of these diseases. Therefore, other systems, like the yeast *Saccharomyces cerevisiae*, can be used to dissect the mechanisms at the intracellular level underlying these disorders. The development of CRISPR/Cas9 technology in yeast has enabled a scar-less editing method that creates an efficient humanized yeast model. This project focuses on humanizing the core TRAPP complex subunits in yeast to generate a platform for studying TRAPP variants associated with disease in humans. Core yeast subunits were humanized by replacing with their human orthologs and TRAPPC1, TRAPPC2, TRAPPC2L, TRAPPC6A, and TRAPPC6B were found to successfully replace their yeast counterparts. This system was used for studying the first reported TRAPPC1 variant identified in humans, which is a compound heterozygous mutation. I show that the maternal variant (TRAPPC1 p.Val121Alafs*3) is non-functional while the paternal variant (TRAPPC1 p.His22_Lys24del*)* is conditional-lethal in yeast. Results show that the paternal TRAPPC1 variant affects non-selective autophagy in yeast whereas membrane trafficking and autophagy are defective in patient fibroblasts. This study suggests that humanized yeast can be an efficient means to study TRAPP subunit variants in the absence of human cells, and it lays the foundation for characterizing further TRAPP variants through this system.

Acknowledgements

I would like to address a heartfelt thank you to my supervisor, Dr. Michael Sacher, for trusting me to be part of his lab and research. Thank you for your continuous support, constructional advice, patience, and guidance through all of this project. This has been an exceptional experience which has helped me grow in many ways, and your contribution has been immense.

To each and every one of my labmates at Sacher Lab, I feel nothing but gratitude to have worked with amazing colleagues like you. Your everyday support and friendship have eased everything and your thoughtful discussions and troubleshooting tips made my research project go smoothly. I will always cherish the laughs and beautiful moments we had together.

I would like to express my appreciation for our collaborators, Dr. Aashiq Kachroo for providing the plasmid for my humanization project, Brittany Greco for designing the sgRNA sequences used in this study and Dr. Mudabir Abdullah for all the thoughtful and constructive advice throughout this research project.

To my husband, for all the incredible support in pursuing my dreams and goals, thank you from the bottom of my heart. My amazing daughters, Oksana and Orkidea, you are my everything! Thank you for following me throughout this whole journey, your kisses and hugs in between exhaustion moments have been the best medicine.

To my family: my mother, my sister, and my brother, thank you for your unconditional love and for always believing in me. I could have never been here without you by my side, it is your enormous support that motivated me to undertake this journey, I am lucky to have you in my life.

Most importantly, this work is dedicated to my father, Shkëlqim.

Contribution of Authors

Figure 3.14A, B – Dr. Miroslav Milev performed the neon transfection of the fibroblasts and the microscopy for the RUSH assay. I completed the quantifications with Image J.

Figure 3.14C – Dr. Hashem Almousa performed the staining of the fibroblasts and the microscopy for the Golgi fragmentation experiment. I completed the quantification with Image J and Imaris.

Table of Contents

List of Figures viii
List of Tables ix
List of Abbreviations x
1. INTRODUCTION 1
1.1 Rare diseases, their prevalence, and link with membrane traffic 1
1.1.1 Rare diseases 1
1.1.2 Membrane traffic and rare diseases 2
1.2 TRAPP complexes 4
1.2.1 Yeast TRAPP complexes 4
1.2.2 Human TRAPP complexes 5
1.2.3 TRAPP complexes and rare diseases 7
1.3 Classic and new approaches for studying rare diseases 9
1.4 Humanized yeast as a platform for studying rare diseases 10
1.5 Objective 12
2. MATERIALS AND METHODS 14
2.1 Plasmids 14
2.2 Yeast strains 14
2.3 Serial dilutions 16
2.4 Preparation of sgRNAs that target the yeast TRAPP genes 16
2.5 Golden Gate cloning 17
2.6 Preparation of repair template DNA 18
2.7 Yeast transformations 19
2.8 Primer design for confirmation via colony PCR 20
2.9 Colony screening via PCR 21
2.10 Yeast liquid growth assays 21
2.11 Autophagy assays in yeast 22
2.12 Preparation of yeast cell lysates 23
2.13 RNA extraction from human fibroblasts 23
2.14 Western blot analysis 24
2.15 Cell culture 24
2.16 Autophagy assays in mammalian cells 24
2.17 Antibodies and dyes 25
2.18 Immunostaining of mammalian cells 25

2.19 Retention using selective hooks (RUSH) assay....26
3. RESULTS....28
3.1 *TRAPPC1*, *TRAPPC2*, *TRAPPC2L*, *TRAPPC6A* and *TRAPPC6B* successfully replace their yeast orthologs *BET5*, *TRS20*, *TCA17* and *TRS33*....28
3.2 *TRAPPC3*, *TRAPPC4* and *TRAPPC5* cannot complement the loss of *BET3*, *TRS23* and *TRS31* in yeast....32
3.3 Humanized yeast strains show a slower growth phenotype compared to the parental yeast strains....33
3.4 Detection of protein expression in humanized yeast strains....35
3.5 Humanized yeast as a platform for characterizing the first reported mutation in *TRAPPC1*....37
3.6 Humanized yeast with *C1 (c.64_72del)* is a conditional-lethal mutant....42
3.7 Non-selective autophagy is defective in the humanized *C1 (c.64_72del)* yeast strain 44
3.8 Fibroblasts from the affected individual with *TRAPPC1* mutations do not show an accumulation of LC3-II during starvation....47
3.9 Wild type *TRAPPC1* rescues a membrane trafficking defect and Golgi fragmentation in patient fibroblasts....49
4. DISCUSSION....52
4.1 An efficient humanized yeast system for characterizing TRAPP mutations....52
4.2 Future directions....56
5. REFERENCES....61

List of Figures

Figure 3. 1 Yeast humanization with core TRAPP genes using CRISPR/Cas9 editing tool. 29
Figure 3. 2 Colony screening via PCR confirms humanization of *C1*, *C2*, *C2L*, *C6A* and *C6B* strains 30
Figure 3. 3 DNA sequencing electropherograms confirm the scar-less replacement of the humanized yeast loci.....31
Figure 3. 4 *C3, C4 and C5* cannot compensate for the loss of *BET3, TRS23 and TRS31* in yeast 33
Figure 3. 5 Growth efficiency of the humanized yeast strains in solid and liquid medium. 35
Figure 3. 6 Detection of protein expression in humanized yeast strains 36
Figure 3. 7 The compound heterozygous mutation in the C1 protein highlighted in the primary and tertiary structure and standard nomenclature for *C1* mutations and variants 39
Figure 3. 8 *C1 (c.64_72del)* but not *C1 (c.362_363del)* can compensate for the loss of *BET5* in yeast 40
Figure 3. 9 Yeast humanization with *C1 (c.362_363del)* and *C1 (c.64_72del)* using CRISPR/Cas9 editing tool 41
Figure 3. 10 Colony PCR screening and DNA sequencing confirm humanization of the yeast *BET5* locus with *C1 (c.64_72del)* 42
Figure 3. 11 Growth efficiency of humanized *C1 (c.64_72del)* strain in solid and liquid medium 43
Figure 3. 12 Non-selective autophagy is affected in the humanized *C1 (c.64_72del)* strain 46
Figure 3. 13 Patient fibroblasts harboring the compound heterozygous TRAPPC1 variant show a defect in autophagy compared to control cells.....48
Figure 3. 14 Trafficking from the ER-to-Golgi is delayed and Golgi morphology is altered in patient fibroblasts harboring a compound heterozygous *TRAPPC1* variant.....50

List of Tables

Table 1. 1 Mammalian and yeast TRAPP subunits 6

Table 2. 1 Plasmids used in this study 14
Table 2. 2 Yeast strains used in this study 14
Table 2. 3 The list of oligonucleotides designed for each sgRNA targeting the yeast TRAPP genes.....17
Table 2. 4 The list of oligonucleotides designed for each repair template.....19
Table 2. 5 Primers used to confirm humanization of yeast 21

Table 4. 1 Humanization of yeast with human core TRAPP genes and the conservation between yeast and human proteins.....57

List of Abbreviations

ER	Endoplasmic reticulum
GDP	Guanosine diphosphate
GTP	Guanosine triphosphate
GEFs	Guanine nucleotide exchange factors
GAPs	GTPase-activating proteins
COP	Coat protein complex
SNARE	Soluble *N*-ethylmaleimide-sensitive factor attachment protein receptor
MTCs	Multisubunit tethering complexes
TRAPP	Transport protein particle
SEDT	Spondyloepiphyseal dysplasia tarda
iPSCs	Induced pluripotent stem cells
ECM	Extracellular matrix
HDF	Human dermal fibroblasts
ESCs	Embryonic stem cells
ORF	Open reading frame
CRISPR	Clustered regularly interspaced short palindromic repeats
sgRNA	single guide RNA
UTR	Untranslated region
LC3I/LC3II	Microtubule-associated protein 1A/1B-light chain 3
ApeI	Aminopeptidase I
Atg8	Autophagy-related protein 8
GFP	Green fluorescent protein
SBP	Streptavidin binding peptide
5-FOA	5-Fluoroorotic acid
GPD	Glyceraldehyde 3-phosphate dehydrogenase
ADH1	Alcohol dehydrogenase I
ST-eGFP	Sialyl transferase – enhanced GFP
RFP	Red fluorescent protein
SEC	Size exclusion chromatography
VUSs	Variants of unknown significance

1. INTRODUCTION

1.1 Rare diseases, their prevalence, and link with membrane traffic

1.1.1 Rare diseases

The term ‘rare diseases’ emerged in the United States by the middle of the 1970s, and it was not until the *Orphan Drug Act of 1984* that it acquired a more stable meaning (Huyard, 2009). Being abandoned or ‘orphaned’ for many years due to their low prevalence in the population, rare diseases are also referred to as orphan diseases (Richter et al., 2015; Schieppati et al., 2008). Since many of the characteristics that determine a certain disease are region and context dependent, nowadays there are still many controversies over the definition of rare conditions, mainly due to the lack of agreement (Haendel et al., 2020). According to the Rare Disease Act of 2002, rare diseases are considered those that affect 200,000 individuals or fewer in the United States (Khosla and Valdez, 2018). In the European Union, according to the EU Regulation on orphan medicinal products of 1999, rare diseases are conditions with a prevalence not more than 50 per 100,000 individuals (Baldovino et al., 2016). Globally, rare conditions affect 3.5-5.9% of the population (Nguengang Wakap et al., 2020) with an estimation of around 30 million affected people in the U.S. (Yang et al., 2022) and over 30 million affected people in Europe (Talarico et al., 2022). Despite their low prevalence individually, more than 10,000 rare diseases are known worldwide (Haendel et al., 2020), and with the rapid improvement of genetic technologies, new diseases are continuously being identified (Nguengang Wakap et al., 2020). Rare variant analysis through exome sequencing in families with individuals that suffer from undiagnosed diseases is a potent method to discover ‘orphan’ gene versions (Lipatova et al., 2020).

While it is difficult to define the precise cause of a rare disorder, most of them are generated by single-gene mutations (Yang et al., 2022). The burden that rare conditions pose for the patients, caregivers and society is tremendous (Cardinali et al., 2019; Garrino et al., 2015). Because of

their chronic and degenerative nature, these diseases extensively affect their patient's quality of life. Rare disorders take time to diagnose and due to their low frequency, researchers and pharmaceutical companies lack incentives to invest scientific interest or money into discovering their underlying causes (Garrino et al., 2015). Nonetheless, it is essential to precisely and timely diagnose these diseases, to better guide treatments (Bick et al., 2019; Nguengang Wakap et al., 2020).

1.1.2 Membrane traffic and rare diseases

Compartmentalization of eukaryotic cells confines metabolic activities into individual organelles. Macromolecules of the endomembrane system need transportation to their proper destination (Aridor and Hannan, 2000; Palade, 1966). This process, referred to as membrane trafficking, is essential for the cells and ensures that proteins are properly sorted and carried to the right location in the cell (Palade, 1975). Two key organelles that participate in bidirectional membrane trafficking are the endoplasmic reticulum (ER) and the Golgi apparatus. Entering the secretory pathway at the ER, proteins are then trafficked to the Golgi through transport vesicles, and the final destination can be either another endomembrane organelle, the plasma membrane or the extracellular space (Howell et al., 2006). Main regulators of intracellular trafficking are small GTP binding proteins of the Rab and Arf families (Cherfils and Zeghouf, 2013; Zerial and McBride, 2001). These proteins are molecular switches that turn 'on' (when GTP is bound) and 'off' (when GDP is bound). Cycling between these two states is regulated by Guanine nucleotide Exchange Factors (GEFs) and GTPase Activating Proteins (GAPs), respectively. Once activated, the small GTPases interact with downstream effectors required for vesicle formation, transport and fusion (Behnia and Munro, 2005).

Intracellular trafficking follows four important and highly regulated steps: 1. vesicle budding from a donor compartment, 2. vesicle transport, 3. vesicle targeting and tethering, 4. vesicle docking and fusion with an acceptor compartment (Bonifacino and Glick, 2004; Kaiser and Schekman,

1990; Sztul and Lupashin, 2006). The budding step results in the formation of membrane-enclosed transporters (vesicles) that detach from a donor membrane with the help of coat protein complexes (COP). These vesicles are loaded with specific cargos selected for certain trafficking events (Bonifacino and Lippincott-Schwartz, 2003; Bröcker et al., 2010). Coat protein complexes can be classified into three main classes: clathrin, COPI and COPII (Bannykh et al., 1996; Barlowe et al., 1994; Bi et al., 2002; Fath et al., 2007; Kreis et al., 1995; Pearse and Robinson, 1990; Stephens et al., 2000).

Following the budding process, the vesicle heads towards an acceptor membrane with the aid of cytoskeletal filaments (Klann et al., 2012). Once the vesicle is in proximity to its destination, tethering and then fusion take place. Tethering elements are proteins or complexes that can physically attach two distinct membranes together (Brunet and Sacher, 2014). They fall into one of two groups: coiled-coil proteins and multisubunit tethering complexes (MTCs) (Whyte and Munro, 2002). Amongst the multisubunit tethering complexes, the TRAnsport Protein Particle (TRAPP) family of complexes are well characterized in yeasts and humans (see below) (Sacher et al., 1998, 2000). Lastly, it is the interaction between tethering and SNARE (soluble *N*-ethylmaleimide-sensitive factor attachment protein receptor) proteins that enables the process of fusion (Fasshauer et al., 1998; Nichols et al., 1997; Sutton et al., 1998).

An increasing number of disorders linked to defects in membrane traffic proteins have been reported in recent years and the number of genes known to cause these predominantly monogenic disorders has grown from 49 genes in 2011 to 346 genes to date (García-Cazorla et al., 2022). Diseases caused by defects in these constituents involve multiple systems or can be manifested as more tissue or organ specific (Yarwood et al., 2020). One of the most sensitive systems to the cellular trafficking distress is the nervous system. Approximately 70% of rare monogenic disorders are manifested with neurodevelopmental symptoms (Condò, 2022; Olkkonen and Ikonen, 2006). By studying these rare Mendelian disorders, we can gain important

insights into the function of membrane traffic genes and their complex molecular interactions. At the same time, we can gather useful information which can lead to possible treatments (Antonietta and Alberto, 2011).

1.2 TRAPP complexes

1.2.1 Yeast TRAPP complexes

TRAPPs are multisubunit tethering complexes initially identified in the yeast *Saccharomyces cerevisiae* as a single large complex that copurified with Bet3p (Blocked Early in Transport 3) and are highly conserved throughout eukaryotes (Sacher et al., 1998). At first, Bet3p was found associated with nine other subunits: Bet5p, Trs20p, Trs23p, Trs31p, Trs33p, Trs65p, Trs85p, Trs120p and Trs130p, named according to their apparent molecular weight, except Bet5p, which was identified in an earlier screen (Jiang et al., 1998). Subsequent work in yeast have reported the purification of at least three separate complexes *in vitro*: TRAPP I, TRAPP II and TRAPP III (Cai et al., 2005; Lynch-Day et al., 2010; Sacher et al., 2001). In most other species analyzed, only two main physiological forms are seen *in vivo*: TRAPP II and TRAPP III (Galindo and Munro, 2023), while TRAPP I is suggested to be a purification artefact and a byproduct of TRAPP II and TRAPP III destabilization *in vitro* (Brunet et al., 2012, 2013; Thomas et al., 2018). This suggestion is further supported by studies in the filamentous fungi *Aspergillus nidulans* that also lack TRAPP I (Pinar et al., 2015, 2019) while other evidence argues that previously reported functions of TRAPP I are carried out by TRAPP III (Thomas et al., 2018).

All TRAPPs in yeast are comprised of a common ‘core’ (TRAPP I) that includes the subunits Bet5p, Trs20p, two copies of Bet3p, Trs23p, Trs31p and Trs33p (Sacher et al., 2019). With the exception of Trs33p, all of the other core subunits are essential for cell viability (Kim et al., 2016). This core is present in each complex but it cannot be detected as a distinguished complex in living yeast cells (Thomas et al., 2018). Apart from the core, TRAPP II has four additional subunits

(Tca17p, Trs65p, Trs120p and Trs130p) (Choi et al., 2011; Liang et al., 2007), while TRAPP III has one additional subunit (Trs85p) (Lynch-Day et al., 2010) (**see Table 1.1, page 6**). Although the exact function of these extra subunits is still ambiguous, they are thought to stabilize the complexes by giving them substrate and compartmental specificity (Joiner and Fromme, 2018).

TRAPPs are tethering elements and although their role as bona fide tethers remains to be proven, it is thought that they carry out this function indirectly through their activity as Rab-GEFs (Brunet and Sacher, 2014). In yeast, the three TRAPP complexes act as GEFs for the small GTPase Ypt1 while TRAPP II has shown GEF activity for Ypt31 (Lipatova and Segev, 2019) and its related GTPase, Ypt32 (Thomas and Fromme, 2016). TRAPP II is known to function in the late Golgi, regulating processes like endocytosis and post-Golgi trafficking (Cai et al., 2005; Montpetit and Conibear, 2009), while TRAPP III is implicated in ER-to-Golgi trafficking and autophagy (Brunet et al., 2013; Joiner et al., 2021; Zhao et al., 2017).

1.2.2 Human TRAPP complexes

Two main forms of TRAPPs identified in humans are TRAPP II and TRAPP III (Bassik et al., 2013; Zhao et al., 2017). Even though yeast TRAPP subunits are well-conserved in higher eukaryotes where each yeast subunit corresponds to a mammalian orthologue, humans and metazoans contain extra subunits for which no counterpart in yeast has been identified (Scrivens et al., 2011). The two distinct TRAPP complexes share a common core of 7 proteins: TRAPPC1 (Bet5p ortholog), TRAPPC2 (Trs20p ortholog), TRAPPC2L (Tca17p ortholog), two copies of TRAPPC3 (Bet3p ortholog), TRAPPC4 (Trs23p ortholog), TRAPPC5 (Trs31p ortholog) and TRAPPC6A/C6B (Trs33p ortholog). Besides the core, TRAPP II includes TRAPPC9 (Trs120p ortholog) and TRAPPC10 (Trs130p ortholog), while TRAPP III includes TRAPPC8 (Trs85p ortholog), TRAPPC11, TRAPPC12 and TRAPPC13, where TRAPPC11 and TRAPPC12 are metazoan specific subunits (Riedel et al., 2018) (**see Table 1.1 below**).

MAMMALIAN SUBUNITS	YEAST SUBUNITS	TRAPP COMPLEX
TRAPPC1	Bet5p	I/ II/ III
TRAPPC2	Trs20p	I/ II/ III
TRAPPC2L	Tca17p	II
TRAPPC3	Bet3p	I/ II/ III
TRAPPC4	Trs23p	I/ II/ III
TRAPPC5	Trs31p	I/ II/ III
TRAPPC6A/C6B	Trs33p	I/ II/ III
TRAPPC8	Trs85p	III
TRAPPC9	Trs120p	II
TRAPPC10	Trs130p	II
TRAPPC11	-	III
TRAPPC12	-	III
TRAPPC13	Trs65	III/II*

Essential

Non essential

*TRAPPC13 is part of TRAPP III complex in mammals and Trs65p is part of TRAPP II complex in yeast.

Table 1. 1 Mammalian and yeast TRAPP subunits. Mammalian subunits together with their yeast counterparts are listed and their presence in TRAPP I (I), TRAPP II (II) and/or TRAPPIII (III) is shown. Note that TRAPP I is only described in yeast. Essential TRAPP subunits are shaded in light yellow, and non essential TRAPP subunits are shaded in light blue. Orthologues between yeast and mammals are listed on the same row.

Crystallographic studies of separate TRAPP core subunits show a center occupied by two longin domain proteins TRAPPC1 and TRAPPC4 flanked by TRAPPC5, TRAPPC6 and two copies of TRAPPC3. This forms a core region where the GTPase Rab1 attaches and subunits TRAPPC1, TRAPPC3, TRAPPC4 and TRAPPC5 prove to be sufficient for ensuring GEF activity *in vitro* (Cai et al., 2008; Kim et al., 2006; Levine et al., 2013; Montpetit and Conibear, 2009). The two extremities of the core bind to TRAPPC2 and TRAPPC2L which anchor the core to the unique subunits of TRAPP II and TRAPP III complexes.

Both human TRAPP complexes act as GEFs on specific Rabs. TRAPP III activates Rab1 GTPase which is a master regulator of ER-to-Golgi trafficking and autophagy while TRAPP II typically

activates Rab11 that plays a key role in late Golgi transport (Cai et al., 2005; Jones et al., 2000; Wang et al., 2000). TRAPP complexes participate in crucial processes in cells with roles in vesicle tethering, ciliogenesis, cytokinesis, lipid droplet homeostasis, and secretion arrest induced by stress granule assembly (Cai et al., 2007; Li et al., 2017; Robinett et al., 2009; Westlake et al., 2011; Zappa et al., 2019). Additionally, many studies have reported well-defined roles of specific TRAPP subunits in the cells, apart from their role within the TRAPP complex (Bögershausen et al., 2013; Milev et al., 2015; Ramírez-Peinado et al., 2017; Xu et al., 2023; Zong et al., 2011).

1.2.3 TRAPP complexes and rare diseases

The detrimental effects of mutations in genes that code for TRAPP subunits are a proof of the importance of TRAPP complexes in humans (Zappa et al., 2019). In recent years, numerous mutations have been reported in TRAPP genes and the number of diseases associated with these mutations is growing rapidly (Sacher et al., 2019). Characterizing these mutations helps elucidate functions of TRAPP proteins within the complex, but also specific activities outside the complex. Variants in TRAPP proteins result in a set of rare disorders that collectively are known as TRAPPopathies and fall mainly into three categories: neurodevelopmental disorders, muscular dystrophies and skeletal dysplasias (Gedeon et al., 1999; Matalonga et al., 2017; Sacher et al., 2019).

Defective vesicular trafficking and/or autophagy contribute to a diverse range of neurological disorders, mostly neurodegenerative in nature but also with neonatal manifestations. Some known mutations that impair neurodevelopment are those related to *TRAPPC2L*, *TRAPPC4*, *TRAPPC6A/B*, *TRAPPC11* and *TRAPPC12* (Harripaul et al., 2018; Milev et al., 2017, 2018; Mohamoud et al., 2018). Since some of the resulting proteins are part of the core shared by the two distinct complexes in humans, mutations in a core subunit are predicted to affect both complexes (Lipatova et al., 2020). Therefore, deficiency for TRAPP II and TRAPP III in trafficking and autophagy might lead to impairment of neurological functions (Tang, 2021).

Previously reported homozygous mutations in *TRAPPC4* cause seizures, developmental delay, microcephaly and cerebellar atrophy and result in low levels of this core protein. Since TRAPP complexes are crucial in the secretory pathway and autophagy, both processes are expected to be affected with a more severe phenotype manifested in autophagy. Neuronal cells rely heavily on autophagy for removal of toxins and damaging components, which may explain the severe symptoms developed in the individuals who carry these mutations (Lipatova et al., 2020; Van Bergen et al., 2020).

Variants in the *TRAPPC2* gene are linked to the skeletal disorder spondyloepiphyseal dysplasia tarda (SEDT). This disorder affects the bones, with short-stature individuals and dysplasia of the extremities of large bones (Gedeon et al., 1999). All individuals with *TRAPPC2* mutations suffer from SEDT. The skeletal defects may be explained by the role of TRAPPC2 in the transport of collagen from the ER (Venditti et al., 2012). Since collagen secretion is crucial for bone development, the impairment of this process can most likely explain the link with this skeletal disorder.

Mutations in *TRAPPC11* affect muscle, eye, brain and liver. Some mutations can cause limb girdle muscular dystrophy 2S (LGMD2S) (Bögershausen et al., 2013) while other reported variants cause symptoms of ataxia, myopathy and intellectual disability (Fee et al., 2017; Koehler et al., 2017; Larson et al., 2018; Liang et al., 2015; Matalonga et al., 2017; Munot et al., 2022). TRAPPC11 is an essential protein known to be involved in ER-to-Golgi trafficking (Scrivens et al., 2011), autophagy (Stanga et al., 2019) and N-linked protein glycosylation (DeRossi et al., 2016), and impairment of these processes might lead to the phenotypes observed in disorders caused by TRAPPC11 variants.

With the expansion of TRAPP-related disorders, it becomes increasingly important to understand shared clinical features and also clinical divergences between TRAPP variants. This can ease future diagnosis, therapeutic approaches and treatments for this spectrum of rare disorders (Sacher et al., 2019).

1.3 Classic and new approaches for studying rare diseases

The next-generation-sequencing era has enabled the identification of many genes that cause a wide range of rare diseases and still, therapeutic approaches for these disorders continue to advance slowly (Hentschel et al., 2021). For studying cellular phenotypes related to a certain disease, one of the most suitable sources are cells derived from the affected individual carrying that particular variant (Vangipuram et al., 2013). Some common types of such cells are cultured fibroblasts and patient-derived induced pluripotent stem cells (iPSCs). Human dermal fibroblasts (HDF) represent an efficient cellular model for studying human diseases (Hentschel et al., 2021). They originate from mesenchymal cells and play an important role in the generation of the extracellular matrix (ECM). The most common source of fibroblasts is the skin and by performing a minimally invasive biopsy, HDFs can be isolated and then cultured *in vitro*. They adhere and proliferate quickly and after 3 passages a bank of 15 to 20 million cells can be obtained from just a 4 mm^2 skin biopsy (Vangipuram et al., 2013).

The advantages of using fibroblasts as a cellular disease model are: 1. they are easily obtainable from the individual (Vangipuram et al., 2013), 2. they are easy to maintain, 3. they can proliferate for long periods of time (Auburger et al., 2012), 4. they are genetically stable even after many passages which means that a single biopsy can provide sufficient material for numerous experiments, 5. they can be used to generate iPSCs. HDFs have been used in many studies as cellular models for characterizing mutations that are linked to rare diseases (Al-Deri et al., 2021;

Bögershausen et al., 2013; Milev et al., 2017), and also neurodegenerative diseases such as Parkinson's (Auburger et al., 2012) and Alzheimer's (Mocali et al., 2014; Pérez et al., 2017).

Patient-derived induced pluripotent stem cells originate from reprogrammed somatic cells and they provide a potent approach for disease modeling and therapeutic progress for human diseases (Bell et al., 2017; Deyle, 2021; Kim et al., 2011). They show similar morphology and growth features with embryonic stem cells (ESCs) and are usually derived from fibroblasts or other types of somatic cells. Using different protocols, iPSCs can be differentiated into many types of human cells (Bayzigitov et al., 2016). iPSCs have been used for modelling many Mendelian diseases like neurodegenerative disorders (Ebert et al., 2009; Lee et al., 2009), cardiac disorders (Itzhaki et al., 2011; Moretti et al., 2010), hepatic disorders (Zhang et al., 2011) and hematopoietic disorders (Ye et al., 2009).

Although patient-derived cells make an ideal model system for studying the molecular mechanism of many diseases, the procedure for obtaining these cells is more invasive than a simple blood test. Therefore the number of patients that agree to undergo a skin biopsy is relatively small (Mesdom et al., 2020). This poses a limitation when it comes to characterizing disease-causing mutations in humans, and therefore, other approaches that do not rely on patient cells offer new possibilities for studying these disorders.

1.4 Humanized yeast as a platform for studying rare diseases

Saccharomyces cerevisiae, has long been used as a model system for studying human biology due to its evolutionarily conserved genes and pathways that are very similar to those in humans (Kachroo et al., 2022; Kim et al., 2020). Most of our understanding of processes like the cell cycle, replication of DNA, vesicular trafficking, aging and cell death comes from studies on *S. cerevisiae* (Botstein and Fink, 2011; Hohmann, 2016). Yeast and humans share roughly 2,100 orthologous

genes with similar functions (Laurent et al., 2016; Remm et al., 2001) while 30% of disease-associated genes in humans have their orthologs in yeast and can functionally replace their yeast counterparts (Foury, 1997).

An efficient way for using yeast as an experimental tool to study human diseases is by humanizing yeast cells. By definition, humanization of yeast is the replacement of yeast genes with human orthologs (Kim et al., 2020). Laurent and colleagues have considered five degrees of yeast humanization: (degree 0) nonhumanized yeasts as systems for analyzing human-specific processes, (degree 1) heterologous expression of human genes in yeast, (degree 2) humanization of specific sites in yeast genes, (degree 3) humanization of complete yeast genes, (degree 4) humanization of entire pathways in yeast (Laurent et al., 2016).

Highly conserved amino acid residues play a crucial role for protein function and they are often more related to human diseases (Miller and Kumar, 2001). Therefore, when a mutation in such residues is linked to a certain disease in humans, mimicking this mutation in the yeast homologous gene may indicate the impact in the protein or in the individual related to this mutation (Laurent et al., 2016). Because of the limited conservation, the generation of equivalent mutations in yeast orthologous genes is not always feasible. Many mutations in humans are due to splicing variants which result in truncated proteins with complete loss of structure and function (Li et al., 2019) and these kind of mutations are difficult to replicate in yeasts due to differences in splicing mechanisms between these organisms and the relative paucity of introns in yeasts (Kupfer et al., 2004; Lander et al., 2001).

Hence, an alternative way for studying these mutations is the replacement of the entire yeast gene with the open reading frame (ORF) of its human ortholog. In the last 30 years, there have been many attempts to humanize yeast genes (Garge et al., 2021; Kachroo et al., 2015; Kim et al., 2020; Laurent et al., 2016), mainly due to the simplicity and effectiveness of this process

(Kachroo et al., 2022). The emerge and advancement of CRISPR/Cas9 technology in yeast has proved to be an extremely useful tool (DiCarlo et al., 2013). Unlike conventional methods, it has enabled the efficient replacement of yeast genes with their human orthologs in a scar-less way and with no need for a selectable marker (Akhmetov et al., 2018). Utilizing a method developed by Dueber and colleagues (Lee et al., 2015), Akhmetov et al have humanized the essential yeast gene *HEM2* with its human ortholog *ALAD* (Akhmetov et al., 2018). This approach consists of generating single plasmids that express both the Cas9 nuclease, acting as a pair of molecular scissors for creating a double-strand break in the DNA, and the guide RNA which will target any desired locus in the yeast genome. These plasmids, when transformed together with a repair template (i.e. human ORF), enable the efficient replacement of yeast genes with their human orthologs (Akhmetov et al., 2018; Brzáčová et al., 2021).

Humanized yeast models provide efficient systems for studying the function of human genes and the impact of mutations in health and disease. They are invaluable tools in this regard, especially when human models for characterizing different disease-causing mutations are not available.

1.5 Objective

With the increasing number of rare diseases reported and the subgroup of TRAPP related disorders, there is a high demand for models to study these human disease-causing variants. Although patient-derived cells provide an ideal system for studying the molecular mechanisms underlying these disorders, they are not always readily obtainable, posing a limitation for the investigation of the gene-function relationship.

My main objective is to create an efficient humanized yeast strain which can be used as a platform to study TRAPP variants, especially when there are restrictions in obtaining cells from an affected individual. Using the CRISPR/Cas9 editing tool, I will replace core TRAPP genes in yeast with

their human counterparts and evaluate the ability of each of them to replace their yeast ortholog. Secondly, I will test the applicability of this system by characterizing the first reported mutation in the *TRAPPC1* gene. This variant is a compound heterozygous mutation in an individual that suffers from a severe neurodevelopmental disorder. Human *TRAPPC1* and its yeast ortholog *BET5* are both essential genes and part of the core of TRAPP II and TRAPP III complexes. I will perform functional experiments using humanized strains and patient-derived fibroblasts to look for defects in different pathways that might be affected by this mutation.

2. MATERIALS AND METHODS

2.1 Plasmids

Table 2. 1 Plasmids used in this study

Plasmid	Backbone
MSB2	pRS315
MSB206	pRS313
MSB230	pRS313-TRS20
MSB1253	pRS416-GFP-ATG8
MSB1790	pmRFP-N1-TRAPPC1
MSB1791	pmRFP-C1-TRAPPC1
MSB1797	pRS413-ADH1-TRAPPC1
MSB1800	pRS413-ADH1-TRAPPC1 (c.362_363del)
MSB1801	pRS413-ADH1-TRAPPC1 (c.64_72del)
MSB1805	pCEN6-Cas9-GFP-KanMX
MSB1806	pCEN6-Cas9-GFP-KanMX BET5 sgRNA1
MSB1820	pCEN6-Cas9-GFP-KanMX TRS20 sgRNA1
MSB1821	pCEN6-Cas9-GFP-KanMX TRS23 sgRNA1
MSB1823	pCEN6-Cas9-GFP-KanMX BET3 sgRNA1
MSB1824	pCEN6-Cas9-GFP-KanMX TRS31 sgRNA1
MSB1826	pCEN6-Cas9-GFP-KanMX TCA17 sgRNA1
MSB1829	pCEN6-Cas9-GFP-KanMX TRS33 sgRNA1
MSB1839	pRS413-ADH1-TRAPPC5
MSB1840	pRS413-GPD-TRAPPC5
MSB1841	pRS423-GPD-TRAPPC5
MSB1855	pRS413-ADH1-TRAPPC3
MSB1856	pRS413-GPD-TRAPPC3
MSB1857	pRS423-GPD-TRAPPC3
MSB1858	pRS413-ADH1-TRAPPC4
MSB1859	pRS413-GPD-TRAPPC4
MSB1860	pRS423-GPD-TRAPPC4

2.2 Yeast strains

Table 2. 2 Yeast strains used in this study

Yeast strain	Genotype	Source
MSY61	*MATα his3Δ1 leu2Δ0 ura3Δ0 MET15 bet3Δ::KanMX pRS315-BET3*	Sacher Lab
MSY62	*MATα his3Δ1 leu2Δ0 ura3Δ0 MET15 trs23Δ::KanMX pRS316-TRS23*	Sacher Lab
MSY64	*MATα his3Δ1 leu2Δ0 ura3Δ0 MET15 bet5Δ::KanMX pRS316-BET5*	Sacher Lab

MSY65	*MATα his3Δ1 leu2Δ0 ura3Δ0 MET15 trs31Δ::KanMX pRS316-TRS31*	Sacher Lab
MSY135	*MATα his3Δ1 leu2Δ0 lys2Δ0 ura3Δ0*	Sacher Lab
MSY362	*MATα his3Δ1 leu2Δ0 lys2Δ0 ura3Δ0 trs85Δ::KanMX*	Titorenko Lab
MSY563	*MATα his3Δ1 leu2Δ0 ura3ΔMET15 trs23Δ::KanMX pRS315-TRS23 TRS85–3xHA::HIS3*	Sacher Lab
MSY706	*MATα his3Δ1 leu2Δ0 lys2Δ0 ura3Δ0 atg1Δ::KanMX*	Brett Lab
MSY710	*MATα his3Δ1 leu2Δ0 lys2Δ0 ura3Δ0 atg1Δ::KanMX pRS416-GFP-ATG8*	Sacher Lab
MSY740	*MATα his3Δ1 leu2Δ0 lys2Δ0 ura3Δ0 trs85Δ::KanMX pRS416-GFP-ATG8*	Sacher Lab
MSY766	*MATα his3Δ1 leu2Δ0 lys2Δ0 ura3Δ0 pRS416-GFP-ATG8*	Sacher Lab
MSY901	*MATα his3Δ1 leu2Δ0 lys2Δ0 ura3Δ0 TRS130-3xHA::HIS3*	Sacher Lab
MSY950	*MATα his3Δ1 leu2Δ0 ura3Δ0 MET15 bet5Δ::KanMX pRS316-BET5 pRS413-ADH1*	Zykaj E.
MSY951	*MATα his3Δ1 leu2Δ0 ura3Δ0 MET15 bet5Δ::KanMX pRS316-BET5 pRS413-ADH1-TRAPPC1*	Zykaj E.
MSY952	*MATα his3Δ1 leu2Δ0 ura3Δ0 MET15 bet5Δ::KanMX pRS316-BET5 pRS313-BET5*	Zykaj E.
MSY955	*MATα his3Δ1 leu2Δ0 lys2Δ0 ura3Δ0 bet5Δ with TRAPPC1*	Zykaj E.
MSY956	*MATα his3Δ1 leu2Δ0 lys2Δ0 ura3Δ0 bet5Δ with TRAPPC1 ΔHRK (c.64_72del)*	Zykaj E.
MSY957	*MATα his3Δ1 leu2Δ0 lys2Δ0 ura3Δ0 trs20Δ with TRAPPC2*	Zykaj E.
MSY958	*MATα his3Δ1 leu2Δ0 lys2Δ0 ura3Δ0 TRS130-3xHA::HIS3 tca17Δ with TRAPPC2L*	Zykaj E.
MSY959	*MATα his3Δ1 leu2Δ0 lys2Δ0 ura3Δ0 TRS130-3XHA::HIS3 trs33Δ with TRAPPC6A*	Zykaj E.
MSY960	*MATα his3Δ1 leu2Δ0 lys2Δ0 ura3Δ0 TRS130-3XHA::HIS3 trs33Δ with TRAPPC6B*	Zykaj E.
MSY963	*MATα his3Δ1 leu2Δ0 ura3Δ0 MET15 trs31Δ::KanMX pRS316-TRS31 pRS413-ADH1-TRAPPC5*	Zykaj E.
MSY964	*MATα his3Δ1 leu2Δ0 ura3Δ0 MET15 trs31Δ::KanMX pRS316-TRS31 pRS413-GPD-TRAPPC5*	Zykaj E.
MSY965	*MATα his3Δ1 leu2Δ0 ura3Δ0 MET15 trs31Δ::KanMX pRS316-TRS31 pRS423-GPD-TRAPPC5*	Zykaj E.
MSY967	*MATα his3Δ1 leu2Δ0 ura3Δ0 MET15 trs31Δ::KanMX pRS316-TRS31 pRS315*	Zykaj E.
MSY968	*MATα his3Δ1 leu2Δ0 ura3Δ0 MET15 trs31Δ::KanMX pRS316-TRS31 pRS315-TRS31*	Zykaj E.
MSY971	*MATα his3Δ1 leu2Δ0 ura3Δ0 MET15 trs23Δ::KanMX pRS316-TRS23 pRS313*	Zykaj E.
MSY972	*MATα his3Δ1 leu2Δ0 ura3Δ0 MET15 trs23Δ::KanMX pRS316-TRS23 pRS313-TRS23*	Zykaj E.
MSY973	*MATα his3Δ1 leu2Δ0 ura3Δ0 MET15 trs23Δ::KanMX pRS316-TRS23 pRS413-ADH1-TRAPPC4*	Zykaj E.
MSY974	*MATα his3Δ1 leu2Δ0 ura3Δ0 MET15 trs23Δ::KanMX pRS316-TRS23 pRS413-GPD-TRAPPC4*	Zykaj E.

MSY975	*MATα his3Δ1 leu2Δ0 ura3Δ0 MET15 trs23Δ::KanMX pRS316-TRS23 pRS423-GPD-TRAPPC4*	Zykaj E.
MSY976	*MATα his3Δ1 leu2Δ0 ura3Δ0 MET15 bet3Δ::KanMX pRS315-BET3 pRS313*	Zykaj E.
MSY977	*MATα his3Δ1 leu2Δ0 ura3Δ0 MET15 bet3Δ::KanMX pRS315-BET3 pRS313–BET3*	Zykaj E.
MSY978	*MATα his3Δ1 leu2Δ0 ura3Δ0 MET15 bet3Δ::KanMX pRS315-BET3 pRS413-ADH1-TRAPPC3*	Zykaj E.
MSY979	*MATα his3Δ1 leu2Δ0 ura3Δ0 MET15 bet3Δ::KanMX pRS315-BET3 pRS413-GPD-TRAPPC3*	Zykaj E.
MSY980	*MATα his3Δ1 leu2Δ0 ura3Δ0 MET15 bet3Δ::KanMX pRS315-BET3 pRS423-GPD-TRAPPC3*	Zykaj E.
MSY981	*MATα his3Δ1 leu2Δ0 lys2Δ0 ura3Δ0 bet5Δ with TRAPPC1* pRS416-GFP-ATG8	Zykaj E.
MSY982	*MATα his3Δ1 leu2Δ0 lys2Δ0 ura3Δ0 bet5Δ with TRAPPC1 ΔHRK (c.64_72del) pRS416-GFP-ATG8*	Zykaj E.
MSY983	*MATα his3Δ1 leu2Δ0 lys2Δ0 ura3Δ0 TRS130-3xHA::HIS3 bet5Δ with TRAPPC1*	Zykaj E.
MSY984	*MATα his3Δ1 leu2Δ0 lys2Δ0 ura3Δ0 TRS130-3xHA::HIS3 bet5Δ with TRAPPC1 ΔHRK (c.64_72del)*	Zykaj E.
MSY987	*MATα his3Δ1 leu2Δ0 lys2Δ0 ura3Δ0 tca17Δ with TRAPPC2L*	Zykaj E.
MSY988	*MATα his3Δ1 leu2Δ0 lys2Δ0 ura3Δ0 trs33Δ with TRAPPC6B*	Zykaj E.
MSY993	*MATα his3Δ1 leu2Δ0 lys2Δ0 ura3Δ0 trs33Δ with TRAPPC6A*	Zykaj E.

2.3 Serial dilutions

Yeast strains inoculated in liquid YPD (3 ml), were grown overnight in a shaker incubator at 30°C. The OD600 was measured, normalized to the lowest value and three or four sets of 10-fold serial dilutions were spotted (2 µl) onto YPD plates. Yeast plates were incubated at 30°C as the permissive temperature and at 35°C and 37°C, as possible restrictive temperatures.

2.4 Preparation of sgRNAs that target the yeast TRAPP genes

All the single guide RNA oligonucleotides (sgRNA) targeting the yeast TRAPP genes were designed by Brittany Greco (a graduate student from the Kachroo Lab) using the Geneious software and the Doench algorithm to score sgRNA for high on target and low off target activity (Doench et al., 2016; Kearse et al., 2012).

Table 2. 3 The list of oligonucleotides designed for each sgRNA targeting the yeast TRAPP genes

sgRNA oligos	Sequence
BET5 sgRNA1-Fp	GACTTTTTACACAAAAGCTCTCCAAA
BET5 sgRNA1-Rp	AAACTTTGGAGAGCTTTTGTGTAAAA
BET5 sgRNA2-Fp	GACTTTGGTCTGTTAAAAATGACATA
BET5 sgRNA2-Rp	AAACTATGTCATTTTTAACAGACCAA
TRS20 sgRNA1-Fp	GACTTTACCAATGCAGAAAATCCACA
TRS20 sgRNA1-Rp	AAACTGTGGATTTTCTGCATTGGTAA
TRS20 sgRNA2-Fp	GACTTTAGTGATGCATGCAGTATGAA
TRS20 sgRNA2-Rp	AAACTTCATACTGCATGCATCACTA
TCA17 sgRNA1-Fp	GACTTTGATTTACGTCCCTAATGAGG
TCA17 sgRNA1-Rp	AAACCCTCATTAGGGACGTAAATCAA
TCA17 sgRNA2-Fp	GACTTTTCTGAAGTCAATTTTTCAAT
TCA17 sgRNA2-Rp	AAACATTGAAAAATTGACTTCAGAAA
BET3 sgRNA1-Fp	GACTTTCTTCAAAGACCTCGATTGCG
BET3 sgRNA1-Rp	AAACCGCAATCGAGGTCTTTGAAGAA
BET3 sgRNA2-Fp	GACTTTGCTAACATATGGGTCCATAG
BET3 sgRNA2-Rp	AAACCTATGGACCCATATGTTAGCAA
TRS23 sgRNA1-Fp	GACTTTCTTGTAATAAACAAATCAGG
TRS23 sgRNA1-Rp	AAACCCTGATTTGTTTATTACAAGAA
TRS23 sgRNA2-Fp	GACTTTATTCTTGCTAGTACACTGCA
TRS23 sgRNA2-Rp	AAACTGCAGTGTACTAGCAAGAATAA
TRS31 sgRNA1-Fp	GACTTTGCATCTGACCAACAATTCCC
TRS31 sgRNA1-Rp	AAACGGGAATTGTTGGTCAGATGCAA
TRS31 sgRNA2-Fp	GACTTTAGAAGCGTCTTTATCAGCAA
TRS31 sgRNA2-Rp	AAACTTGCTGATAAAGACGCTTCTAA
TRS33 sgRNA1-Fp	GACTTTGGACCTTGTGGAGAAGATTG
TRS33 sgRNA1-Rp	AAACCAATCTTCTCCACAAGGTCCAA
TRS33 sgRNA2-Fp	GACTTTCTCTAGCTATGGGCATTGAG
TRS33 sgRNA2-Rp	AAACCTCAATGCCCATAGCTAGAGAA

Forward and reverse oligonucleotides with the sgRNA sequence and Golden Gate compatible overlaps were mixed (10μM each) in a total volume of 20 μl and annealed with each other using a thermocycler programmed to start at 95ºC and reduce the temperature in 5ºC increments every 15 minutes.

2.5 Golden Gate cloning

Golden Gate cloning is an efficient cloning method that is based on using Type IIs restriction enzymes (endonucleases), which cut the DNA outside of their recognition site, generating 5’ or 3’ DNA overhangs. Therefore, through the correct design of the cleavage sites, two digested DNA

fragments can ligate to produce a final product that lacks the initial cleavage site. This quality has been used to combine numerous DNA 'parts' in a one pot assembly reaction where the two-step reaction of digestion and ligation is changed to a single step of restriction and ligation (Engler et al., 2008).

2 µl of annealed oligonucleotides (1:500 dilution) was used in the Golden Gate reaction for the assembly of the sgRNA cassette into the CRISPR/Cas9 plasmid (pCEN6-Cas9-GFP-KanMX). The CRISPR/Cas9 plasmid was a generous gift from Dr. Aashiq Kachroo, Centre for Applied Synthetic Biology, Concordia University.

CEN6ura direct cloning vector	20 fmol (NEB biocalculator to calculate moles to mass)
sgRNA annealed oligos (10µM)	2 µl
NEB T4 buffer 10x	1 µl
NEB BsmBI fast digestion	1 µl
10mM ATP	1 µl
T7 ligase	1 µl
dH_2O	to 10 µl final volume

The following program was set in the thermocycler for the Golden Gate reaction:

37°C for 5 min
16°C for 5 min
Repeat 30x
37°C for 60 min
85°C for 15 min

2.6 Preparation of repair template DNA

The repair templates (human ORFs) were amplified using oligonucleotides designed for each of the human TRAPP genes.

Table 2. 4 The list of oligonucleotides designed for each repair template

Primer name	Sequence
TRAPPC1-Fp	AATACAAAAAAAAAATACAGAACTATCGTAAGATAATCTGCTTTTGATATA AATCATAAATCAGTGGAGCATGACTGTCCACAACCTGTAC
TRAPPC1-Rp	TATACGATGAATGCAATTCAATTCATCGCTTCTATTTATTTTAGGTTTTTC TTCTGCTCATGGTTCGTGCTCAGCCAGCCCGGGCGGAGAAG
TRAPPC2-Fp	AAGAAAAAAAAGAGAAGGTAAACACTAATACGAATAGAGAATACAGAAA AAACATACAAAGCACATTGAGATGTCTGGGAGCTTCTACTTTG
TRAPPC2-Rp	AAAAAAAAAAAAATACATACTACATATACATATACGCCATAAAAAATCTCT GCATCTATCTTATTTCCCATCAGCTTAAAAGGTGTTTCTTC
TRAPPC2L-Fp	AAGTTATTGAGTTGAAAATTGAGTAAATATTCTCTCCAAAAATCAAATTGT ACGTTTATATCACCAAACTATGGCGGTGTGCATCGCGGTG
TRAPPC2L-Rp	GCTCTCACTCCAAAGCAGTGACATTAAATTTTGCTTTCATTCGTGAAAGA ATCGACTAATAAATTATCATTCAGCACACCTGTATCATCATC
TRAPPC3-Fp	CCATAGCTATAGAGATGGGAATGCAGAGTAAAGCTTCAAGTGTTCATTG ATAACCAAAACTGGGTCAAAAATGTCGAGGCAGGCGAACCGTG
TRAPPC3-Rp	AAATAATGTATACCTAAATAACGACACCAATAATAACAAAAATCACGAAA AAAAAAAGCTTACATGTCCATTATTCCTCTCCAGCTGGAAG
TRAPPC4-Fp	AAAAGGAATCTGCCTTTGCATAAGTTCAAAAGTGCAATTTTAGTGTTGGA TTTAAACGGGAAAAATTGAAATGGCGATTTTTAGTGTGTATG
TRAPPC4-Rp	CTTAGTTCTAGAAGTACGTAGTATTTATTTTCTTGGTGTGAATGCGTTTA TCTTCCGATGGCGCGTGCGTCTATGACCCAGGTCCAAAAG
TRAPPC5-Fp	AGGACAAGAGACACGGAAGCGACAGAAAGACAGGGAGTACTATCACCA TCCATAATACTGGAGTAACATTATGGAGGCGCGCTTCACGCGC
TRAPPC5-Rp	TCAACAGTAAATATACAAACTCTTTATCCTTTTCTTGGTTTTAGGTATTTA CCGATGTTTTGAGATGATATCAGCGGCCCTCCAGGGCCCG
TRAPPC6A-Fp	AGCTGAGAGTGAAGACCTCATGCCATAAAAGAAAACATACACCGGTTAT AAAGTTGGAAGATAAACAATTATGGCGGATACTGTGTTGTTTG
TRAPPC6A-Rp	TCTTTTATATACACACTTATATCTATCTATATGTCGATGTACATTCTTAGA ACAAAAATCTGTCGGACCTTTAGGATTTCGGAATCACCACC
TRAPPC6B-Fp	AGCTGAGAGTGAAGACCTCATGCCATAAAAGAAAACATACACCGGTTAT AAAGTTGGAAGATAAACAATTATGGCGGATGAGGCGTTGTTTTTG
TRAPPC6B-Rp	TCTTTTATATACACACTTATATCTATCTATATGTCGATGTACATTCTTAGA ACAAAAATCTGTCGGACCTCTACAGCTTCTGTATCATCAC

To obtain 5 μg or more of the repair template DNA needed, PCR reactions of 150 μl were set in the thermocycler, using a high-fidelity polymerase. Each template PCR was verified by agarose gel electrophoresis and then purified to use for yeast transformation.

2.7 Yeast transformations

Yeast transformation for the genomic replacement via CRISPR/Cas9 plasmid

Yeast strains were transformed using the Frozen-EZ Yeast Transformation II Kit (Zymo Research). EZI solution was used to generate competent cells, although it can be replaced with

100 mM lithium acetate with no considerable change in the efficiency of transformation (Akhmetov et al., 2018). EZII solution was used to store competent cells in a -80°C freezer. EZIII solution was used to transform yeast strains. The transformation reaction consisted of 50 µl of competent yeast, 500 µl EZIII solution, 500 ng of CRISPR plasmid and up to 5 µg repair template DNA (final volume 600 µl). Tubes were mixed gently by flicking with a finger and incubated at 30°C for 45 min. After incubation, the tubes were centrifuged at 3500 rpm for 4 min, resuspended in 750 µl YPD and recovered for 1 h at 30°C without shaking. After recovery, 500 µl of the cell culture was discarded and the remaining volume of 250 µl was plated on selective media (YPD + G418).

Regular yeast transformation

Yeast cells were pelleted for 2 min at 2500 rpm in tabletop centrifuge. The pellet was resuspended in 500 µl of sterile water and transferred to a sterile tube. The tube was centrifuged at 13000 rpm for 30 sec in a microfuge. The supernatant was removed, and the pellet was resuspended in 250 µl of sterile water. 50 µl of cell suspension was added to each transformation tube and the tubes were centrifuged in a microfuge at 13000 rpm for 30 sec. The supernatant was removed and 163 µl of transformation mix (120 µl 50% PEG 3350, 25 µl carrier DNA, 18 µl 1M lithium acetate) was added to each transformation tube along with 3 µl of appropriate plasmid. The transformation tubes were mixed well by vortexing and/or pipetting and were incubated in 42°C water bath for 45 min. After incubation, the tubes were centrifuged in a microfuge at 13000 rpm for 30 sec and the supernatant was removed. The pellet was gently resuspended in 300 µl of sterile water and 150 µl was plated on selective media.

2.8 Primer design for confirmation via colony PCR

PCR primers to confirm gene replacement were designed for each of the human ORFs replacing their yeast counterparts such that the forward primers annealed to the yeast 5' untranslated region (UTR) and the reverse primers annealed only to the new human ORF.

Table 2. 5 Primers used to confirm humanization of yeast

Primer name	Sequence
TRAPPC1-Fp	GTCCTTTACTATTGACTAGTG
TRAPPC1-Rp	CATCCCGTACATCAGCTTATAC
TRAPPC2-Fp	CCCTTTACCTCTTCAAAGCCT
TRAPPC2-Rp	AAGTACATGTTGTTCGATAGC
TRAPPC2L-Fp	AAGTTCTGCCGGAAGAGCTCATC
TRAPPC2L-Rp	ATTGCGGAGATCTTCTCATCC
TRAPPC6A-Fp	GGAATCTGGTATGCACTCAC
TRAPPC6A-Rp	TGTTGTCTTGCAGGACGTAG
TRAPPC6B-Fp	GGAATCTGGTATGCACTCAC
TRAPPC6B-Rp	AACTCATCCTTGAACCTTGCAG

2.9 Colony screening via PCR

Colonies from YPD + G418 plates were picked using a pipette tip, suspended in 50 µl of water and microwaved at the highest power for 2 min to lyse the cells for a genomic DNA (gDNA) template. Using Phire Plant Direct PCR Master Mix Kit (Thermo Scientific) as the polymerase, a 10 µl PCR reaction was set up, with confirmation primers and 2 µl of the gDNA template as listed below.

PCR reaction	
2x Phire MIX	5 µl
Primer F	0.5 µl
Primer R	0.5 µl
Template	2 µl
H_2O	2 µl
Total	10 µl

The colony PCR reactions were fractionated by agarose electrophoresis to assess successful replacement of the yeast gene with its human ortholog.

2.10 Yeast liquid growth assays

BioTek Synergy HT incubating spectrophotometer was used to perform the liquid growth assays. Yeast cultures of 150 µl were seeded in a 96-well plate with an initial cell density of 2.5 - 5 x 10^5

cells/ml by normalizing them to approximately 0.01 – 0.02 OD600 units, across 3 replicates. The cultures were grown and OD600 was measured in the microplate reader, with continuous double orbital shaking. The assays were performed at 30°C, 35°C or 37°C and reads were taken every 10 - 20 min over a 30 h time period.

2.11 Autophagy assays in yeast

Processing of pre-Ape1p was assessed by monitoring different forms of the protein using western blot analysis (Klionsky et al., 1992). Yeast cultures of 10 ml were grown overnight to an early-to-mid-log phase at OD600 = 0.5 – 0.8 in YPD at 30°C. 5 OD units of cells were pelleted at 2500 rpm in a table top centrifuge for 3 min, the supernatant was removed and the pellet was resuspended in 5 ml pre-warmed YPD medium and incubated at 35°C or 37°C (for temperature-sensitive mutants) or 30°C in a water bath for 1 h. For selective autophagy, 1 OD unit of cells (1 ml culture) was immediately processed for lysis (see below). For non-selective autophagy, the remaining 4 OD units of cells (4 ml culture) were pelleted at 2500 rpm for 3 min, and resuspended in pre-warmed synthetic medium lacking nitrogen (SD-N with 0.17% yeast nitrogen base without ammonium sulphate and amino acids and 2% glucose), incubated for 4 h at 35°C or 37°C (for temperature-sensitive mutants) or 30°C and then 1 ml of culture was processed for lysis (see below).

Processing of GFP-Atg8p was performed by monitoring the cleavage of this fusion protein using western analysis. 10 ml yeast cultures were grown overnight to an early-to-mid-log phase at OD600 = 0.5 – 0.8 in uracil drop-out medium at 30°C. 5 OD units of cells were pelleted as above at 2500 rpm for 3 min, the supernatant was removed and the pellet was resuspended in 5 ml pre-warmed uracil drop-out medium and incubated at 30°C in a water bath for 1 h. After incubation, 1 OD unit of cells (1 ml culture) was immediately processed for lysis (0 h time point) (see below). The remaining 4 OD units of cells (4 ml culture) were pelleted at 2500 rpm for 3 min, resuspended

in pre-warmed synthetic medium lacking nitrogen (SD-N with 0.17% yeast nitrogen base without ammonium sulphate and amino acids and 2% glucose), incubated at 30°C and 1 ml of culture was taken out after 1 h, 2 h, and 4 h to process for lysis (see below).

2.12 Preparation of yeast cell lysates

For pre-Ape1p and GFP-Atg8p processing, 1 ml of culture was transferred immediately on ice and 100% trichloroacetic acid (TCA) was added to 10% final concentration (100 µl) and samples were incubated on ice for 20 min. The precipitated proteins were pelleted by centrifugation at 15000xg for 3 min in a microfuge. After washing 2x with 1 ml of ice-cold acetone, the pellet was air-dried. The dried pellet was resuspended in 1x Sample Buffer (4x SB recipe: 250mM Tris-HCl pH 6.8, 40% Glycerol [vol/vol], 8% SDS [w/vol], 0.2% Bromophenol Blue [w/vol]) and then an equal volume of glass beads was added keeping the glass beads below the level of the liquid. The samples were vortexed for 5 min and incubated at 70°C for 10 min. Unlysed cells were removed by centrifugation at 10000xg for 1 min in a microfuge and protein extracts equivalent to an OD600 = 0.2 units of cells (20 µl) were loaded on a 12% gel (for pre-Ape1p) or 10% gel (for GFP-Atg8p), resolved by SDS-PAGE and processed for western blotting using anti-Ape1 antibody or anti-GFP antibody (see below).

2.13 RNA extraction from human fibroblasts

For the purification of messenger RNA from human fibroblasts, Quick-RNA™ Miniprep Plus Kit (Zymo Research) was used. Lysed cells were pelleted by centrifugation (500xg for 1 min) and the supernatant was removed. The cell pellet was resuspended in 300 µl RNA lysis buffer, centrifuged to remove the particulate debris and the supernatant was transferred to a nuclease-free microfuge tube. This sample was then passed through a Spin-Away Filter in a Collection Tube and centrifuged for discarding the majority of genomic DNA. Flow through was kept and mixed with 1 volume of ethanol (99% [vol/vol]) (1:1). This mix was transferred to a Zymo-Spin IIICG Column in

a Collection Tube, centrifuged and flow-through was discarded. After a three-step DNase I treatment for removing genomic DNA, 400 µl of RNA Prep Buffer was added to the column. The column was then washed twice with 700 µl and 400 µl of RNA Wash Buffer, transferred to a nuclease-free tube and eluted with 50 µl of DNase/RNase-Free Water. The eluted RNA was stored at -20°C. All the steps were performed at room temperature and centrifuged at 16000xg for 30 sec, unless otherwise specified.

2.14 Western blot analysis

Samples (0.2 OD units of cells for yeast lysates and 20 µg total protein for human fibroblast lysates) were fractionated on SDS-polyacrylamide gels (different concentrations depending on the protein analyzed) for 1 h and 30 min at 110 V. The proteins were transferred to a nitrocellulose membrane or PVDF membrane (for LC3-II blot) for 1 h at 100 V in transfer buffer (25mM Tris, 192mM glycine, and 20% methanol [vol/vol]). Membranes were blocked with 5% skim milk powder in PBS-T (PBS with 0.1% Tween 20 [vol/vol]) for 2 h and incubated overnight at 4°C with primary antibodies diluted in PBS-T. The secondary antibodies diluted in PBS-T were added for 1 h at room temperature. After incubation with ECL reagent (Thermo Fisher) for 1 min, membranes were visualized on an Amersham Imager 600.

2.15 Cell culture

Primary fibroblasts were cultivated and propagated using Dulbecco's modified eagle medium (DMEM) (Wisent) supplemented with 10% (vol/vol) fetal bovine serum (FBS; Thermo Fisher Scientific). Cells were then incubated at 37°C in a humidified incubator with 5% CO_2.

2.16 Autophagy assays in mammalian cells

Primary fibroblasts seeded in 6-cm diameter dishes, were washed twice with phosphate buffered saline (PBS) and incubated with Earl’s balanced salt solution (EBSS) (Wisent) for 0 h, 1 h and 2

h to induce autophagy. The cells were then lysed using 150 µl lysis buffer (150mM NaCl, 50mM Tris pH 7.2, 1mM DTT, 1% Triton X-100, 0.5mM EDTA, complete protease inhibitors (Roche) and analyzed by western blotting for the processing of LC3. The data were normalized to the tubulin signal developed from the same membrane as the LC3 blot.

2.17 Antibodies and dyes

The antibodies used were rabbit anti-Ape1 (1:2500) (gift from Dr. Daniel Klionsky, University of Michigan), mouse anti-GFP (1:1000) (Roche Diagnostics), rabbit anti-LC3 (1:2500) (Abcam), mouse anti-tubulin (1:10000) (Sigma-Aldrich), rabbit anti-mCherry (1:4000) (Abnova), rabbit anti-mannosidase II (1:500) (gift from Dr. Kelly Moreman, University of Georgia), rabbit anti-Bet5 (1:1000) (Sacher Laboratory), rabbit anti-Trs20 (1:1000) (Sacher Laboratory), rabbit anti-Tca17 (1:1000) (Sacher Laboratory), rabbit anti-Trs33 (1:1000) (Sacher Laboratory), rabbit anti-TRAPPC1 (1:1000) (Sigma), rabbit anti-TRAPPC2 (1:500) (Sacher Laboratory), mouse anti-TRAPPC2L (1:500) (Santa Cruz), mouse anti-TRAPPC6A (1:500) (Santa Cruz) and rabbit anti-TRAPPC6B (1:1000) (Sacher Laboratory). To visualize the DNA, staining with Hoechst 33342 (1:2000) (Invitrogen) was used. Except for anti-mannosidase II and Hoechst which were used for immunofluorescence microscopy all the other antibodies were used for western blotting. The secondary antibodies used in this study for western analysis were goat anti-Rabbit (1:5000) (Seracare) and goat anti-Mouse (1:5000) (Seracare), while for immunofluorescence anti-Rabbit Alexafluor647 (Life Technologies) was used. The membranes in all the western blots were cut close to the specific region where the protein migrates for the purpose of maximizing the detected signal.

2.18 Immunostaining of mammalian cells

Fibroblast cells cultured in 12 or 6-well plates on coverslips were washed twice with PBS, fixed for 15 min at room temperature with 4% paraformaldehyde (PFA), quenched for 10 min in 0.1M glycine, and then permeabilized for 7 min in 0.1% Triton X-100 in PBS. The cells were blocked

with 5% blocking solution (BS) (5% normal goat serum in PBS) for 45 min at room temperature and then incubated with primary antibodies resuspended in 5% blocking solution (BS) overnight at 4°C. The cells were washed twice with PBS for 10 min each time and secondary antibodies resuspended in 5% blocking solution (BS) were added for 45 min at room temperature. The coverslips were washed one time with Hoescht in PBS for 2 min and two other times with PBS for 10 min each wash. The coverslips were then dried for 2-3 min and mounted on clean slides using Prolong Gold AntiFade (Life Technologies). Nikon confocal laser scanning microscope C2 TIRF was used to take images of the cells. The Golgi fragmentation images were obtained with 0.20 µm increment size and ImageJ was used to delineate the cells for each condition. The delineated cell images were converted to IMS files and conveyed to Imaris, a software pre-set to recognize Golgi structures as spherical-shaped structures (fragments) with a size no smaller than 0.550 µm. The number of fragments together with the area per each fragment were identified by the software and listed, but for this experiment, only the number of fragments was quantified. The N value for control cells was 75 and the N values for S1 (patient cells) and S1 + RFP-TRAPPC1 (rescued cells) were 78 and 81, respectively.

2.19 Retention using selective hooks (RUSH) assay

Fibroblasts cultured in DMEM supplemented with 10% fetal bovine serum (FBS) were used to monitor ER-to-Golgi vesicle transport through the Retention Using Selective Hooks (RUSH) system, a methodology that enables the assessment of synchronized cargo trafficking by examining vesicles of fluorescent cargo in the cells when biotin is added. The RUSH assay was carried out as previously described (Boncompain et al., 2012) and ImageJ software was used for quantification.

RUSH system is comprised of two main components: a reporter protein tagged with a fluorophore and bound to a streptavidin binding peptide (SBP) and a streptavidin molecule coupled with an

anchored hook protein. In the absence of biotin, this complex is maintained in the donor compartment while upon biotin addition, the complex of the reporter protein-fluorophore-SBP will be released from the hook protein at the donor compartment and then transported to the acceptor compartment. In this way, the reporter protein can be followed up at different time points using confocal microscopy.

Here, fibroblasts were transfected with a fluorescent cargo protein (Sialyl transferase (ST)-eGFP) through electroporation. This cargo protein is retained in the ER and with the addition of biotin, it is monitored as it leaves the ER and is transported to the Golgi. ImageJ software was used to quantify the fluorescence intensity in individual cells. First, the fluorescence intensity of the Golgi was measured in each cell to be quantified. By using images taken every two minutes, the Golgi was distinguished and outlined manually in every cell and for each time point, the fluorescence intensity was measured. With the same Golgi outlining, a random spot was chosen as “background” and this “background” value was used to correct the Golgi fluorescence intensity at each time point. Next, the total fluorescence intensity was measured for each time point by outlining the entire cell. With the same cell outlining, a “background” measurement was taken. For each time point, the background-corrected Golgi fluorescence intensity was divided by the background-corrected total cell fluorescence intensity. The produced values (the ratio of Golgi fluorescence intensity / total cell fluorescence intensity) were used to generate the graph.

3. RESULTS

3.1 *TRAPPC1*, *TRAPPC2*, *TRAPPC2L*, *TRAPPC6A* and *TRAPPC6B* successfully replace their yeast orthologs *BET5*, *TRS20*, *TCA17* and *TRS33*

In an effort to create a platform in yeast that can be used for characterizing mutations in TRAPP subunits in the absence of patient-derived cells and since many reported mutations affect the core subunits, I started the humanization project within the core of the TRAPP complex. The human TRAPP genes and proteins, TRAPPC1, TRAPPC2, TRAPPC2L, TRAPPC3, TRAPPC4, TRAPPC5, TRAPPC6A and TRAPPC6B, will be referred to as C1, C2, C2L, C3, C4, C5, C6A and C6B, respectively. These proteins are part of the core, common to both TRAPP complexes, except for C2L (Tca17p ortholog), which is only found in the TRAPP II complex (**see Table 1.1, page 6**). Each human open reading frame (ORF) was PCR amplified as a repair template with flanking homology to the locus of interest in yeast and was assessed by replacing its yeast ortholog using CRISPR/Cas9 as an editing tool.

For targeting the yeast locus, I prepared the yeast compatible CRISPR/Cas9 plasmid by inserting the sequence for a single guide RNA (sgRNA). For this, I used the CEN6 direct cloning vector which contains the gene for Cas9 nuclease, a KanMX resistance gene as a yeast selectable marker and a GFP gene which is silenced upon successful cloning of the sgRNA cassette. To increase the chances of replacing the yeast genes with their human orthologs, two sgRNA sequences (sgRNA1 and sgRNA2) targeting each yeast locus were designed, but only sgRNA1 (**see Table 2.3, page 17**) was used for the purpose of this study. The Golden Gate reaction was used to assemble the sgRNA cassette designed for each locus and the CEN6ura direct cloning vector. This reaction was then utilized to transform competent bacterial cells where the white colonies, because of GFP gene loss, were an indication of successful constructs, while fluorescent colonies were an indication of non-recombinant constructs (Akhmetov et al., 2018). All the assembled constructs were sequence verified to verify the cloning and to check for errors.

Upon successful generation of the CRISPR/Cas9 plasmids and the respective repair templates (human ORFs), eight human TRAPP genes (*C1, C2, C2L, C3, C4, C5, C6A* and *C6B*) were tested for their ability to complement their yeast orthologs (*BET5, TRS20, TCA17, BET3, TRS23, TRS31* and *TRS33*, respectively) one by one. These genes were expressed as a single copy in the haploid yeast strain MSY135 (the parental strain). As seen in **Figure 3.1**, after the transformation of the yeast cells, reactions containing *C1, C2, C2L, C6A* and *C6B* repair templates showed colony growth in the selective media while those containing *C3, C4* and *C5* did not show any colony growth at all.

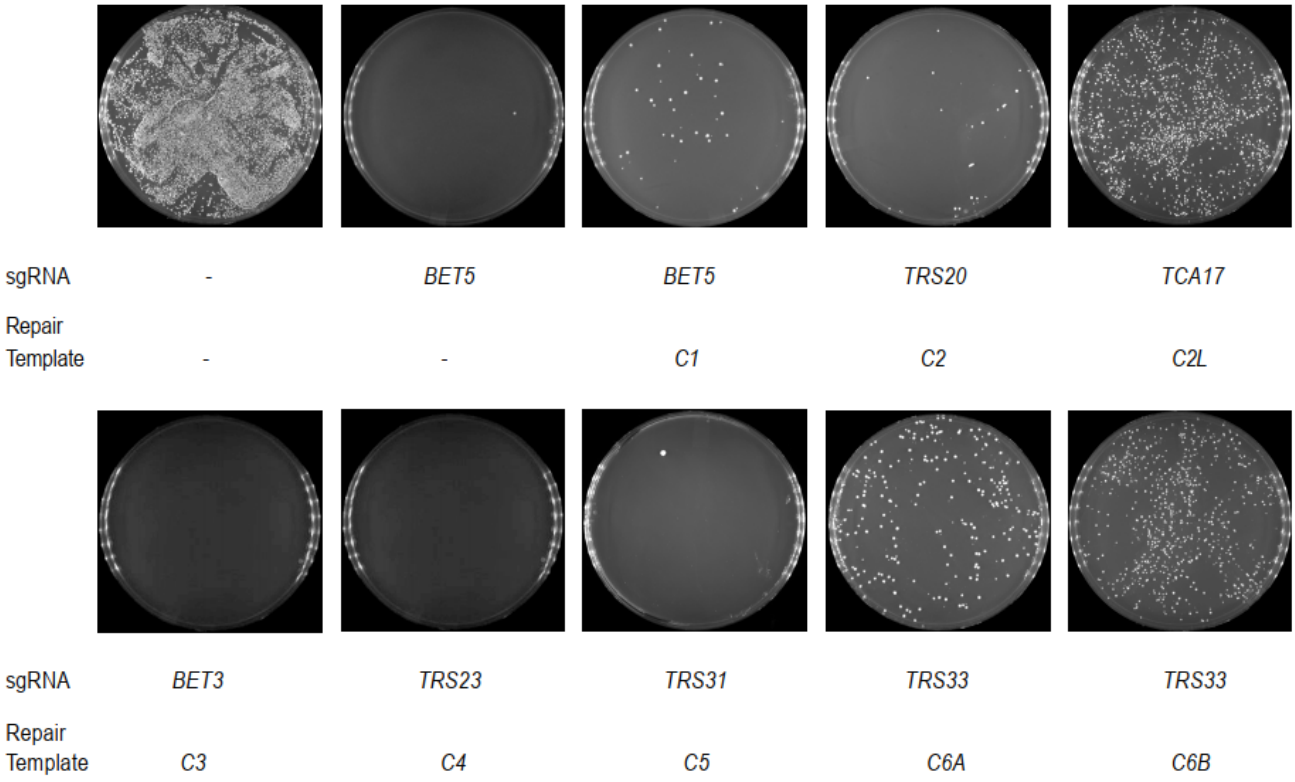

Figure 3. 1 Yeast humanization with core TRAPP genes using CRISPR/Cas9 editing tool. Yeast cells were transformed with ORFs from human *C1, C2, C2L, C3, C4, C5, C6A* or *C6B* as repair templates, in the presence of the self-containing CRISPR/Cas9 plasmid to replace their yeast orthologs *BET5, TRS20, TCA17, BET3, TRS23, TRS31* and *TRS33*, respectively. The upper left plate is a control of cells transformed with the empty CRISPR/Cas9 plasmid that contains no sgRNA and no repair template is provided, therefore, it is used to evaluate the transformation efficiency of the yeast strains being used. The remaining plates show the results of the indicated sgRNA with or without (second plate from left at top as an example of the double stranded break (DSB)-induced lethality) repair template. The presence or absence of growth in

the remaining plates is an indication of rescue or not rescue from the DSB lethality of the Cas9 nuclease when an appropriate repair template is provided.

To confirm the success of replacement for *C1, C2, C2L, C6A* and *C6B* genes, I performed colony PCR using confirmation primers designed for each of the transformed loci in yeast (**see Table 2.5, page 21**). As indicated in **Figure 3.2**, all the replaced loci in yeast show a band of the expected size, suggesting successful integration of the repair templates.

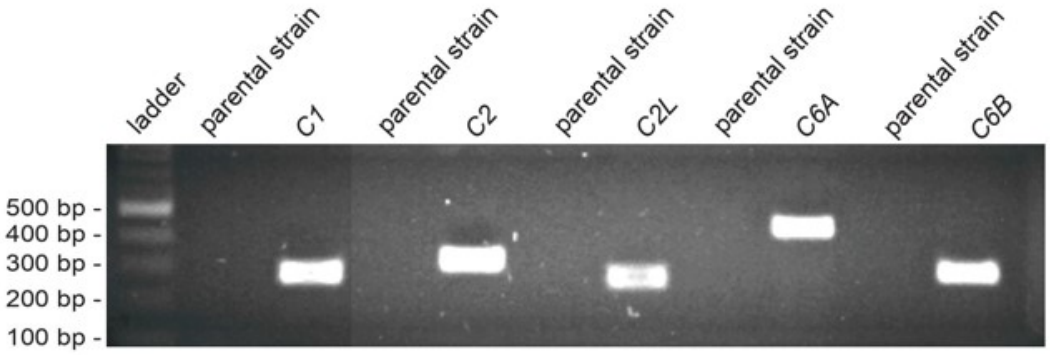

Figure 3. 2 Colony screening via PCR confirms humanization of *C1*, *C2*, *C2L*, *C6A* and *C6B* strains. Colonies from plates transformed with the empty CRISPR/Cas9 plasmid and from plates transformed with *C1, C2, C2L, C6A* or *C6B* repair templates were picked and analyzed by PCR for correct integration of the human ORF. Lanes labeled parental strain represent negative controls from the parental strain transformed with the empty plasmid. The remaining lanes represent the lysates from cells transformed with the appropriate repair templates. The expected band size for each successful transformation is 274 bp for *C1*, 311 bp for *C2*, 255 bp for *C2L*, 428 bp for *C6A* and 276 bp for *C6B*.

For further verification and to confirm a scar-less replacement of the yeast gene with the human ORF, I sequenced the humanized loci (**Figure 3.3**) and all the sequences confirmed the presence of human ORFs in their respective yeast loci, replacing only the sequence between the start and stop codons and not affecting the 5' or 3' untranslated regions. The results from these experiments suggest that *C1, C2, C2L, C6A* and *C6B* are able to complement their yeast orthologs while this complementation was not successful for *C3, C4* and *C5*.

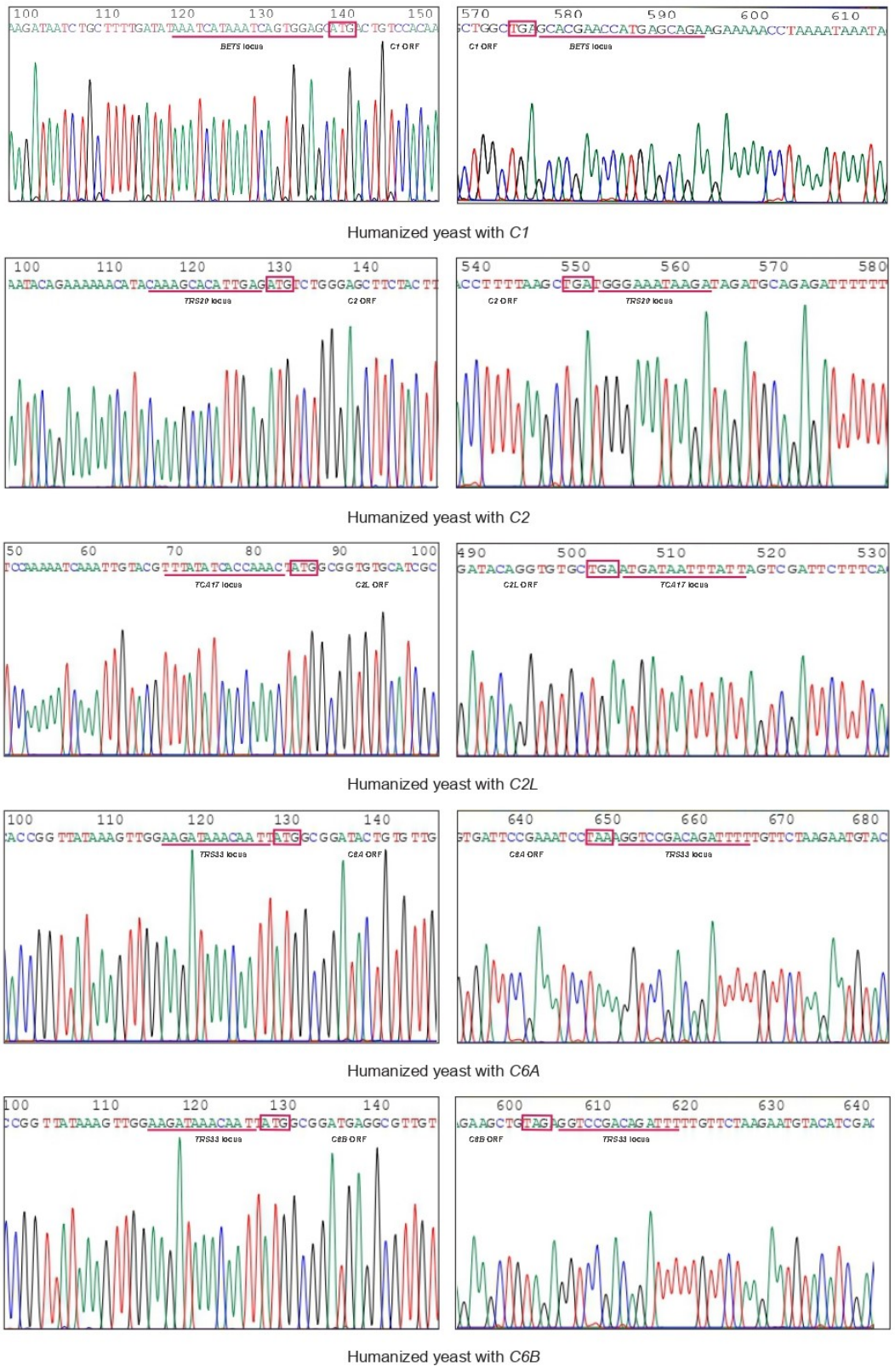

Figure 3. 3 DNA sequencing electropherograms confirm the scar-less replacement of the humanized yeast loci. Each of the humanized yeast strains with *C1, C2, C2L, C6A* or *C6B* repair templates was lysed, and genomic DNA was subjected to PCR reactions with primers annealing

to the 5'UTR and 3'UTR regions of the humanized yeast loci. The PCR products were sequenced by Sanger sequencing. The start and stop codons for each of the human ORFs are shown in red boxes and the corresponding untranslated regions for each yeast locus are underlined in red.

3.2 *TRAPPC3*, *TRAPPC4* and *TRAPPC5* cannot complement the loss of *BET3*, *TRS23* and *TRS31* in yeast

Since the humanized yeast strains express the human gene from the endogenous yeast promotor, the reason for the unsuccessful replacements of *C3, C4* and *C5* might be due to their inability to compensate for the loss of the genes encoding their essential yeast orthologs *BET3, TRS23* and *TRS31*, respectively, at low endogenous levels. I therefore set up a system to examine if they could compensate when overexpressed. I used haploid yeast strains in which the genomic copies of *BET3, TRS23* and *TRS31* are disrupted *(bet3*Δ, *trs23*Δ, *trs31*Δ) but the cells are kept alive with *URA3*-based plasmids containing the *BET3, TRS23* or *TRS31*. These plasmids can be counter-selected on plates that contain 5-fluoroortic acid (5-FOA). The product of the *URA3* gene is orotidine 5'-phosphate decarboxylase which is an enzyme required for the biosynthesis of uracil. Selection of cells that have lost a *URA3*-based plasmid is accomplished by plating the cells on media containing 5-FOA. With the action of the enzyme encoded by the *URA3* gene, this compound is transformed in a toxic product, 5-fluorouracil, killing the cells that did not lose the *URA3*-based plasmid while cells that do lose this plasmid are resistant to 5-FOA (Boeke et al., 1984).

The *bet3*Δ, *trs23*Δ and *trs31*Δ strains were transformed with empty vectors, or with vectors containing either *BET3* (the *bet3*Δ strain), *TRS23* (the *trs23*Δ strain), *TRS31* (the *trs31*Δ strain) or either *C3* (the *bet3*Δ strain), *C4* (the *trs23*Δ strain) or *C5* (the *trs31*Δ strain), under the control of different overexpression promoters (GPD or ADH1). As shown in **Figure 3.4**, none of the human TRAPP genes could compensate for the loss of *BET3*, *TRS23* and *TRS31* as indicated by lack of growth on plates containing 5-FOA. These results indicate that *C3, C4* and *C5* are not able to compensate for the disruption of their orthologous genes in yeast and reinforce the previous

results from the humanization experiments in yeast where *C3, C4* and *C5* were shown to be incapable of replacing their yeast counterparts *BET3, TRS23* and *TRS31*, respectively.

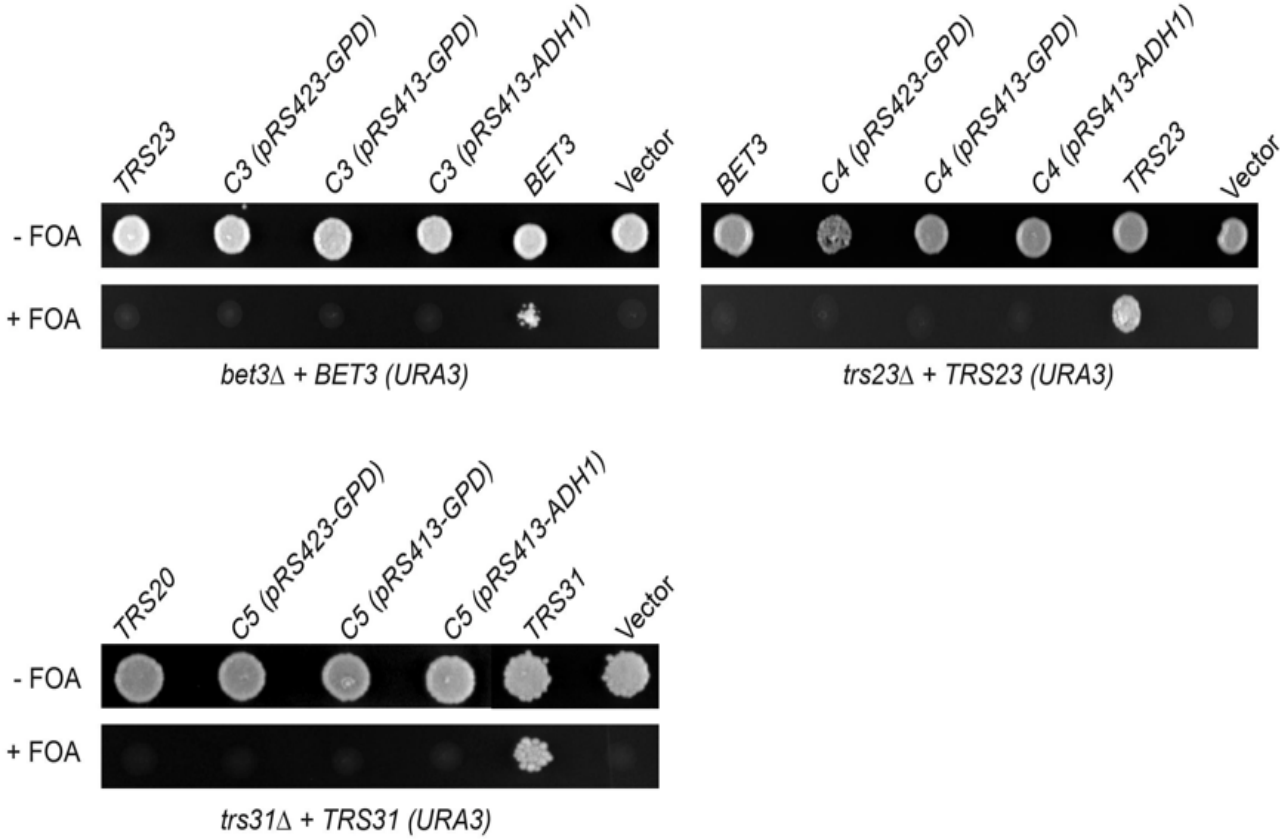

Figure 3. 4 *C3, C4 and C5* cannot compensate for the loss of *BET3, TRS23 and TRS31* in yeast. Haploid yeast strains *bet3*Δ, *trs23*Δ and *trs31*Δ were kept alive with *URA3*-based *BET3*, *TRS23* and *TRS31* plasmids, respectively. These strains were transformed with empty plasmids (vector), or vectors containing either *BET3* (the *bet3*Δ strain), *TRS23* (the *trs23*Δ strain), *TRS31* (the *trs31*Δ strain) under their endogenous promoters or either *C3* (the *bet3*Δ strain), *C4* (the *trs23*Δ strain) and *C5* (the *trs31*Δ strain) under the control of the *ADH1* or *GPD* promoters. Transformed cells were plated on 5-FOA to counter-select for the *URA3*-based plasmids.

3.3 Humanized yeast strains show a slower growth phenotype compared to the parental yeast strains

A previous study with humanized yeast strains revealed that although most yeast strains might be slightly affected by the process of humanization, many other humanized strains show highly

reduced growth rates that can be up to 70% slower (Boonekamp et al., 2022). Therefore, I sought to test the growth rate of the humanized yeast strains with *C1, C2, C2L, C6A* and *C6B* genes.

For this, serial dilutions were spotted onto YPD plates. The plates were incubated at three different temperatures (30°C, 35°C, 37°C) and after 48h, I examined the growth phenotype of the humanized yeast strains. As shown in the images from the plates (**Figure 3.5A**), yeast strains humanized with *C1, C2* and *C2L* showed a slower growth phenotype compared to the parental strain (MSY135) at 30°C, 35°C and 37°C, which is also the optimal temperature for human genes to function. In contrast, yeast strains humanized with *C6A* and *C6B* genes seemed to not be affected by any of the conditions.

Next, I more quantitatively tested the growth rate of the humanized yeast strains in liquid medium. As shown in **Figure 3.5B**, *C1, C2* and *C2L* strains showed slower growth rates compared to the parental strain in all the temperatures with a 2 – 5 h of lag phase. *C6A* and *C6B* strains showed growth rates similar to the parental strain at 30°C and 35°C, while at 37°C, the growth rate of the *C6B* strain was slower compared to the parental strain. This was in contradiction to the previous experiments in solid plates where the *C6B* strain seemed to grow normally even at 37°C. These experiments demonstrate that humanized yeast strains with *C1*, *C2*, and *C2L* overall show a partial reduction in fitness compared to the parental strain, while the growth of humanized yeast strains with *C6A* and *C6B* is not affected at low temperatures and they show similar fitness to the parental strain but *C6B* appears to be heat-sensitive.

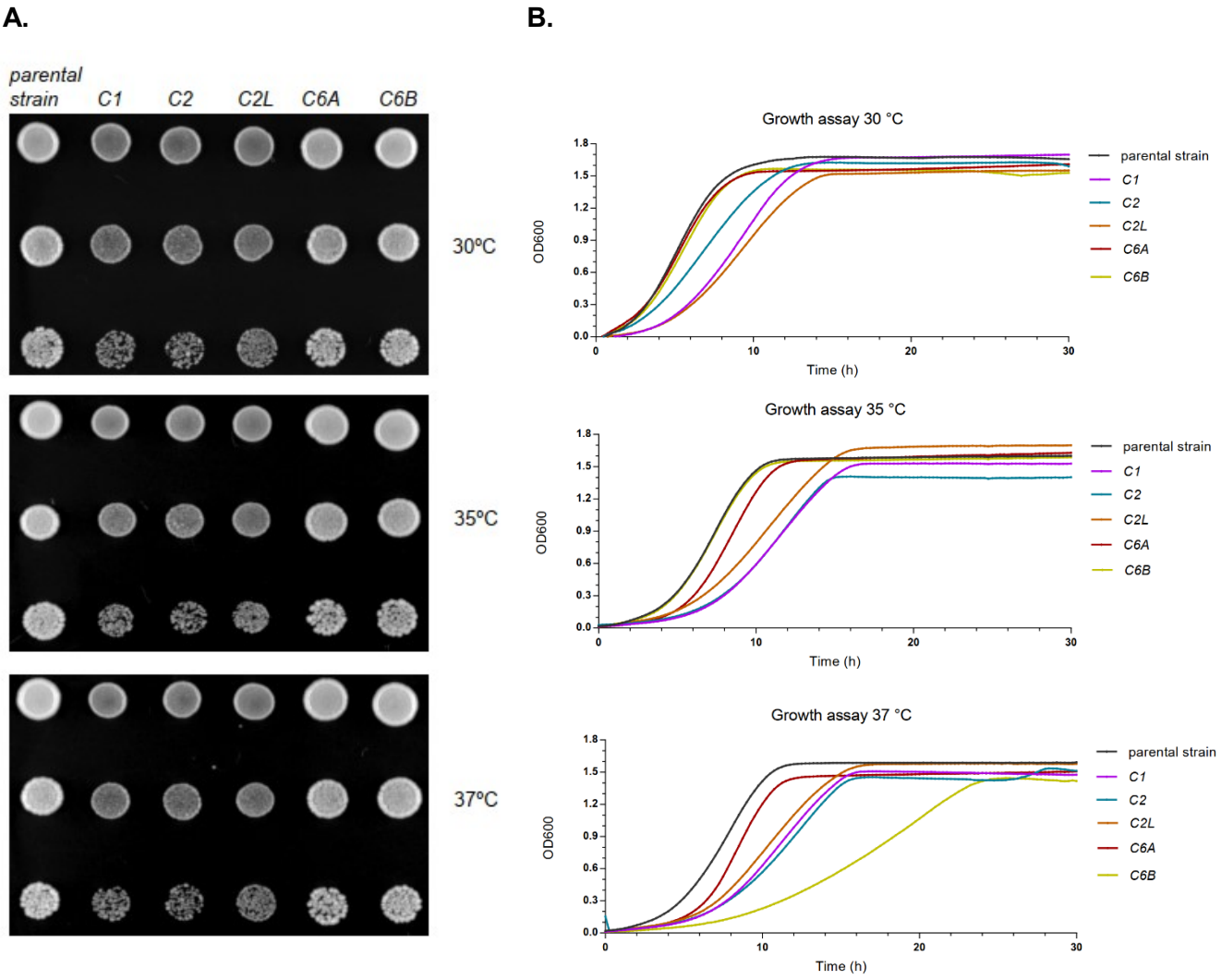

Figure 3. 5 Growth efficiency of the humanized yeast strains in solid and liquid medium. A) Images from the plates of *C1, C2, C2L, C6A* and *C6B* humanized yeast strains. Serial dilutions of the liquid cultures were spotted on YPD plates and incubated for 48 h at three different temperatures, 30°C, 35°C and 37°C. B) Representation of the growth curves for *C1, C2, C2L, C6A* and *C6B* humanized yeast strains in 30°C, 35°C and 37°C. Shown are the averages of OD600 for three replicates.

3.4 Detection of protein expression in humanized yeast strains

Although PCR confirmation and sequencing data prove the correct integration of human ORFs in their ortholog yeast loci, they do not reveal the expression of these genes in the yeast background. Detection of protein expression can also help address the slight defects in fitness noticed in some of our humanized strains which might be related to poor expression of human proteins in yeast. Therefore, I assessed the protein expression in humanized yeast strains through western

analysis. Lysates from the parental strain and the humanized yeast strains were fractionated by SDS-PAGE and screened with antibodies against human and yeast proteins. Depending on the essentiality of each yeast ortholog (**see Table 1.1, page 6**), I also prepared lysates from knock-out strains (*tca17*Δ and *trs33*Δ) and from strains that overexpress Bet5p Trs20p, Tca17p and Trs33p, as controls.

When lysates of humanized yeast strains with *C1*, *C2*, *C2L*, *C6A* and *C6B* were blotted individually with antibodies against yeast proteins Bet5p, Trs20p, Tca17p and Trs33p, respectively, in the humanized yeast strain with *C1,* I did not detect any yeast protein expression (Bet5p) in any of the lysates, suggesting the yeast antibody was not capable of detecting this protein. For the humanized yeast strains with *C2*, *C2L*, *C6A* and *C6B*, yeast protein expression was detected in the parental strain and in the overexpression strains, while no expression of yeast proteins was observed in the humanized yeast strains or the knock-out strains (**Figure 3.6**). Next, lysates of the humanized yeast strains were tested with human antibodies against C1, C2, C2L, C6A and C6B proteins but none of the blots showed any expression of the human proteins in the yeast background.

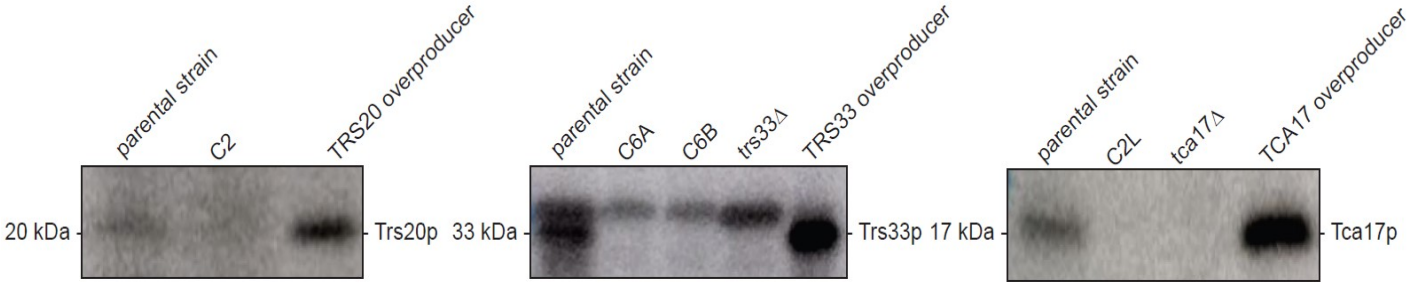

Figure 3. 6 Detection of protein expression in humanized yeast strains. Lysates from the parental strain and the humanized yeast strains with *C2*, *C2L*, *C6A* and *C6B* were fractionated by SDS-PAGE and analyzed by western analysis with antibodies against yeast proteins Trs20p, Tca17p and Trs33p, respectively. The expected band sizes for each blot are 20 kDa for Trs20p, 17 kDa for Tca17p and 33 kDa for Trs33p.

The absence of yeast protein expression in the humanized yeast strains is consistent with the replacement of the yeast genes from human orthologs. The inability to detect the human proteins by western analysis suggests an antibody detection issue or that the human proteins are expressed at very low levels in the yeast.

3.5 Humanized yeast as a platform for characterizing the first reported mutation in *TRAPPC1*

My next objective was to test whether the humanized platform in yeast provides an optimal system for characterizing mutations in human genes. For this, I decided to study the first reported mutation in *C1* which will be the focus of the following experiments in this thesis.

C1 is an essential gene in humans, encoding for a protein orthologue to Bet5p in yeast that share 33% identity and 54% similarity (**see Table 4.1, page 57**) (Sacher et al., 2019). C1 is part of longin domain (LD) proteins which are comprised of a conserved domain of 120 - 140 amino acids at their N-terminus (Filippini et al., 2001). Longin domains contain a core of a five-stranded β-sheets flanked by a single α-helix on one side and two α-helixes on the other side (Rossi et al., 2004) and they have been proposed to regulate many membrane trafficking processes (Schlenker et al., 2006). C1 and Bet5p are part of the core TRAPP subunits and therefore, they are common to both complexes, TRAPP II and TRAPP III.

The individual who carries this *C1* mutation exhibits a severe neurodevelopmental clinical phenotype with symptoms of global neurodevelopmental delay, lack of speech, autistic features, brain anomalies with delayed myelination and a myopathy with elevated creatine kinase (CK) levels. Whole exome sequencing showed that the best candidate for this condition is a compound heterozygous mutation in *C1*. In the maternal variant, p.(Val121Alafs*3), a deletion of two nucleotides (c.362_363del) results in a frameshift mutation which introduces a premature stop codon, altering the C-terminal 24 amino acids. In the paternal variant, p.(His22_Lys24del), a

deletion of nine nucleotides (c.64_72del) results in an in-frame 3 amino acid deletion in the variant protein (**Figure 3.7A**). As illustrated from the structure of the C1 protein depicted in **Figure 3.7B**, the p.(Val121Alafs*3) mutation deletes an entire α-helix of the longin domain protein while the p.(His22_Lys24del) mutation deletes three amino acids of a short loop connecting two strands of the β-sheet. Therefore, I would speculate that deleting a whole α-helix would have a more dramatic effect on the protein than a small 3 amino acid deletion, which might change the geometry of a portion of the protein.

A.

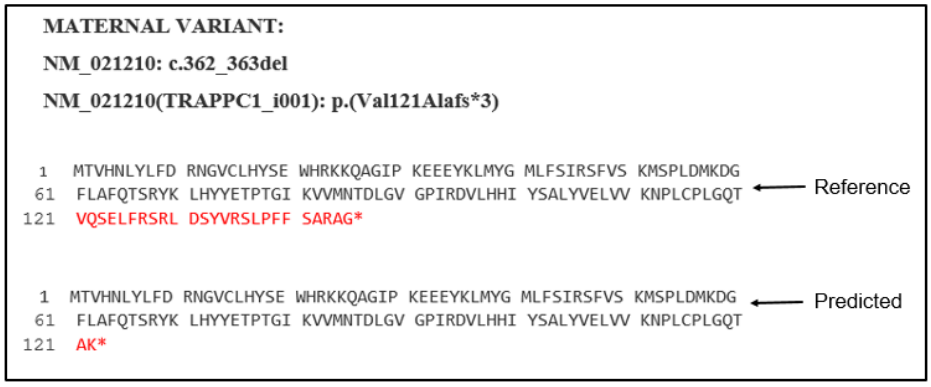

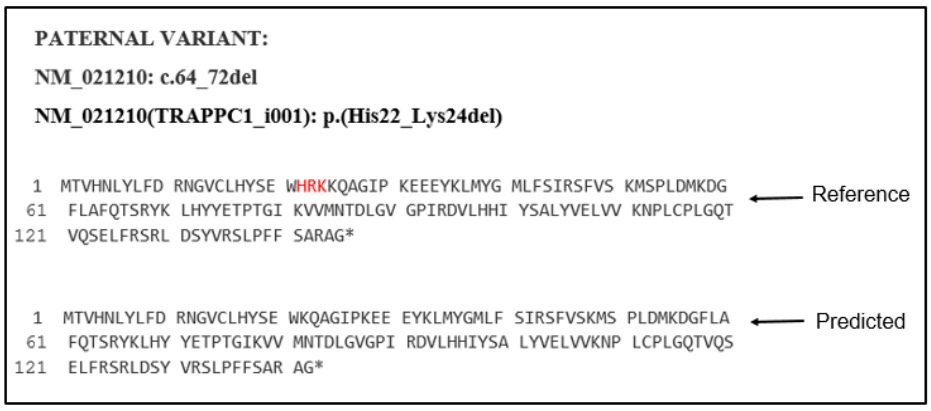

DNA sequence change	Amino acid change (three-letter code)	Mutation
C1 (c.362_363del)	C1 p.Val121Alafs*3	Frameshift
C1 (c.64_72del)	C1 p.His22_Lys24del	In-frame deletion

B.

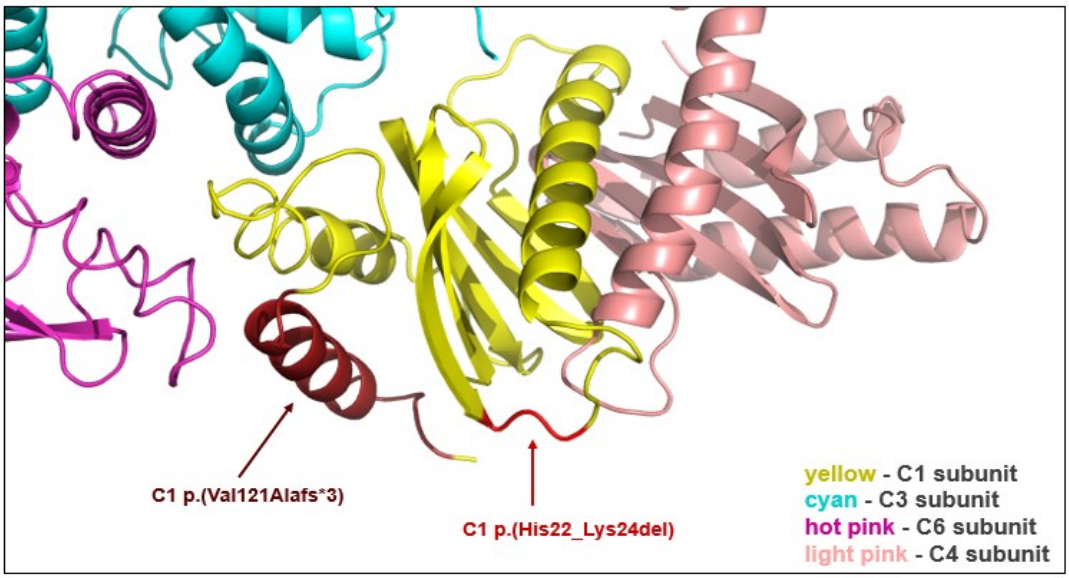

Figure 3. 7 The compound heterozygous mutation in the C1 protein highlighted in the primary and tertiary structure and standard nomenclature for *C1* mutations and variants. A) C1 p.(Val121Alafs*3) and C1 p.(His22_Lys24del) variants are predicted in the amino acid sequence of the C1 protein. Shown are the reference and the predicted sequence of the protein for both variants and the nomenclature for *C1* mutations and variants. B) C1 p.(Val121Alafs*3) and C1 p.(His22_Lys24del) are highlighted in red in the structure of the C1 protein. Interacting subunits of the TRAPP core with C1 are included partially in the figure. Shown are: C1 p.(Val121Alafs*3) variant in dark red, C1 p.(His22_Lys24del) variant in light red, C1 subunit in yellow, C3 subunit in cyan, C4 subunit in light pink and C6 subunit in hot pink.

There were two reasons for using the mutant *C1* as a candidate to test our humanized platform in yeast. First was the fact that wild-type *C1* can replace *BET5* in yeast and second was the presence of fibroblast cells from the patient bearing the *C1* mutation. This would allow me to compare the phenotype of the humanized yeast platform with that of human cells. As a source of each variant, I extracted messenger RNA (mRNA) from the patient fibroblasts and used it to synthesize complementary DNA (cDNA). Utilizing the synthesized cDNA, I performed PCR to generate the repair templates to humanize the yeast for both mutations in *C1*.

As a first estimate to see whether I would be able to humanize yeast strains with both *C1* mutations, I examined the overexpression of each variant in yeast devoid of *BET5* (*bet5*Δ) containing a *URA3*-based wild type *BET5* in the presence of 5-FOA.

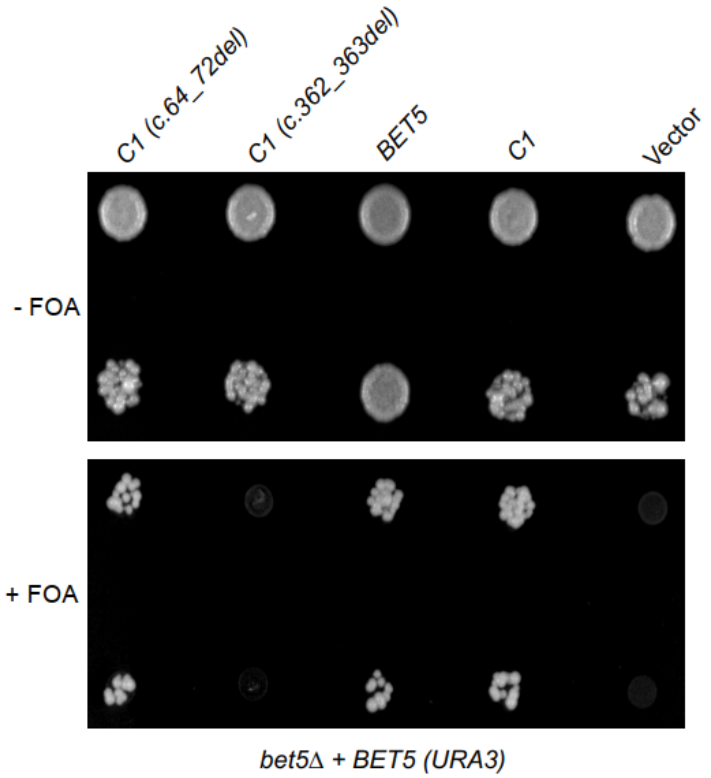

Figure 3. 8 *C1 (c.64_72del)* but not *C1 (c.362_363del)* can compensate for the loss of *BET5* in yeast. Haploid yeast strain *bet5*Δ kept alive with *URA3*-based *BET5* was transformed with an empty plasmid, with a vector containing *BET5* under its endogenous promoter or with vectors expressing either *C1*, *C1 (c.362_363del)* or *C1 (c.64_72del)* under the control of the *ADH1* promoter. Transformed cells were plated on 5-FOA to counter-select for the *URA3*-based plasmids.

As shown in **Figure 3.8**, only *BET5*, *C1* and *C1 (c.64_72del)* could compensate for the loss of *BET5* as indicated by growth on plates containing 5-FOA, while *C1 (c.362_363del)* was non-functional and did not support the growth of *bet5*Δ yeast strains on 5-FOA.

Knowing that when overexpressed, the maternal variant C1 p.Val121Alafs*3 (expressed from *C1 c.362_363del*) is lethal and the paternal variant C1 p.His22_Lys24del (expressed from *C1 c.64_72del*) is functional, I tested their functionality in the humanized yeast platform under the control of the endogenous *BET5* promoter. For this, I used the CRISPR/Cas9 plasmid and *C1 (c.362_363del)* and *C1 (c.64_72del)* as repair templates. As seen in **Figure 3.9**, after the transformation of the yeast cells, humanized strains with *C1* and *C1 (c.64_72del)* showed colony

growth in the selective media while humanized strains with *C1 (c.362_363del)* could not support yeast growth.

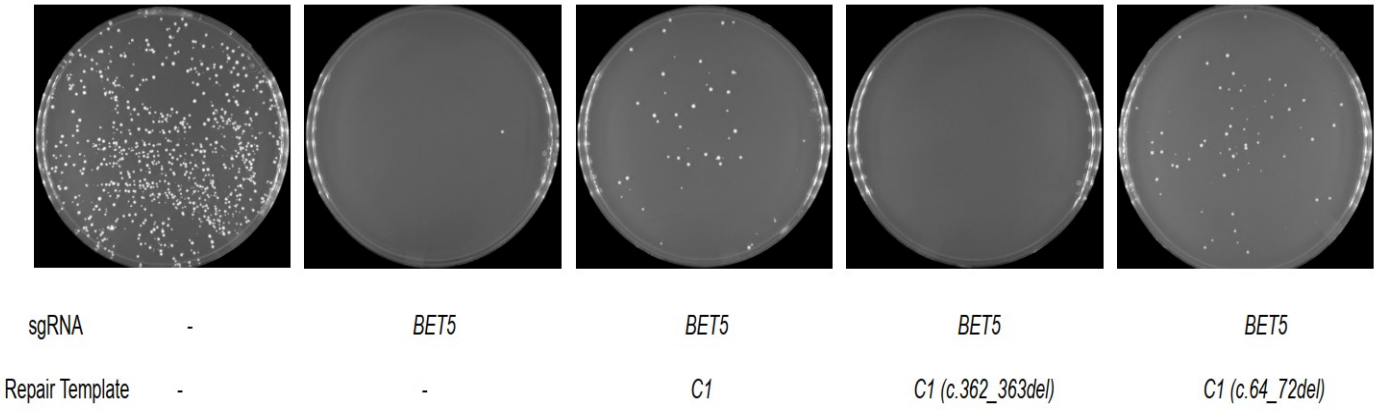

Figure 3. 9 Yeast humanization with *C1 (c.362_363del)* and *C1 (c.64_72del)* using CRISPR/Cas9 editing tool. Yeast cells were transformed with either *C1*, *C1 (c.362_363del)* or *C1 (c.64_72del)* repair templates, in the presence of the self-containing CRISPR/Cas9 plasmid. In one control (left-most), the cells were not transformed with guide RNA or repair template to evaluate the transformation efficiency. A second control (second from left) used only gRNA to demonstrate the lethality of a DSB. The presence or absence of growth in the remaining plates is an indication of rescue or no rescue from the DSB lethality of the Cas9 nuclease when an appropriate repair template is provided.

These results confirmed that the maternal variant C1 p.Val121Alafs*3 (expressed from *C1 c.362_363del*) was lethal and suggested that the paternal variant C1 p.His22_Lys24del (expressed from *C1 c.64_72del*) was functional at endogenous Bet5p levels. Replacement with either wild type *C1* or *C1 (c.64_72del)* was confirmed by colony PCR (**Figure 3.10,** upper panel) and DNA sequencing (**Figure 3.10**, lower panel). These results confirm the functionality of *C1 (c.64_72del)* in yeast and the ability of this mutant to complement the *BET5* gene.

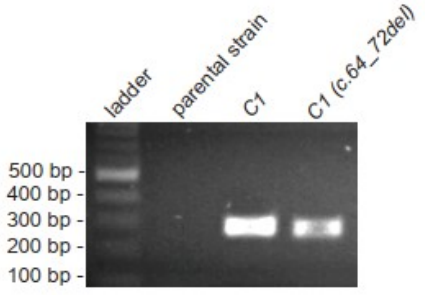

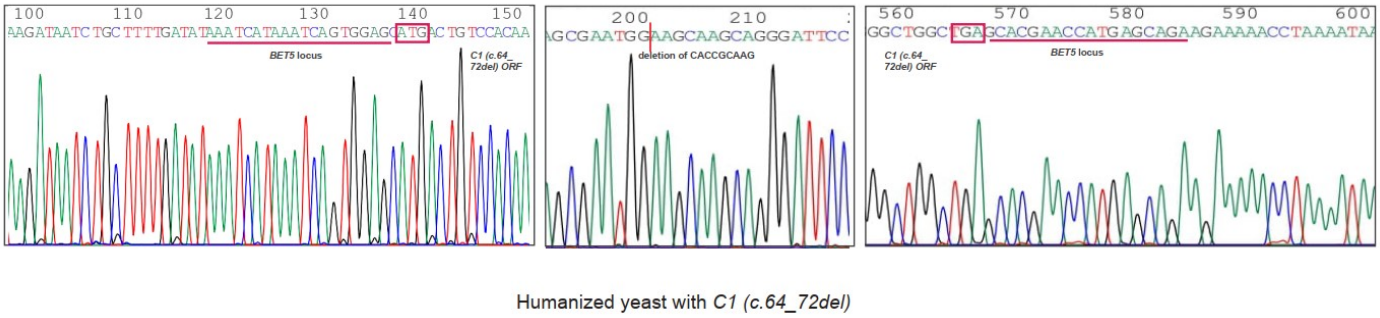

Figure 3. 10 Colony PCR screening and DNA sequencing confirm humanization of the yeast *BET5* locus with *C1 (c.64_72del)*. The upper panel shows an image from the colony PCR products of the transformation of yeast strains with *C1 (c.64_72del)* using humanized *C1* strain and parental strain as controls. The expected band size for each successful transformation is 274 bp for *C1* and 265 bp for *C1 (c.64_72del)*. The lower panel shows the electropherogram of the humanized yeast locus with *C1 (c.64_72del)*. The start and stop codons are shown in red boxes, the location of the 9-nucleotide deletion for *C1 (c.64_72del)* ORF is indicated and the corresponding UTR regions for the *BET5* yeast locus are underlined in red.

3.6 Humanized yeast with *C1 (c.64_72del)* is a conditional-lethal mutant

Since the *C1 (c.64_72del)* mutant was functional and could replace the *BET5* gene in yeast, I decided to look at the growth efficiency of this mutant in solid and liquid media using the parental strain (MSY135) and the humanized *C1* strain as controls. The solid plates were incubated at three different temperatures (30°C, 35°C, 37°C) and after 48h, I examined the growth phenotype of the humanized strain.

As shown in **Figure 3.11A**, yeast strains humanized with *C1 (c.64_72del)* showed a slower growth phenotype compared to the parental strain (MSY135) at 30°C, an even slower growth at 35ºC and no growth at 37°C. These observations are consistent with the results from the liquid growth curves (**Figure 3.11B**) where the *C1 (c.64_72del)* strain shows a slower growth rate at 30°C compared to the parental MSY135 strain and is essentially non-functional at 35°C and 37°C. These results demonstrate that *C1 (c.64_72del)* humanized yeast strain is a conditional-lethal mutant, and its growth is sensitive to temperatures above 30°C. Although the *C1 (c.64_72del)* mutation complements *BET5* in yeast, its functionality is not comparable to the wild type *C1* at 30°C.

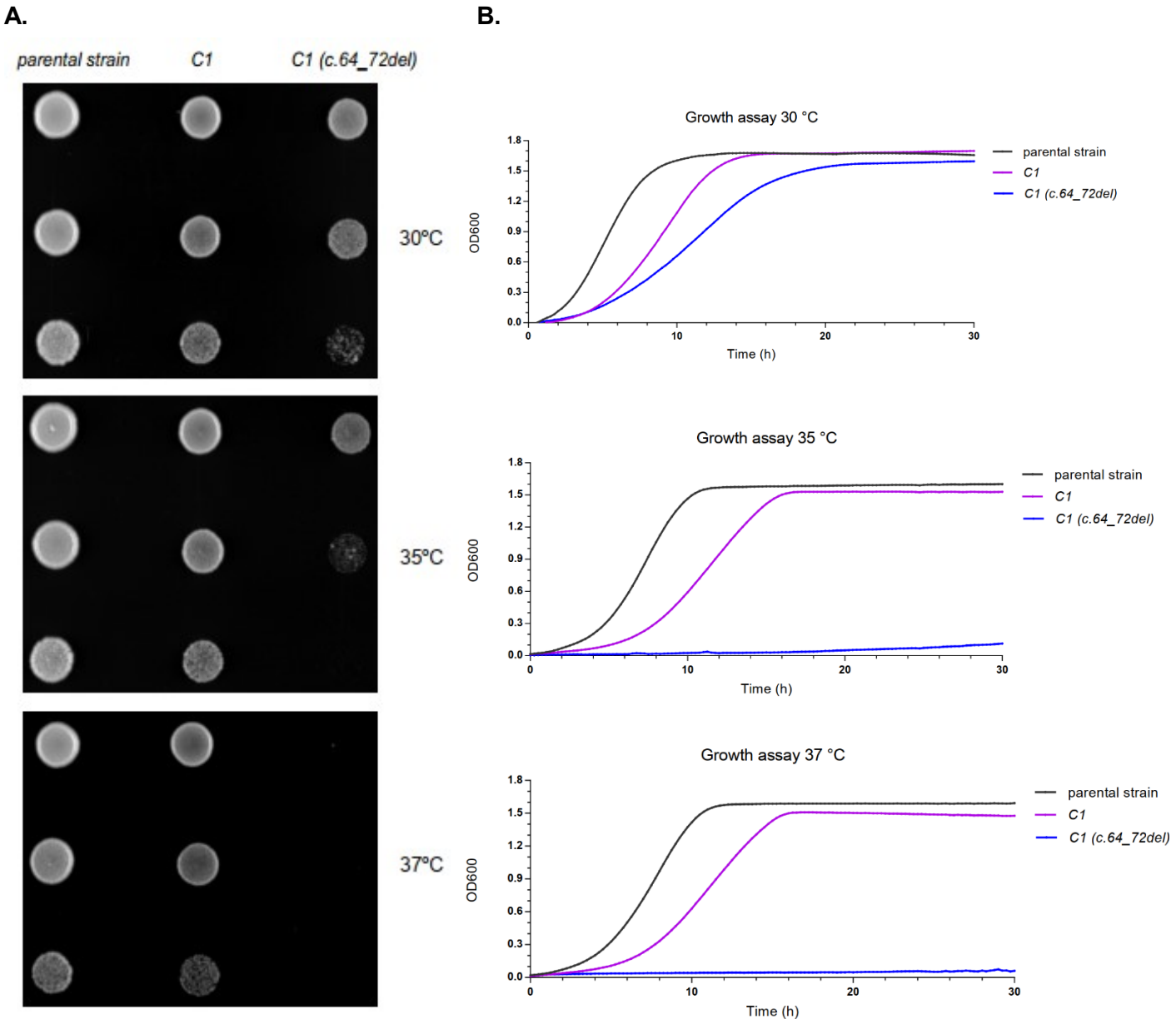

Figure 3. 11 Growth efficiency of humanized *C1 (c.64_72del)* strain in solid and liquid medium. A) Images from the plates of parental strain (MSY135) and humanized yeast strains with *C1* and *C1 (c.64_72del)*. Serial dilutions of the liquid cultures were spotted on YPD plates and incubated for 48 h at three different temperatures, 30°C, 35°C and 37°C. B) Representation of the growth curves for MSY135 and humanized yeast strains with *C1* and *C1 (c.64_72del)* at 30°C, 35°C and 37°C. Shown are the averages of OD600 for three replicates.

3.7 Non-selective autophagy is defective in the humanized *C1 (c.64_72del)* yeast strain

The fact that the mutant *C1 (c.64_72del)* showed to be conditional-lethal presented me with the ability to characterize this mutation in our humanized platform by growing this strain at permissive and restrictive temperatures. Since C1 subunit is part of both TRAPP complexes in humans and knowing that TRAPP III functions in autophagy, I tested whether *C1 (c.64_72del)* affected autophagy.

Depending on the media in which the cells are grown, the presence of a nitrogen source (rich media) or the absence of a nitrogen source (starvation media) can help distinguish between the selective cytosol-to-vacuole (Cvt) autophagic pathway (+ nitrogen) and the non-selective pathway (- nitrogen). Cvt pathway occurs continuously during the cell growth in conditions rich in nutrients while the non-selective pathway is usually triggered by starvation (Cheong and Klionsky, 2008). I probed first for the marker protein Ape1p which in the presence of nitrogen undergoes the selective pathway and in the absence of nitrogen is transported to the vacuole in a non-selective manner (Scott et al., 1996). The processing of Ape1p is monitored by detecting the levels of the precursor of the protein and its processed form by SDS-PAGE/western analysis. When an antibody against Ape1p is used, the latter form appears as a faster migrating species compared to the former. As shown in **Figure 3.12A**, the processing of Ape1p in the presence of nitrogen (+N panel) was completely blocked for the humanized strain with *C1* and *C1 (c.64_72del)* compared to the parental strain, suggesting that selective autophagy is impaired in the two humanized strains. In starvation conditions, when Ape1p is processed by non-selective autophagy (-N panel), at 30°C, there was a notable amount of precursor Ape1p and a very small amount of mature Ape1p detected in the humanized *C1 (c.64_72del)* strain compared to the humanized *C1* strain and the parental strain, suggesting a defect in non-selective autophagy of Ape1p in the *C1 (c.64_72del)* strain. At 35°C, no processing of the Ape1p was detected from the precursor to the mature form in the humanized *C1 (c.64_72del)* strain compared to the humanized

C1 strain and the parental strain, although the humanized *C1* strain at this temperature, showed less processing of Ape1 marker protein compared to the parental strain. At 37°C, both humanized strains with *C1* and *C1 (c.64_72del)* were defective in non-selective autophagy and showed no processing of Ape1p compared to the parental strain. These results indicate that humanized strains with *C1* and *C1 (c.64_72del)* are both defective in selective autophagy while *C1 (c.64_72del)* impairs non-selective autophagy of Ape1p.

To further evaluate whether the *C1 (c.64_72del)* mutation affects non-selective autophagy, we examined the processing of GFP-Atg8p. Under starvation conditions, this fusion protein is taken up in the vacuole in a non-selective manner and cleaved, releasing GFP which is resistant to the proteolytic enzymes of the vacuole. The appearance of free GFP can be used as a marker which can be detected through western analysis over time (Shintani and Klionsky, 2004). As seen in **Figure 3.12B**, at 30°C, in the parental strain and the humanized *C1* strain, there was an increase in the amount of free GFP over time, whereas the humanized *C1 (c.64_72del)* strain accumulated only the full-length GFP-Atg8p but not the GFP. Collectively, these results demonstrate that *C1 (c.64_72del)* affects the non-selective autophagy of Ape1p and GFP-Atg8p while both the mutant and wild type *C1* appear to affect selective autophagy.

A.

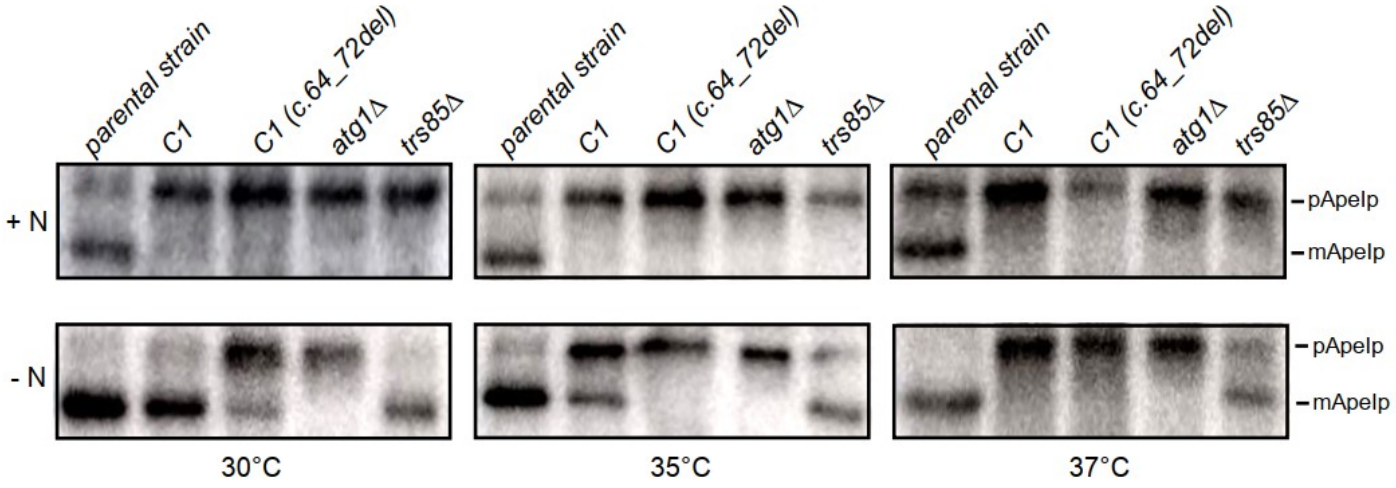

B.

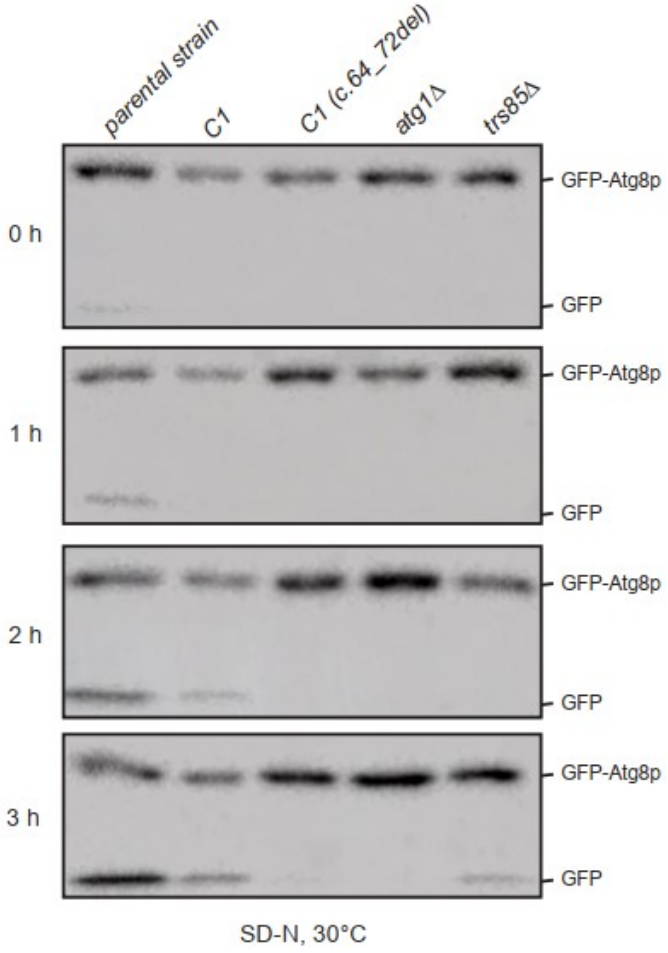

Figure 3. 12 Non-selective autophagy is affected in the humanized *C1 (c.64_72del)* strain. A) The parental strain MSY135 and the humanized strains with *C1* and *C1 (c.64_72del)* were grown in rich (+N panel) or nitrogen starvation (-N panel) medium to induce autophagy at three different temperatures, 30°C, 35°C and 37°C, as described in *Materials and Methods* section. The mutant strains *atg1*Δ and *trs85*Δ were used as controls to show defects in autophagy. Equal amounts of protein were fractionated by SDS–PAGE and analyzed by western analysis using anti-Ape1p IgG. The parental strain is normal for processing Ape1p in both rich and starvation conditions at all temperatures. The humanized *C1* strain is defective for selective autophagy but shows full processing of Ape1p when switched to starvation medium at 30°C and partial processing of the marker protein at 35°C. The humanized *C1 (c.64_72del)* strain is defective for selective autophagy and shows little processing of Ape1p when switched to starvation medium at 30°C and no processing at other temperatures. B) The parental strain MSY135 and the humanized strains with *C1* and *C1 (c.64_72del)* expressing plasmid-based GFP-Atg8 under the control of the endogenous ATG8 promoter were grown in nitrogen starvation medium (SD-N) to induce autophagy at 30°C. The mutant strains *atg1*Δ and *trs85*Δ were used as controls to show defects in autophagy. At the indicated times, aliquots were removed and protein extracts prepared and fractionated by SDS-PAGE. Using anti-GFP antibody, full-length GFP-Atg8p and free GFP were detected by western analysis. The parental strain and the humanized *C1* strain show accumulation of free GFP over time while the humanized *C1 (c.64_72del)* strain does not show generation of free GFP under these conditions.

3.8 Fibroblasts from the affected individual with *TRAPPC1* mutations do not show an accumulation of LC3-II during starvation

Since we had received fibroblast cells from the individual with the compound heterozygous mutation in *C1*, I sought to perform experiments to characterize the cellular defects. I first characterized these cells for an autophagic defect to assess whether the results from this experiment would parallel those in yeasts.

For this purpose, I used a starvation assay in which the fibroblasts are deprived of nutrients and serum, and which allows the monitoring of LC3-II expression levels through western analysis. LC3, the mammalian ortholog of yeast Atg8p, is synthesized as proLC3, a soluble unprocessed form that is proteolytically processed into LC3-I and finally is modified into LC3-II (the phosphatidylethanolamine-conjugated form), which is associated with membranes. The cells need to be deprived of nutrients, otherwise it is difficult to interpret LC3-I and LC3-II protein levels (Klionsky et al., 2021).

Initially, control and patient fibroblasts were starved for up to 2 h in EBSS starvation medium to induce autophagy. Cell lysates were collected at 0 h, 1 h and 2 h time points. As indicated in **Figure 3.13A** and quantified in **Figure 3.13B**, control cells showed an increase of LC3-II over the 2 h period. In contrast, patient cells did not show significant differences in the level of LC3-II over time compared to the control cells, while they show stable levels of LC3-I over the same 2 h period. The failure to convert LC3-I to LC3-II suggests a defect in autophagosome formation in these cells. It is worth noting though that autophagy is a highly dynamic process and the detection of LC3-II levels only at a specific time point is not sufficient for evaluating the overall autophagic flux.

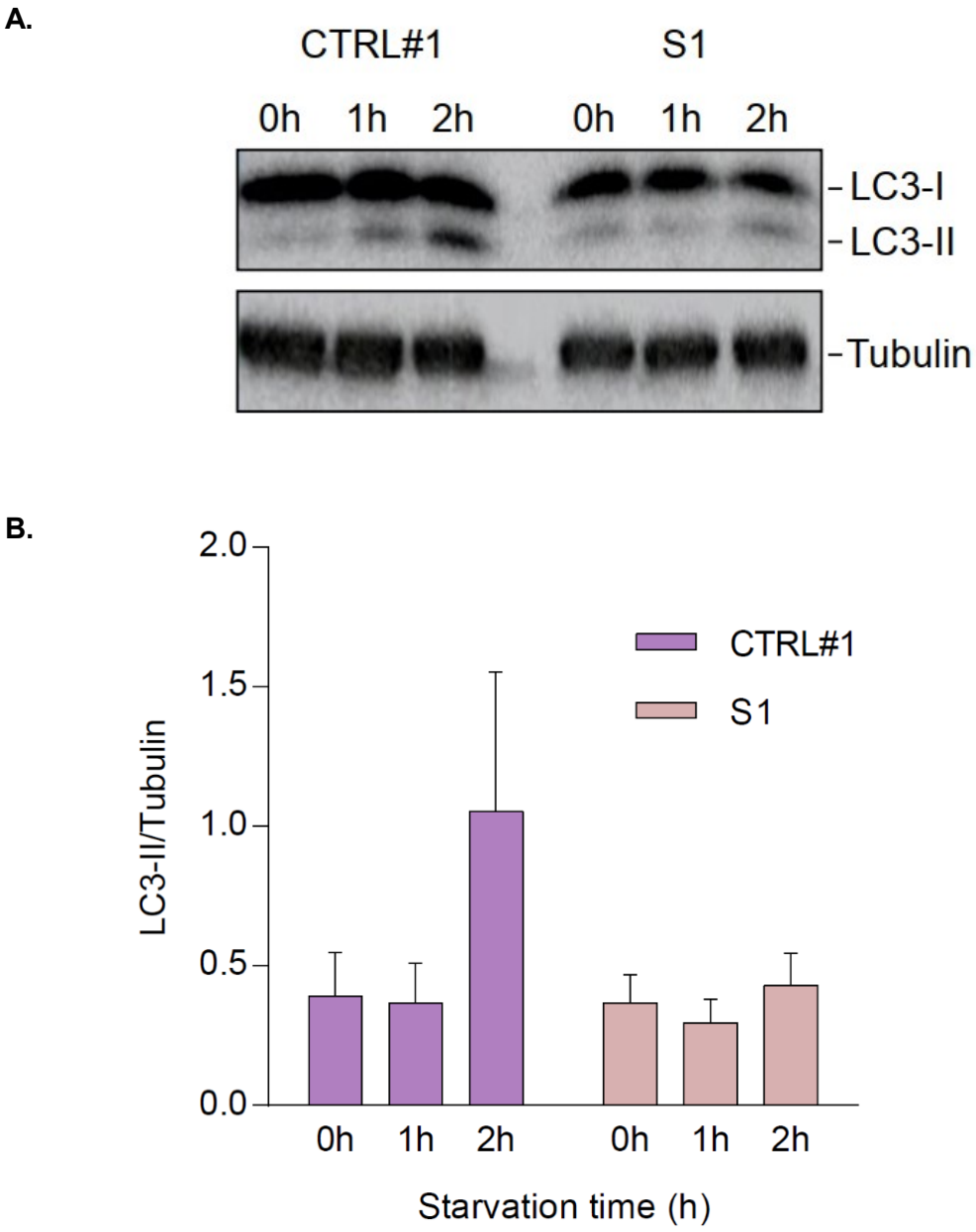

Figure 3. 13 Patient fibroblasts harboring the compound heterozygous *TRAPPC1* mutation show a defect in autophagy compared to control cells. A) Control (CTRL#1) and patient fibroblasts (S1) were starved (EBSS medium) for up to 2 h and cell lysates were collected at 0 h, 1 h and 2 h time points. Shown is a representative western blot where the expected bands for LC3-I, LC3-II and tubulin (loading control) are indicated. LC3-I migrates at ~17 kDa and LC3-II migrates at ~15 kDa. B) Quantification of the western blots with LC3-II signal normalized to the tubulin loading control. Quantification was done with ImageJ. The error bars indicate SEM.

3.9 Wild type *TRAPPC1* rescues a membrane trafficking defect and Golgi fragmentation in patient fibroblasts

TRAPP complexes are involved in ER-to-Golgi trafficking and late Golgi transport in mammals and C1 protein is part of the core TRAPP subunits of the two TRAPP complexes involved. Hence, patient fibroblasts were examined for defects in membrane trafficking using the RUSH system. In this assay, a fluorescent cargo protein (ST-eGFP) is kept in the ER until biotin is administered. Upon biotin addition, the cargo exits the ER and is transported to the Golgi and the fluorescent signal is monitored and quantified as it occupies the Golgi, indicating therefore the ER-to-Golgi traffic (Boncompain et al., 2012; Milev et al., 2019).

As illustrated in **Figure 3.14A,B**, the fluorescence intensity in the control cells increased over time as the cargo protein arrived at the Golgi. In contrast, the patient fibroblasts (S1) displayed a delay in the arrival of the cargo protein at the Golgi compared to the control cells. These results demonstrate that patient fibroblasts are defective in membrane trafficking events along the biosynthetic pathway. This defect is due to non-functional *C1* since patient cells transfected with a construct of the wild type *C1* tagged with red fluorescent protein (RFP) rescued the trafficking defect.

Next, I looked at the Golgi alterations in patient fibroblasts. Previous studies have reported changes in the Golgi morphology in patients with mutations in TRAPP subunits (Bögershausen et al., 2013; Milev et al., 2017, 2019). With this is mind, the fragmentation of the Golgi into small structures was quantified in the patient fibroblasts (S1) and was compared to the control cells. To visualize the Golgi, an antibody that recognizes the Golgi resident protein mannosidase-II (Man-II) was used. As shown in **Figure 3.14C**, the number of Golgi fragments in patient cells is significantly higher compared to the control. The transfection of patient cells with a construct of the wild type *C1* fused to RFP significantly rescued this phenotype, confirming that the Golgi morphological alterations are *C1*-dependent.

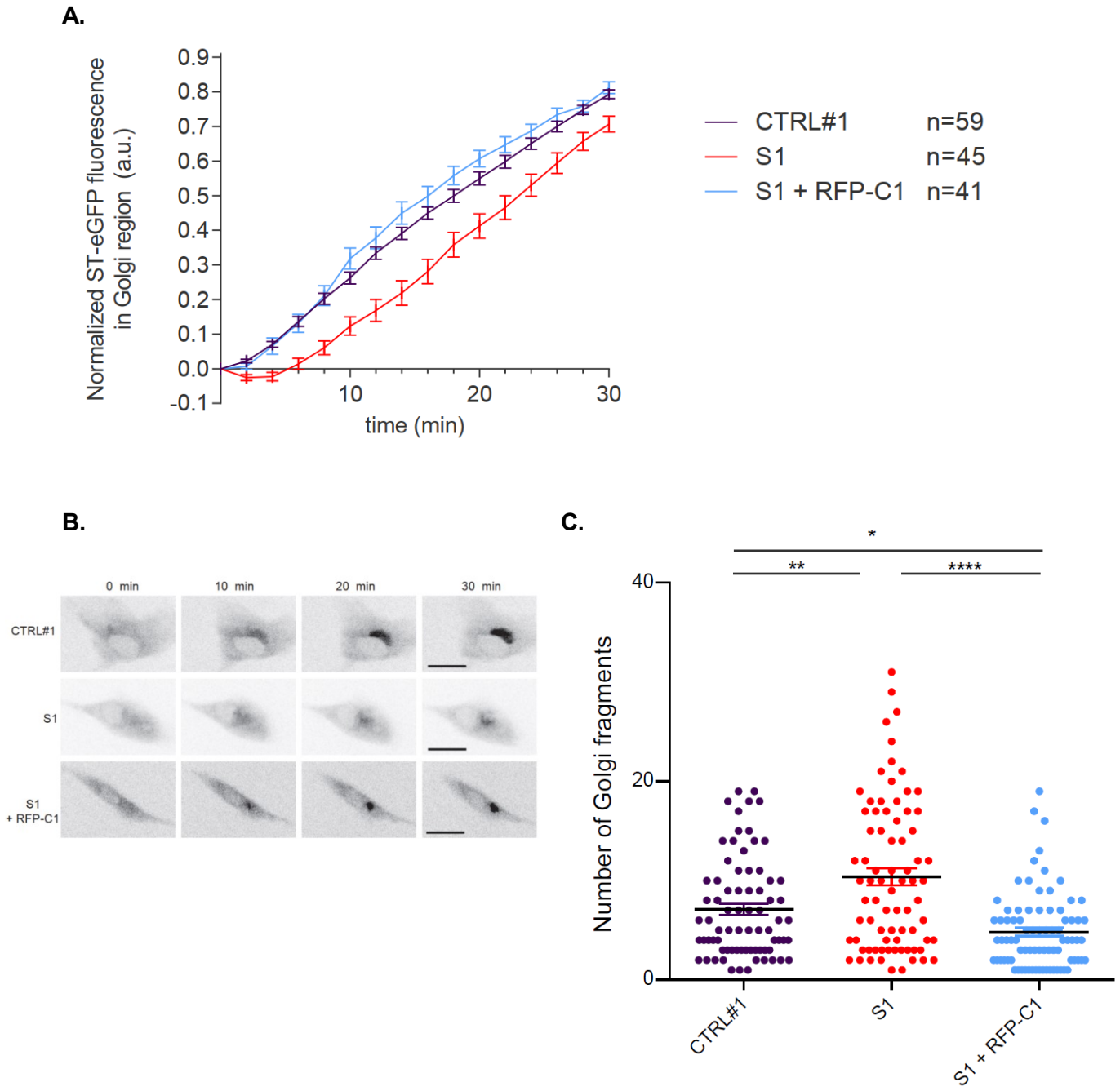

Figure 3. 14 Trafficking from the ER-to-Golgi is delayed, and Golgi morphology is altered in patient fibroblasts harboring a compound heterozygous *TRAPPC1* mutation. A) The RUSH assay was performed on control, S1 patient fibroblasts and S1 + RFP-C1 patient fibroblasts using ST-eGFP cargo protein. The cells were imaged every 2 min over a period of 30 min upon biotin addition, which causes the release of the cargo protein from the ER. Fluorescence intensity in the Golgi was quantified using ImageJ as described in Koehler et al., 2017. B) Representative images of the cells in each condition for the time points indicated are shown. C) Control fibroblasts, patient fibroblasts untransfected or transfected with a *C1* construct fused to RFP were

fixed and stained for Man-II to visualize Golgi and Hoechst to visualize the nucleus. The number of Golgi fragments per cell was quantified using Imaris as described in the *Materials and Methods* section. For estimating the statistical significance, one-way ANOVA was used with post hoc Tukey HSD analysis. The error bars indicate SEM. The N values for control, S1 and S1 + RFP-C1 are 75, 78 and 81 respectively in three different replicates.

4. DISCUSSION

4.1 An efficient humanized yeast system for characterizing TRAPP mutations

The scarcity in human cellular models represents a major challenge for studying the globally increasing number of rare diseases in general and TRAPPopathies in particular. This can be attributed at least in part to the limited number of patients diagnosed with rare conditions who agree to provide cells through invasive techniques such as skin and deeper tissue biopsies. To overcome this difficulty, there is a need for using other models to characterize disease-causing variants in humans. The yeast, *Saccharomyces cerevisiae*, has long been used as a model organism for studying human processes due to the remarkable degree of gene conservation between the two organisms. Therefore, using CRISPR/Cas9 as an editing tool, I generated a platform in yeast that would enable the characterization of mutations in human TRAPP genes in the absence of patient-derived cells. Analyzing first the core TRAPP genes, my project has demonstrated that *C1, C2, C2L, C6A* and *C6B* can complement individually their orthologs *BET5, TRS20, TCA17* and *TRS33*, respectively, in yeast. However, *C3, C4* and *C5* could not replace their corresponding yeast counterparts, *BET3*, *TRS23* and *TRS31* respectively (**Figure 3.1**). These results were confirmed by plasmid-based assays in yeast which proved that none of these genes, even when expressed under strong promoters, were able to compensate for the loss of their yeast orthologs (**Figure 3.4**). Despite the successful and scar-less replacement of their yeast equivalents by some of the human core TRAPP genes, *C1, C2* and *C2L* humanized strains revealed slightly compromised fitness compared to the parental yeast strain, a feature more pronounced in temperatures above 30°C while the *C6B* humanized strain was found to be heat-sensitive (**Figure 3.5A,B**).

The growth-delays observed in the humanized strains here have also been reported in other studies that explored humanized yeast systems (Boonekamp et al., 2022; Garge et al., 2020). Although the exact mechanisms that contribute to this decrease in growth efficiency are not

known, the adverse environment in yeast, alterations in function and regulation of human genes or failure of human orthologs to complement the yeast protein's moonlighting functions might be contributing factors. Therefore, a more detailed assessment of other specific phenotypes might help to better explore the underlying causes of growth differences that characterize humanized yeasts.

After generating a set of individually engineered strains with human TRAPP genes expressed at their native loci, the applicability of this system in studying human variants was investigated. Within the context of this study, the focus was to use this system as a test platform to characterize the first reported compound heterozygous mutation in *C1*, where a deletion of two nucleotides (c.362_363del) in the maternal variant (C1 p.Val121Alafs*3) alters an entire α-helix at the C-terminus of this longin domain protein while a deletion of nine nucleotides (c.64_72del) in the paternal variant (C1 p.His22_Lys24del) affects a short loop bridging two strands of the β-sheet structure (**Figure 3.7**). Towards this goal, yeast humanization with both mutants individually showed that the *C1 (c.362_363del)* is lethal and cannot replace *BET5* in yeast while the *C1 (c.64_72del)* is functional and can complement its ortholog *BET5*. The *C1 (c.64_72del)* mutant was tested for its growth efficiency under different temperature conditions (30°C, 35°C and 37°C) and the growth rate of this mutant was substantially compromised at 35°C and 37°C, indicating that it is a conditional-lethal mutant (**Figure 3.11A,B**).

The phenotypes observed for these two mutants might be better explained by looking at the structure of the C1 protein (**Figure 3.7B**) and the data that comes from crystallographic and cryo-EM studies which have revealed the structure of the TRAPP core (Galindo et al., 2021; Galindo and Munro, 2023; Kim et al., 2006; Mi et al., 2022; Tan et al., 2013; Yip et al., 2010). The octameric core forms an elongated rod with two flattened surfaces which accommodates the C1 and C4 proteins in the center. As two longin domain proteins, C1 and C4 also form most of the catalytic site for activating Rab GTPases. As shown in **Figure 3.7B**, C1 has three close core interactors,

C4 (in light pink), C3 (in cyan) and C6 (in hot pink). In the C1 p.Val121Alafs*3 variant (expressed from *C1 c.362_363del*), the entire α-helix at the C-terminus of the protein, which is in close proximity to the C6 subunit, is deleted. Therefore, the removal of this α-helix would be expected to have a major effect on the protein as it would interfere with the structure of this longin domain protein. This might explain the non-functionality of the maternal variant C1 p.Val121Alafs*3 in the yeast. On the other hand, in the C1 p.His22_Lys24del variant (expressed from *C1 c.64_72del*), the 3 amino acid deletion affects a portion of the protein which is a short peptide that connects two domains of a secondary structure and is close to the catalytic site where C1 and C4 accommodate and activate Rab GTPases. Although previous reports have revealed the importance of loops in the folding/geometry of proteins (Jappelli et al., 1992; Rose et al., 1985), the partial truncation of this loop might reflect less severe effects on the geometry of the protein. Indeed, previous studies have revealed that when perturbations are introduced by mutations in the structure of the protein, they might change the connection between elements of the system (atoms/residues) which in turn might provoke changes in the functional site and other sites of the structure (DuBay et al., 2015; Guarnera and Berezovsky, 2019; Prabantu et al., 2020). This might explain why in fact the paternal variant C1 p.His22_Lys24del, contrary to C1 p.Val121Alafs*3, acts as a conditional-lethal variant.

The *C1 (c.64_72del)* mutant was further characterized for defects in autophagy. Based on preApe1p processing in rich medium under permissive and restrictive temperatures, this mutant affected the cvt pathway while in starvation conditions, the *C1 (c.64_72del)* showed considerable defects in preApe1p processing in temperatures above 30°C (**Figure 3.12A**). Examination of the processing of GFP-Atg8p fusion protein under starvation conditions revealed that non-selective autophagy was also strongly affected in the *C1 (c.64_72del)* mutant (**Figure 3.12B**). Although these results imply that non-selective autophagy might be substantially affected by this mutation, it is difficult to draw a similar conclusion for selective autophagy (cvt pathway) since also the *C1* humanized strain seemed defective for preApe1 processing in rich conditions compared to the

parental wild type strain. Therefore, further optimization of these experiments would help draw more conclusive results to the degree that this mutation might affect autophagy.

In an effort to reinforce these results, I performed parallel experiments in fibroblasts derived from the patient who carries the compound heterozygous mutation in *C1*. These cells were tested for defects in autophagy, membrane trafficking and for alterations in Golgi morphology, phenotypes which have been previously reported in different TRAPPopathies (Bögershausen et al., 2013; Milev et al., 2017, 2018, 2019). Autophagy was examined by looking at the levels of LC3-II over time induced by starvation conditions since the amount of LC3-II is associated with the number of autophagosomes (Mizushima and Yoshimori, 2007). Patient fibroblasts did not show changes in the levels of LC3-II over the course of starvation compared to the control cells in which the level of this protein increased with time (**Figure 3.13A**). This suggests a defect in the autophagosome formation in patient cells although it is not yet clear if there are also defects in the autophagic flux. Hence, in the future, treatment with lysosome inhibitors that block the autophagosome-lysosome fusion and partially inhibit the degradation of LC3-II, would enable a more accurate assessment of the precise step in this pathway that is blocked.

Membrane trafficking defects were studied using the RUSH assay in which patient fibroblasts showed weaker Golgi fluorescence intensity over time compared to the control (**Figure 3.14A**). This suggests a delay in the trafficking process and less cargo-transporting vesicles since at the end of the 30 min movie the maximum Golgi intensity was less than the control. This defect was rescued through the transfection of patient cells with a wild type *C1-RFP* construct confirming that it is related to the *C1* mutation. Investigation of Golgi alterations showed that the number of Golgi fragments in the patient fibroblasts is significantly higher compared to the control cells, a phenotype that was rescued when these cells were transfected with a wild type *C1-RFP* construct (**Figure 3.14C**). The term Golgi ‘fragmentation’ here describes the alterations in the Golgi

morphology. However, it is important to emphasize that the Golgi structure is very dynamic and can very quickly go through remodeling on certain physiological or pathological conditions. Since the pattern of Golgi fragments depends on the nature of the cellular pathway that modifies the Golgi ribbon, we should be careful to discriminate between different types of Golgi fragmentation taking place. Therefore, the inclusion of additional information from other methods of observation such as electron microscopy, high resolution optical microscopy or staining with various Golgi markers, would be more beneficial in observing this phenotype related to Golgi morphology (Makhoul et al., 2019).

Taken together, all these data highlight the efficiency of the humanized yeast as a platform to characterize mutations in TRAPP genes and also suggest a possible correlation between the C1 variant and the severe neurodevelopmental delay from which the individual bearing the *C1* mutations suffers. This latter suggestion is related with the use of this system for addressing variants of unknown or uncertain significance (VUSs). VUSs are variants for which the clinical significance, therefore the association with the risk of disease, is not clear (Hoffman-Andrews, 2018). In this study, I applied this platform to address the significance of a compound heterozygous mutation in *TRAPPC1* identified as a VUS from genetic testing data, where the maternal variant showed to be lethal and could not replace its yeast counterpart while the paternal variant manifested as a conditional phenotype. Therefore, setting up this system with other TRAPP proteins will allow us to rapidly test additional VUSs and find out whether they show any clinical significance. Such a system would also have more general benefits to quickly analyze an VUS if its yeast orthologue can be humanized.

4.2 Future directions

In this study, I individually humanized core TRAPP genes in yeast using CRISPR/Cas9 in a single step and scar-less approach for engineering genes in yeast. These efforts lead to the generation of five novel individually humanized strains with *C1, C2, C2L, C6A* and C6B and to one novel

humanized strain with *C1 (c.64_72del)*. Since *C3, C4* and *C5* did not complement their yeast orthologs, work towards humanizing these remaining core genes is in progress. Looking at the percentage of identity and similarity for these genes, it was surprising why these replacements were not permitted (**see Table 4.1 below**).

Table 4. 1 Humanization of yeast with human core TRAPP genes and the conservation between yeast and human proteins

HUMAN PROTEIN	YEAST PROTEIN	REPLACEMENT IN YEAST	% IDENTITY/SIMILARITY	GROWTH PHENOTYPE
C1	Bet5p	+	33/54	partially affected
C1 p.Val121Alafs*3	Bet5p	-	N/A	N/A
C1 p.His22_Lys24del	Bet5p	+	N/A	conditional-lethal
C2	Trs20p	+	34/52	partially affected
C2L	Tca17p	+	24/43	partially affected
C3	Bet3p	-	56/76	N/A
C4	Trs23p	-	29/44	N/A
C5	Trs31p	-	31/52	N/A
C6A	Trs33p	+	35/51	normal
C6B	Trs33p	+	33/47	partially affected

With respect to C3, the best conserved protein that shows the highest percentage of identity and similarity with its yeast counterpart Bet3p (56/76), I expected success in humanizing its ortholog at the native locus in yeast. It is important to emphasize that C3 is the only core protein that is present in two copies (C3a and C3b) by flanking both sides of the core center formed by C1 and C4. The dimeric nature of C3 and its yeast equivalent Bet3p, which determines the stoichiometry of the TRAPP complex, might explain this intolerable substitution since the single gene replacement should generate in a sense a double protein replacement in the complex. Therefore, a major challenge in the future will be to make these genes humanizable in yeast. For this, we could employ increased homology arm length up to several hundred base pairs which might improve the efficiency of the replacement. Since certain genes require local interactions for

functional replaceability, another track to follow could be combinations of replacements, such as humanized *C1* strain with *C3* repair template or humanized *C2* strain with *C5* repair template. As we progressively humanize additional TRAPP genes in yeast, our final goal would be to assemble all these replacements in one strain, generating in this way a fully humanized TRAPP complex in yeast.

A bottleneck in this study was the inability to characterize the expression among humanized strains via western analysis. Indeed, attempts to look at the expression of *C1* in humanized yeast were unsuccessful due to an inefficient antibody against C1. Therefore, attempts in other humanized strains with C2, *C2L, C6A* and *C6B* to look at the expression of these genes in the yeast background showed the absence of the specific bands for yeast proteins when blotted with yeast antibodies against Trs20p, Tca17p and Trs33p, respectively (**Figure 3.6**). Still, more convincing proof will be needed to show expression of the human genes in the humanized system and future ongoing work aims at performing mass spectrometry as an analytic approach to quantify the expression of the yeast and human proteins in these strains. I fully expect that for the humanized C2 strain I will detect C2 since both the yeast and human proteins are essential.

Through the humanized system, I was able to characterize the first reported mutations in *C1* by performing functional experiments that explore pathways where this protein is involved such as selective and non-selective autophagy. The results from these experiments were supported by similar outcomes in patient fibroblasts confirming the applicability of this system as a reliable tool for characterizing other gene mutations as well. Although these experiments need additional optimization to generate more conclusive data, other functional assays would provide more compelling data for the characterization of the C1 variant and other variants in the future.

Indeed, I attempted looking into two other aspects of the humanized strains with *C1* and *C1 (c.64_72del)*. First was the incorporation of human proteins into the yeast TRAPP complexes

which would be a measure of the stability of the complexes after the replacement. For this, I performed size exclusion chromatography (SEC). With C1 as a core protein, my expectations were to detect all the fractionated TRAPP complexes in the wild-type *C1* humanized strain, while for the *C1 (c.64_72del)* humanized strain, shifts in growth conditions from permissive to restrictive temperatures might indicate changes in stability for the three TRAPP complexes, reflected as shifting or absence of TRAPP peak fractions. The results from these experiments were not conclusive and I could not show the presence of all TRAPP complexes in the wild-type *C1* humanized strain or detect any changes in the *C1 (c.64_72del)* humanized strain. Next, since TRAPP complexes are tethers involved in membrane trafficking, I assessed trafficking in the humanized strains with *C1* and *C1 (c.64_72del)*. For this, I performed a general secretion assay and immunoprecipitation of carboxypeptidase Y (CPY), a vacuolar protein that traverses the secretory pathway. These functional assays involve the radiolabeling of yeast cells with [^{35}S]-methionine followed by a chase with non-labeled methionine. While in the general secretion assay I looked at the full tableau of the secretion process, the immunoprecipitation of CPY enabled the detection of only this protein. To date, the generated data from the general secretion assay were inconsistent and I could not draw definite conclusions for either the *C1* or the *C1 (c.64_72del)* humanized strains while for the CPY assay, I managed to detect the processing of this protein in both humanized strains at 30°C. This work is still in progress, and I am working on optimizing conditions and normalizing the levels of CPY detected in all of the samples. Next, I will need to perform this experiment at a restrictive temperature (37°C) to observe any differences between the wild-type *C1* and *C1 (c.64_72del)* humanized strains.

Since the *TRAPPC1* mutation in this study is a compound heterozygous mutation, another direction would be to test this mutation in diploid yeasts with one allele as the maternal copy and the other allele as the paternal copy. Such a system might better reflect the human situation and may allow me to tease out additional phenotypes not seen by either single variant alone.

In conclusion, this study together with many others before, highlights the crucial importance of using yeast as a model organism for exploring human genetics and disease in a simplified background. The engineered strains in this study will be further used as effective platforms to characterize other disease-causing mutations. Therefore, I conclude that the humanization of TRAPP in yeast will be a useful model system to study mutations, particularly when human cells are not available.

5. REFERENCES

Akhmetov, A., Laurent, J. M., Gollihar, J., Gardner, E. C., Garge, R. K., Ellington, A. D., Kachroo, A. H., & Marcotte, E. M. (2018). Single-step Precision Genome Editing in Yeast Using CRISPR-Cas9. *Bio-Protocol*, *8*(6), e2765. https://doi.org/10.21769/BioProtoc.2765

Al-Deri, N., Okur, V., Ahimaz, P., Milev, M., Valivullah, Z., Hagen, J., Sheng, Y., Chung, W., Sacher, M., & Ganapathi, M. (2021). A novel homozygous variant in TRAPPC2L results in a neurodevelopmental disorder and disrupts TRAPP complex function. *Journal of Medical Genetics*, *58*(9), 592–601. https://doi.org/10.1136/jmedgenet-2020-107016

Antonietta, D. M. M., & Alberto, L. (2011). Mendelian Disorders of Membrane Trafficking. *The New England Journal of Medicine*.

Aridor, M., & Hannan, L. A. (2000). Traffic jam: A compendium of human diseases that affect intracellular transport processes. *Traffic (Copenhagen, Denmark)*, *1*(11), 836–851. https://doi.org/10.1034/j.1600-0854.2000.011104.x

Auburger, G., Klinkenberg, M., Drost, J., Marcus, K., Morales-Gordo, B., Kunz, W. S., Brandt, U., Broccoli, V., Reichmann, H., Gispert, S., & Jendrach, M. (2012). Primary skin fibroblasts as a model of Parkinson's disease. *Molecular Neurobiology*, *46*(1), 20–27. https://doi.org/10.1007/s12035-012-8245-1

Baldovino, S., Moliner, A. M., Taruscio, D., Daina, E., & Roccatello, D. (2016). Rare Diseases in Europe: From a Wide to a Local Perspective. *The Israel Medical Association Journal: IMAJ*, *18*(6), 359–363.

Bannykh, S. I., Rowe, T., & Balch, W. E. (1996). The organization of endoplasmic reticulum export complexes. *The Journal of Cell Biology*, *135*(1), 19–35. https://doi.org/10.1083/jcb.135.1.19

Barlowe, C., Orci, L., Yeung, T., Hosobuchi, M., Hamamoto, S., Salama, N., Rexach, M. F., Ravazzola, M., Amherdt, M., & Schekman, R. (1994). COPII: A membrane coat formed by Sec proteins that drive vesicle budding from the endoplasmic reticulum. *Cell*, *77*(6), 895–907. https://doi.org/10.1016/0092-8674(94)90138-4

Bassik, M. C., Kampmann, M., Lebbink, R. J., Wang, S., Hein, M. Y., Poser, I., Weibezahn, J., Horlbeck, M. A., Chen, S., Mann, M., Hyman, A. A., LeProust, E. M., McManus, M. T., & Weissman, J. S. (2013). A Systematic Mammalian Genetic Interaction Map Reveals Pathways Underlying Ricin Susceptibility. *Cell*, *152*(4), 909–922. https://doi.org/10.1016/j.cell.2013.01.030

Bayzigitov, D. R., Medvedev, S. P., Dementyeva, E. V., Bayramova, S. A., Pokushalov, E. A., Karaskov, A. M., & Zakian, S. M. (2016). Human Induced Pluripotent Stem Cell-Derived Cardiomyocytes Afford New Opportunities in Inherited Cardiovascular Disease Modeling. *Cardiology Research and Practice*, *2016*, 3582380. https://doi.org/10.1155/2016/3582380

Behnia, R., & Munro, S. (2005). Organelle identity and the signposts for membrane traffic. *Nature*, *438*(7068), Article 7068. https://doi.org/10.1038/nature04397

Bell, S., Peng, H., Crapper, L., Kolobova, I., Maussion, G., Vasuta, C., Yerko, V., Wong, T. P., & Ernst, C. (2017). A Rapid Pipeline to Model Rare Neurodevelopmental Disorders with Simultaneous CRISPR/Cas9 Gene Editing. *Stem Cells Translational Medicine*, *6*(3), 886–896. https://doi.org/10.1002/sctm.16-0158

Bi, X., Corpina, R. A., & Goldberg, J. (2002). Structure of the Sec23/24-Sar1 pre-budding complex of the COPII vesicle coat. *Nature*, *419*(6904), 271–277. https://doi.org/10.1038/nature01040

Bick, D., Jones, M., Taylor, S. L., Taft, R. J., & Belmont, J. (2019). Case for genome sequencing in infants and children with rare, undiagnosed or genetic diseases. *Journal of Medical Genetics*, *56*(12), 783–791. https://doi.org/10.1136/jmedgenet-2019-106111

Boeke, J. D., La Croute, F., & Fink, G. R. (1984). A positive selection for mutants lacking orotidine-5′-phosphate decarboxylase activity in yeast: 5-fluoro-orotic acid resistance. *Molecular and General Genetics MGG*, *197*(2), 345–346. https://doi.org/10.1007/BF00330984

Bögershausen, N., Shahrzad, N., Chong, J. X., Von Kleist-Retzow, J. C., Stanga, D., Li, Y., Bernier, F. P., Loucks, C. M., Wirth, R., Puffenberger, E. G., Hegele, R. A., Schreml, J., Lapointe, G., Keupp, K., Brett, C. L., Anderson, R., Hahn, A., Innes, A. M., Suchowersky, O., … Lamont, R. E. (2013). Recessive TRAPPC11 mutations cause a disease spectrum of limb girdle muscular dystrophy and myopathy with movement disorder and intellectual disability. *American Journal of Human Genetics*, *93*(1), 181–190. https://doi.org/10.1016/j.ajhg.2013.05.028

Boncompain, G., Divoux, S., Gareil, N., de Forges, H., Lescure, A., Latreche, L., Mercanti, V., Jollivet, F., Raposo, G., & Perez, F. (2012). Synchronization of secretory protein traffic in populations of cells. *Nature Methods*, *9*(5), 493–498. https://doi.org/10.1038/nmeth.1928

Bonifacino, J. S., & Glick, B. S. (2004). The mechanisms of vesicle budding and fusion. *Cell*, *116*(2), 153–166. https://doi.org/10.1016/s0092-8674(03)01079-1

Bonifacino, J. S., & Lippincott-Schwartz, J. (2003). Coat proteins: Shaping membrane transport. *Nature Reviews. Molecular Cell Biology*, *4*(5), 409–414. https://doi.org/10.1038/nrm1099

Boonekamp, F. J., Knibbe, E., Vieira-Lara, M. A., Wijsman, M., Luttik, M. A. H., van Eunen, K., Ridder, M. den, Bron, R., Almonacid Suarez, A. M., van Rijn, P., Wolters, J. C., Pabst, M., Daran, J.-M., Bakker, B. M., & Daran-Lapujade, P. (2022). Full humanization of the glycolytic pathway in Saccharomyces cerevisiae. *Cell Reports*, *39*(13), 111010. https://doi.org/10.1016/j.celrep.2022.111010

Botstein, D., & Fink, G. R. (2011). Yeast: An experimental organism for 21st Century biology. *Genetics*, *189*(3), 695–704. https://doi.org/10.1534/genetics.111.130765

Bröcker, C., Engelbrecht-Vandré, S., & Ungermann, C. (2010). Multisubunit tethering complexes and their role in membrane fusion. *Current Biology: CB*, *20*(21), R943-952. https://doi.org/10.1016/j.cub.2010.09.015

Brunet, S., Noueihed, B., Shahrzad, N., Saint-Dic, D., Hasaj, B., Guan, T. L., Moores, A., Barlowe, C., & Sacher, M. (2012). The SMS domain of Trs23p is responsible for the in vitro appearance of the TRAPP I complex in Saccharomyces cerevisiae. *Cellular Logistics*, *2*(1), 28–42. https://doi.org/10.4161/cl.19414

Brunet, S., & Sacher, M. (2014). Are all multisubunit tethering complexes bona fide tethers? *Traffic (Copenhagen, Denmark)*, *15*(11), 1282–1287. https://doi.org/10.1111/tra.12200

Brunet, S., Shahrzad, N., Saint-Dic, D., Dutczak, H., & Sacher, M. (2013). A trs20 mutation that mimics an SEDT-causing mutation blocks selective and non-selective autophagy: A model for TRAPP III organization. *Traffic (Copenhagen, Denmark)*, *14*(10), 1091–1104. https://doi.org/10.1111/tra.12095

Brzáčová, Z., Peťková, M., Veljačiková, K., Zajičková, T., & Tomáška, Ľ. (2021). Reconstruction of human genome evolution in yeast: An educational primer for use with “systematic humanization of the yeast cytoskeleton discerns functionally replaceable from divergent human genes.” *Genetics*, *219*(2), iyab118. https://doi.org/10.1093/genetics/iyab118

Cai, H., Yu, S., Menon, S., Cai, Y., Lazarova, D., Fu, C., Reinisch, K., Hay, J. C., & Ferro-Novick, S. (2007). TRAPPI tethers COPII vesicles by binding the coat subunit Sec23. *Nature*, *445*(7130), 941–944. https://doi.org/10.1038/nature05527

Cai, H., Zhang, Y., Pypaert, M., Walker, L., & Ferro-Novick, S. (2005). Mutants in trs120 disrupt traffic from the early endosome to the late Golgi. *The Journal of Cell Biology*, *171*(5), 823–833. https://doi.org/10.1083/jcb.200505145

Cai, Y., Chin, H. F., Lazarova, D., Menon, S., Fu, C., Cai, H., Sclafani, A., Rodgers, D. W., De La Cruz, E. M., Ferro-Novick, S., & Reinisch, K. M. (2008). The structural basis for activation of the Rab Ypt1p by the TRAPP membrane tethering complexes. *Cell*, *133*(7), 1202–1213. https://doi.org/10.1016/j.cell.2008.04.049

Cardinali, P., Migliorini, L., & Rania, N. (2019). The Caregiving Experiences of Fathers and Mothers of Children With Rare Diseases in Italy: Challenges and Social Support Perceptions. *Frontiers in Psychology*, *10*, 1780. https://doi.org/10.3389/fpsyg.2019.01780

Cheong, H., & Klionsky, D. J. (2008). Biochemical methods to monitor autophagy-related processes in yeast. *Methods in Enzymology*, *451*, 1–26. https://doi.org/10.1016/S0076-6879(08)03201-1

Cherfils, J., & Zeghouf, M. (2013). Regulation of Small GTPases by GEFs, GAPs, and GDIs. *Physiological Reviews*, *93*(1), 269–309. https://doi.org/10.1152/physrev.00003.2012

Choi, C., Davey, M., Schluter, C., Pandher, P., Fang, Y., Foster, L. J., & Conibear, E. (2011). Organization and assembly of the TRAPPII complex. *Traffic (Copenhagen, Denmark)*, *12*(6), 715–725. https://doi.org/10.1111/j.1600-0854.2011.01181.x

Condò, I. (2022). Rare Monogenic Diseases: Molecular Pathophysiology and Novel Therapies. *International Journal of Molecular Sciences*, *23*(12), 6525. https://doi.org/10.3390/ijms23126525

DeRossi, C., Vacaru, A., Rafiq, R., Cinaroglu, A., Imrie, D., Nayar, S., Baryshnikova, A., Milev, M. P., Stanga, D., Kadakia, D., Gao, N., Chu, J., Freeze, H. H., Lehrman, M. A., Sacher, M., & Sadler, K. C. (2016). Trappc11 is required for protein glycosylation in zebrafish and humans. *Molecular Biology of the Cell*, *27*(8), 1220–1234. https://doi.org/10.1091/mbc.E15-08-0557

Deyle, D. R. (2021). Generation of Induced Pluripotent Stem Cells. In A. J. van Wijnen & M. S. Ganshina (Eds.), *Osteoporosis and Osteoarthritis* (pp. 71–87). Springer US. https://doi.org/10.1007/978-1-0716-0989-7_6

DiCarlo, J. E., Norville, J. E., Mali, P., Rios, X., Aach, J., & Church, G. M. (2013). Genome engineering in Saccharomyces cerevisiae using CRISPR-Cas systems. *Nucleic Acids Research*, *41*(7), 4336–4343. https://doi.org/10.1093/nar/gkt135

Doench, J. G., Fusi, N., Sullender, M., Hegde, M., Vaimberg, E. W., Donovan, K. F., Smith, I., Tothova, Z., Wilen, C., Orchard, R., Virgin, H. W., Listgarten, J., & Root, D. E. (2016). Optimized sgRNA design to maximize activity and minimize off-target effects of CRISPR-Cas9. *Nature Biotechnology*, *34*(2), 184–191. https://doi.org/10.1038/nbt.3437

DuBay, K. H., Bowman, G. R., & Geissler, P. L. (2015). Fluctuations within folded proteins: Implications for thermodynamic and allosteric regulation. *Accounts of Chemical Research*, *48*(4), 1098–1105. https://doi.org/10.1021/ar500351b

Ebert, A. D., Yu, J., Rose, F. F., Mattis, V. B., Lorson, C. L., Thomson, J. A., & Svendsen, C. N. (2009). Induced pluripotent stem cells from a spinal muscular atrophy patient. *Nature*, *457*(7227), 277–280. https://doi.org/10.1038/nature07677

Engler, C., Kandzia, R., & Marillonnet, S. (2008). A one pot, one step, precision cloning method with high throughput capability. *PloS One*, *3*(11), e3647. https://doi.org/10.1371/journal.pone.0003647

Fasshauer, D., Eliason, W. K., Brünger, A. T., & Jahn, R. (1998). Identification of a minimal core of the synaptic SNARE complex sufficient for reversible assembly and disassembly. *Biochemistry*, *37*(29), 10354–10362. https://doi.org/10.1021/bi980542h

Fath, S., Mancias, J. D., Bi, X., & Goldberg, J. (2007). Structure and organization of coat proteins in the COPII cage. *Cell*, *129*(7), 1325–1336. https://doi.org/10.1016/j.cell.2007.05.036

Fee, D. B., Harmelink, M., Monrad, P., & Pyzik, E. (2017). Siblings With Mutations in TRAPPC11 Presenting With Limb-Girdle Muscular Dystrophy 2S. *Journal of Clinical Neuromuscular Disease*, *19*(1), 27–30. https://doi.org/10.1097/CND.0000000000000173

Filippini, F., Rossi, V., Galli, T., Budillon, A., D'Urso, M., & D'Esposito, M. (2001). Longins: A new evolutionary conserved VAMP family sharing a novel SNARE domain. *Trends in Biochemical Sciences*, *26*(7), 407–409. https://doi.org/10.1016/s0968-0004(01)01861-8

Foury, F. (1997). Human genetic diseases: A cross-talk between man and yeast. *Gene*, *195*(1), 1–10. https://doi.org/10.1016/s0378-1119(97)00140-6

Galindo, A., & Munro, S. (2023). The TRAPP complexes: Oligomeric exchange factors that activate the small GTPases Rab1 and Rab11. *FEBS Letters*, *597*(6), 734–749. https://doi.org/10.1002/1873-3468.14553

Galindo, A., Planelles-Herrero, V. J., Degliesposti, G., & Munro, S. (2021). Cryo-EM structure of metazoan TRAPPIII, the multi-subunit complex that activates the GTPase Rab1. *The EMBO Journal*, *40*(12), e107608. https://doi.org/10.15252/embj.2020107608

García-Cazorla, A., Oyarzábal, A., Saudubray, J.-M., Martinelli, D., & Dionisi-Vici, C. (2022). Genetic disorders of cellular trafficking. *Trends in Genetics: TIG*, *38*(7), 724–751. https://doi.org/10.1016/j.tig.2022.02.012

Garge, R. K., Cha, H. J., Lee, C., Gollihar, J. D., Kachroo, A. H., Wallingford, J. B., & Marcotte, E. M. (2021). Discovery of new vascular disrupting agents based on evolutionarily conserved drug action, pesticide resistance mutations, and humanized yeast. *Genetics*, *219*(1), iyab101. https://doi.org/10.1093/genetics/iyab101

Garge, R. K., Laurent, J. M., Kachroo, A. H., & Marcotte, E. M. (2020). Systematic Humanization of the Yeast Cytoskeleton Discerns Functionally Replaceable from Divergent Human Genes. *Genetics*, *215*(4), 1153–1169. https://doi.org/10.1534/genetics.120.303378

Garrino, L., Picco, E., Finiguerra, I., Rossi, D., Simone, P., & Roccatello, D. (2015). Living with and treating rare diseases: Experiences of patients and professional health care providers. *Qualitative Health Research*, *25*(5), 636–651. https://doi.org/10.1177/1049732315570116

Gedeon, Á. K., Colley, A., Jamieson, R., Thompson, E. M., Rogers, J., Sillence, D., Tiller, G. E., Mulley, J. C., & Gécz, J. (1999). Identification of the gene (SEDL) causing X-linked spondyloepiphyseal dysplasia tarda. *Nature Genetics*, *22*(4), Article 4. https://doi.org/10.1038/11976

Guarnera, E., & Berezovsky, I. N. (2019). On the perturbation nature of allostery: Sites, mutations, and signal modulation. *Current Opinion in Structural Biology*, *56*, 18–27. https://doi.org/10.1016/j.sbi.2018.10.008

Haendel, M., Vasilevsky, N., Unni, D., Bologa, C., Harris, N., Rehm, H., Hamosh, A., Baynam, G., Groza, T., McMurry, J., Dawkins, H., Rath, A., Thaxon, C., Bocci, G., Joachimiak, M. P., Köhler, S., Robinson, P. N., Mungall, C., & Oprea, T. I. (2020). How many rare diseases are there? *Nature Reviews. Drug Discovery*, *19*(2), 77–78. https://doi.org/10.1038/d41573-019-00180-y

Harripaul, R., Vasli, N., Mikhailov, A., Rafiq, M. A., Mittal, K., Windpassinger, C., Sheikh, T. I., Noor, A., Mahmood, H., Downey, S., Johnson, M., Vleuten, K., Bell, L., Ilyas, M., Khan, F. S., Khan, V., Moradi, M., Ayaz, M., Naeem, F., … Vincent, J. B. (2018). Mapping autosomal recessive intellectual disability: Combined microarray and exome sequencing identifies 26 novel candidate genes in 192 consanguineous families. *Molecular Psychiatry*, *23*(4), 973–984. https://doi.org/10.1038/mp.2017.60

Hentschel, A., Czech, A., Münchberg, U., Freier, E., Schara-Schmidt, U., Sickmann, A., Reimann, J., & Roos, A. (2021). Protein signature of human skin fibroblasts allows the study of the molecular etiology of rare neurological diseases. *Orphanet Journal of Rare Diseases*, *16*(1), 73. https://doi.org/10.1186/s13023-020-01669-1

Hoffman-Andrews, L. (2018). The known unknown: The challenges of genetic variants of uncertain significance in clinical practice. *Journal of Law and the Biosciences*, *4*(3), 648–657. https://doi.org/10.1093/jlb/lsx038

Hohmann, S. (2016). Nobel Yeast Research. *FEMS Yeast Research*, *16*(8), fow094. https://doi.org/10.1093/femsyr/fow094

Howell, G. J., Holloway, Z. G., Cobbold, C., Monaco, A. P., & Ponnambalam, S. (2006). Cell biology of membrane trafficking in human disease. *International Review of Cytology*, *252*, 1–69. https://doi.org/10.1016/S0074-7696(06)52005-4

Huyard, C. (2009). How did uncommon disorders become 'rare diseases'? History of a boundary object. *Sociology of Health & Illness*, *31*(4), 463–477. https://doi.org/10.1111/j.1467-9566.2008.01143.x

Itzhaki, I., Maizels, L., Huber, I., Zwi-Dantsis, L., Caspi, O., Winterstern, A., Feldman, O., Gepstein, A., Arbel, G., Hammerman, H., Boulos, M., & Gepstein, L. (2011). Modelling the long QT syndrome with induced pluripotent stem cells. *Nature*, *471*(7337), 225–229. https://doi.org/10.1038/nature09747

Jappelli, R., Luzzago, A., Tataseo, P., Pernice, I., & Cesareni, G. (1992). Loop mutations can cause a substantial conformational change in the carboxy terminus of the ferritin protein. *Journal of Molecular Biology*, *227*(2), 532–543. https://doi.org/10.1016/0022-2836(92)90905-y

Jiang, Y., Scarpa, A., Zhang, L., Stone, S., Feliciano, E., & Ferro-Novick, S. (1998). A high copy suppressor screen reveals genetic interactions between BET3 and a new gene. Evidence for a novel complex in ER-to-Golgi transport. *Genetics*, *149*(2), 833–841.

Joiner, A., & Fromme, C. (2018). Deciphering TRAPP complex function in yeast. *The FASEB Journal*, *32*(S1), 542.17-542.17. https://doi.org/10.1096/fasebj.2018.32.1_supplement.542.17

Joiner, A. M., Phillips, B. P., Yugandhar, K., Sanford, E. J., Smolka, M. B., Yu, H., Miller, E. A., & Fromme, J. C. (2021). Structural basis of TRAPPIII-mediated Rab1 activation. *The EMBO Journal*, *40*(12), e107607. https://doi.org/10.15252/embj.2020107607

Jones, S., Newman, C., Liu, F., & Segev, N. (2000). The TRAPP Complex Is a Nucleotide Exchanger for Ypt1 and Ypt31/32. *Molecular Biology of the Cell*, *11*(12), 4403–4411.

Kachroo, A. H., Laurent, J. M., Yellman, C. M., Meyer, A. G., Wilke, C. O., & Marcotte, E. M. (2015). Systematic humanization of yeast genes reveals conserved functions and genetic modularity. *Science (New York, N.Y.)*, *348*(6237), 921–925. https://doi.org/10.1126/science.aaa0769

Kachroo, A. H., Vandeloo, M., Greco, B. M., & Abdullah, M. (2022). Humanized yeast to model human biology, disease and evolution. *Disease Models & Mechanisms*, *15*(6), dmm049309. https://doi.org/10.1242/dmm.049309

Kaiser, C. A., & Schekman, R. (1990). Distinct sets of SEC genes govern transport vesicle formation and fusion early in the secretory pathway. *Cell*, *61*(4), 723–733. https://doi.org/10.1016/0092-8674(90)90483-u

Kearse, M., Moir, R., Wilson, A., Stones-Havas, S., Cheung, M., Sturrock, S., Buxton, S., Cooper, A., Markowitz, S., Duran, C., Thierer, T., Ashton, B., Meintjes, P., & Drummond, A. (2012). Geneious Basic: An integrated and extendable desktop software platform for the organization and analysis of sequence data. *Bioinformatics*, *28*(12), 1647–1649. https://doi.org/10.1093/bioinformatics/bts199

Khattak, N. A., & Mir, A. (2014). Computational analysis of TRAPPC9: Candidate gene for autosomal recessive non-syndromic mental retardation. *CNS & Neurological Disorders Drug Targets*, *13*(4), 699–711. https://doi.org/10.2174/18715273113129990105

Khosla, N., & Valdez, R. (2018). A compilation of national plans, policies and government actions for rare diseases in 23 countries. *Intractable & Rare Diseases Research*, *7*(4), 213–222. https://doi.org/10.5582/irdr.2018.01085

Kim, J. J., Lipatova, Z., & Segev, N. (2016). TRAPP Complexes in Secretion and Autophagy. *Frontiers in Cell and Developmental Biology*, *4*. https://www.frontiersin.org/articles/10.3389/fcell.2016.00020

Kim, K.-Y., Hysolli, E., & Park, I.-H. (2011). Neuronal maturation defect in induced pluripotent stem cells from patients with Rett syndrome. *Proceedings of the National Academy of Sciences of the United States of America*, *108*(34), 14169–14174. https://doi.org/10.1073/pnas.1018979108

Kim, S., Park, J., Kim, T., & Lee, J.-S. (2020). The functional study of human proteins using humanized yeast. *Journal of Microbiology (Seoul, Korea)*, *58*(5), 343–349. https://doi.org/10.1007/s12275-020-0136-y

Kim, Y.-G., Raunser, S., Munger, C., Wagner, J., Song, Y.-L., Cygler, M., Walz, T., Oh, B.-H., & Sacher, M. (2006). The architecture of the multisubunit TRAPP I complex suggests a model for vesicle tethering. *Cell*, *127*(4), 817–830. https://doi.org/10.1016/j.cell.2006.09.029

Klann, M., Koeppl, H., & Reuss, M. (2012). Spatial modeling of vesicle transport and the cytoskeleton: The challenge of hitting the right road. *PloS One*, *7*(1), e29645. https://doi.org/10.1371/journal.pone.0029645

Klionsky, D. J., Abdel-Aziz, A. K., Abdelfatah, S., Abdellatif, M., Abdoli, A., Abel, S., Abeliovich, H., Abildgaard, M. H., Abudu, Y. P., Acevedo-Arozena, A., Adamopoulos, I. E., Adeli, K., Adolph, T. E., Adornetto, A., Aflaki, E., Agam, G., Agarwal, A., Aggarwal, B. B., Agnello, M., … Tong, C.-K. (2021). Guidelines for the use and interpretation of assays for monitoring autophagy (4th edition)1. *Autophagy*, *17*(1), 1–382. https://doi.org/10.1080/15548627.2020.1797280

Klionsky, D. J., Cueva, R., & Yaver, D. S. (1992). Aminopeptidase I of Saccharomyces cerevisiae is localized to the vacuole independent of the secretory pathway. *The Journal of Cell Biology*, *119*(2), 287–299. https://doi.org/10.1083/jcb.119.2.287

Koehler, K., Milev, M. P., Prematilake, K., Reschke, F., Kutzner, S., Jühlen, R., Landgraf, D., Utine, E., Hazan, F., Diniz, G., Schuelke, M., Huebner, A., & Sacher, M. (2017). A novel TRAPPC11 mutation in two Turkish families associated with cerebral atrophy, global retardation, scoliosis, achalasia and alacrima. *Journal of Medical Genetics*, *54*(3), 176–185. https://doi.org/10.1136/jmedgenet-2016-104108

Kreis, T. E., Lowe, M., & Pepperkok, R. (1995). COPs regulating membrane traffic. *Annual Review of Cell and Developmental Biology*, *11*, 677–706. https://doi.org/10.1146/annurev.cb.11.110195.003333

Kreis, T. E., & Pepperkok, R. (1994). Coat proteins in intracellular membrane transport. *Current Opinion in Cell Biology*, *6*(4), 533–537. https://doi.org/10.1016/0955-0674(94)90073-6

Kupfer, D. M., Drabenstot, S. D., Buchanan, K. L., Lai, H., Zhu, H., Dyer, D. W., Roe, B. A., & Murphy, J. W. (2004). Introns and Splicing Elements of Five Diverse Fungi. *Eukaryotic Cell*, *3*(5), 1088–1100. https://doi.org/10.1128/EC.3.5.1088-1100.2004

Lander, E. S., Linton, L. M., Birren, B., Nusbaum, C., Zody, M. C., Baldwin, J., Devon, K., Dewar, K., Doyle, M., FitzHugh, W., Funke, R., Gage, D., Harris, K., Heaford, A., Howland, J., Kann, L., Lehoczky, J., LeVine, R., McEwan, P., … International Human Genome Sequencing Consortium. (2001). Initial sequencing and analysis of the human genome. *Nature*, *409*(6822), 860–921. https://doi.org/10.1038/35057062

Larson, A. A., Baker, P. R., Milev, M. P., Press, C. A., Sokol, R. J., Cox, M. O., Lekostaj, J. K., Stence, A. A., Bossler, A. D., Mueller, J. M., Prematilake, K., Tadjo, T. F., Williams, C. A., Sacher, M., & Moore, S. A. (2018). TRAPPC11 and GOSR2 mutations associate with hypoglycosylation of α-dystroglycan and muscular dystrophy. *Skeletal Muscle*, *8*(1), 17. https://doi.org/10.1186/s13395-018-0163-0

Laurent, J. M., Young, J. H., Kachroo, A. H., & Marcotte, E. M. (2016). Efforts to make and apply humanized yeast. *Briefings in Functional Genomics*, *15*(2), 155–163. https://doi.org/10.1093/bfgp/elv041

Lee, G., Papapetrou, E. P., Kim, H., Chambers, S. M., Tomishima, M. J., Fasano, C. A., Ganat, Y. M., Menon, J., Shimizu, F., Viale, A., Tabar, V., Sadelain, M., & Studer, L. (2009). Modelling pathogenesis and treatment of familial dysautonomia using patient-specific iPSCs. *Nature*, *461*(7262), 402–406. https://doi.org/10.1038/nature08320

Lee, M. E., DeLoache, W. C., Cervantes, B., & Dueber, J. E. (2015). A Highly Characterized Yeast Toolkit for Modular, Multipart Assembly. *ACS Synthetic Biology*, *4*(9), 975–986. https://doi.org/10.1021/sb500366v

Letourneur, F., Gaynor, E. C., Hennecke, S., Démollière, C., Duden, R., Emr, S. D., Riezman, H., & Cosson, P. (1994). Coatomer is essential for retrieval of dilysine-tagged proteins to the endoplasmic reticulum. *Cell*, *79*(7), 1199–1207. https://doi.org/10.1016/0092-8674(94)90011-6

Levine, T. P., Daniels, R. D., Wong, L. H., Gatta, A. T., Gerondopoulos, A., & Barr, F. A. (2013). Discovery of new Longin and Roadblock domains that form platforms for small GTPases in Ragulator and TRAPP-II. *Small GTPases*, *4*(2), 62–69. https://doi.org/10.4161/sgtp.24262

Li, C., Luo, X., Zhao, S., Siu, G. K., Liang, Y., Chan, H. C., Satoh, A., & Yu, S. S. (2017). COPI-TRAPPII activates Rab18 and regulates its lipid droplet association. *The EMBO Journal*, *36*(4), 441–457. https://doi.org/10.15252/embj.201694866

Li, X., Zhang, W., Zhou, D., Lv, T., Xu, A., Wang, H., Zhao, X., Zhang, B., Li, Y., Jia, S., Wang, Y., Wang, X., Wu, Z., Duan, W., Wang, Q., Nan, Y., Shang, J., Jiang, W., Chen, Y., … Huang, J. (2019). Complex ATP7B mutation patterns in Wilson disease and evaluation of a yeast model for functional analysis of variants. *Human Mutation*, *40*(5), 552–565. https://doi.org/10.1002/humu.23714

Liang, W.-C., Zhu, W., Mitsuhashi, S., Noguchi, S., Sacher, M., Ogawa, M., Shih, H.-H., Jong, Y.-J., & Nishino, I. (2015). Congenital muscular dystrophy with fatty liver and infantile-onset cataract caused by TRAPPC11 mutations: Broadening of the phenotype. *Skeletal Muscle*, *5*, 29. https://doi.org/10.1186/s13395-015-0056-4

Liang, Y., Morozova, N., Tokarev, A. A., Mulholland, J. W., & Segev, N. (2007). The role of Trs65 in the Ypt/Rab guanine nucleotide exchange factor function of the TRAPP II complex. *Molecular Biology of the Cell*, *18*(7), 2533–2541. https://doi.org/10.1091/mbc.e07-03-0221

Lipatova, Z., & Segev, N. (2019). Ypt/Rab GTPases and their TRAPP GEFs at the Golgi. *FEBS Letters*, *593*(17), 2488–2500. https://doi.org/10.1002/1873-3468.13574

Lipatova, Z., Van Bergen, N., Stanga, D., Sacher, M., Christodoulou, J., & Segev, N. (2020). TRAPPing a neurological disorder: From yeast to humans. *Autophagy*, *16*(5), 965–966. https://doi.org/10.1080/15548627.2020.1736873

Lynch-Day, M. A., Bhandari, D., Menon, S., Huang, J., Cai, H., Bartholomew, C. R., Brumell, J. H., Ferro-Novick, S., & Klionsky, D. J. (2010). Trs85 directs a Ypt1 GEF, TRAPPIII, to the phagophore to promote autophagy. *Proceedings of the National Academy of Sciences of the United States of America*, *107*(17), 7811–7816. https://doi.org/10.1073/pnas.1000063107

Makhoul, C., Gosavi, P., & Gleeson, P. A. (2019). Golgi Dynamics: The Morphology of the Mammalian Golgi Apparatus in Health and Disease. *Frontiers in Cell and Developmental Biology*, *7*, 112. https://doi.org/10.3389/fcell.2019.00112

Matalonga, L., Bravo, M., Serra-Peinado, C., García-Pelegrí, E., Ugarteburu, O., Vidal, S., Llambrich, M., Quintana, E., Fuster-Jorge, P., Gonzalez-Bravo, M. N., Beltran, S., Dopazo, J., Garcia-Garcia, F., Foulquier, F., Matthijs, G., Mills, P., Ribes, A., Egea, G., Briones, P., … Girós, M. (2017). Mutations in TRAPPC11 are associated with a congenital disorder of glycosylation. *Human Mutation*, *38*(2), 148–151. https://doi.org/10.1002/humu.23145

Mesdom, P., Colle, R., Lebigot, E., Trabado, S., Deflesselle, E., Fève, B., Becquemont, L., Corruble, E., & Verstuyft, C. (2020). Human Dermal Fibroblast: A Promising Cellular Model to Study Biological Mechanisms of Major Depression and Antidepressant Drug Response. *Current Neuropharmacology*, *18*(4), 301–318. https://doi.org/10.2174/1570159X17666191021141057

Mi, C., Zhang, L., Huang, G., Shao, G., Yang, F., You, X., Dong, M.-Q., Sun, S., & Sui, S.-F. (2022). Structural basis for assembly of TRAPPII complex and specific activation of GTPase Ypt31/32. *Science Advances*, *8*(4), eabi5603. https://doi.org/10.1126/sciadv.abi5603

Milev, M. P., Graziano, C., Karall, D., Kuper, W. F. E., Al-Deri, N., Cordelli, D. M., Haack, T. B., Danhauser, K., Iuso, A., Palombo, F., Pippucci, T., Prokisch, H., Saint-Dic, D., Seri, M., Stanga, D., Cenacchi, G., van Gassen, K. L. I., Zschocke, J., Fauth, C., … van Hasselt, P. M. (2018). Bi-allelic mutations in TRAPPC2L result in a neurodevelopmental disorder and have an impact on RAB11 in fibroblasts. *Journal of Medical Genetics*, *55*(11), 753–764. https://doi.org/10.1136/jmedgenet-2018-105441

Milev, M. P., Grout, M. E., Saint-Dic, D., Cheng, Y.-H. H., Glass, I. A., Hale, C. J., Hanna, D. S., Dorschner, M. O., Prematilake, K., Shaag, A., Elpeleg, O., Sacher, M., Doherty, D., & Edvardson, S. (2017). Mutations in TRAPPC12 Manifest in Progressive Childhood Encephalopathy and Golgi Dysfunction. *American Journal of Human Genetics*, *101*(2), 291–299. https://doi.org/10.1016/j.ajhg.2017.07.006

Milev, M. P., Hasaj, B., Saint-Dic, D., Snounou, S., Zhao, Q., & Sacher, M. (2015). TRAMM/TrappC12 plays a role in chromosome congression, kinetochore stability, and CENP-E recruitment. *The Journal of Cell Biology*, *209*(2), 221–234. https://doi.org/10.1083/jcb.201501090

Milev, M. P., Stanga, D., Schänzer, A., Nascimento, A., Saint-Dic, D., Ortez, C., Natera-de Benito, D., Barrios, D. G., Colomer, J., Badosa, C., Jou, C., Gallano, P., Gonzalez-Quereda, L., Töpf, A., Johnson, K., Straub, V., Hahn, A., Sacher, M., & Jimenez-Mallebrera, C. (2019). Characterization of three TRAPPC11 variants suggests a critical role for the extreme carboxy terminus of the protein. *Scientific Reports*, *9*(1), 14036. https://doi.org/10.1038/s41598-019-50415-6

Miller, M. P., & Kumar, S. (2001). Understanding human disease mutations through the use of interspecific genetic variation. *Human Molecular Genetics*, *10*(21), 2319–2328. https://doi.org/10.1093/hmg/10.21.2319

Mizushima, N., & Yoshimori, T. (2007). How to interpret LC3 immunoblotting. *Autophagy*, *3*(6), 542–545. https://doi.org/10.4161/auto.4600

Mocali, A., Della Malva, N., Abete, C., Mitidieri Costanza, V. A., Bavazzano, A., Boddi, V., Sanchez, L., Dessì, S., Pani, A., & Paoletti, F. (2014). Altered proteolysis in fibroblasts of Alzheimer patients with predictive implications for subjects at risk of disease. *International Journal of Alzheimer's Disease*, *2014*, 520152. https://doi.org/10.1155/2014/520152

Mohamoud, H. S., Ahmed, S., Jelani, M., Alrayes, N., Childs, K., Vadgama, N., Almramhi, M. M., Al-Aama, J. Y., Goodbourn, S., & Nasir, J. (2018). A missense mutation in TRAPPC6A leads to build-up of the protein, in patients with a neurodevelopmental syndrome and dysmorphic features. *Scientific Reports*, *8*(1), Article 1. https://doi.org/10.1038/s41598-018-20658-w

Montpetit, B., & Conibear, E. (2009). Identification of the Novel TRAPP Associated Protein Tca17. *Traffic*, *10*(6), 713–723. https://doi.org/10.1111/j.1600-0854.2009.00895.x

Moretti, A., Bellin, M., Welling, A., Jung, C. B., Lam, J. T., Bott-Flügel, L., Dorn, T., Goedel, A., Höhnke, C., Hofmann, F., Seyfarth, M., Sinnecker, D., Schömig, A., & Laugwitz, K.-L. (2010). Patient-specific induced pluripotent stem-cell models for long-QT syndrome. *The New England Journal of Medicine*, *363*(15), 1397–1409. https://doi.org/10.1056/NEJMoa0908679

Munot, P., McCrea, N., Torelli, S., Manzur, A., Sewry, C., Chambers, D., Feng, L., Ala, P., Zaharieva, I., Ragge, N., Roper, H., Marton, T., Cox, P., Milev, M. P., Liang, W.-C., Maruyama, S., Nishino, I., Sacher, M., Phadke, R., & Muntoni, F. (2022). TRAPPC11-related muscular dystrophy with hypoglycosylation of alpha-dystroglycan in skeletal muscle and brain. *Neuropathology and Applied Neurobiology*, *48*(2), e12771. https://doi.org/10.1111/nan.12771

Nguengang Wakap, S., Lambert, D. M., Olry, A., Rodwell, C., Gueydan, C., Lanneau, V., Murphy, D., Le Cam, Y., & Rath, A. (2020). Estimating cumulative point prevalence of rare diseases: Analysis of the Orphanet database. *European Journal of Human Genetics: EJHG*, *28*(2), 165–173. https://doi.org/10.1038/s41431-019-0508-0

Nichols, B. J., Ungermann, C., Pelham, H. R., Wickner, W. T., & Haas, A. (1997). Homotypic vacuolar fusion mediated by t- and v-SNAREs. *Nature*, *387*(6629), 199–202. https://doi.org/10.1038/387199a0

Olkkonen, V. M., & Ikonen, E. (2006). When intracellular logistics fails—Genetic defects in membrane trafficking. *Journal of Cell Science*, *119*(Pt 24), 5031–5045. https://doi.org/10.1242/jcs.03303

Palade, G. (1975). Intracellular aspects of the process of protein synthesis. *Science (New York, N.Y.)*, *189*(4200), 347–358. https://doi.org/10.1126/science.1096303

Palade, G. E. (1966). Structure and function at the cellular level. *JAMA*, *198*(8), 815–825.

Pearse, B. M., & Robinson, M. S. (1990). Clathrin, adaptors, and sorting. *Annual Review of Cell Biology*, *6*, 151–171. https://doi.org/10.1146/annurev.cb.06.110190.001055

Pérez, M. J., Ponce, D. P., Osorio-Fuentealba, C., Behrens, M. I., & Quintanilla, R. A. (2017). Mitochondrial Bioenergetics Is Altered in Fibroblasts from Patients with Sporadic Alzheimer's Disease. *Frontiers in Neuroscience*, *11*, 553. https://doi.org/10.3389/fnins.2017.00553

Pinar, M., Arias-Palomo, E., Ríos, V. de los, Jr, H. N. A., & Peñalva, M. A. (2019). Characterization of Aspergillus nidulans TRAPPs uncovers unprecedented similarities between fungi and metazoans and reveals the modular assembly of TRAPPII. *PLOS Genetics*, *15*(12), e1008557. https://doi.org/10.1371/journal.pgen.1008557

Pinar, M., Arst, H. N., Pantazopoulou, A., Tagua, V. G., de los Ríos, V., Rodríguez-Salarichs, J., Díaz, J. F., & Peñalva, M. A. (2015). TRAPPII regulates exocytic Golgi exit by mediating nucleotide exchange on the Ypt31 ortholog RabERAB11. *Proceedings of the National Academy of Sciences of the United States of America*, *112*(14), 4346–4351. https://doi.org/10.1073/pnas.1419168112

Prabantu, V. M., Naveenkumar, N., & Srinivasan, N. (2020). Influence of Disease-Causing Mutations on Protein Structural Networks. *Frontiers in Molecular Biosciences*, *7*, 620554. https://doi.org/10.3389/fmolb.2020.620554

Ramírez-Peinado, S., Ignashkova, T. I., van Raam, B. J., Baumann, J., Sennott, E. L., Gendarme, M., Lindemann, R. K., Starnbach, M. N., & Reiling, J. H. (2017). TRAPPC13 modulates autophagy

and the response to Golgi stress. *Journal of Cell Science*, *130*(14), 2251–2265. https://doi.org/10.1242/jcs.199521

Remm, M., Storm, C. E., & Sonnhammer, E. L. (2001). Automatic clustering of orthologs and in-paralogs from pairwise species comparisons. *Journal of Molecular Biology*, *314*(5), 1041–1052. https://doi.org/10.1006/jmbi.2000.5197

Richter, T., Nestler-Parr, S., Babela, R., Khan, Z. M., Tesoro, T., Molsen, E., & Hughes, D. A. (2015). Rare Disease Terminology and Definitions—A Systematic Global Review: Report of the ISPOR Rare Disease Special Interest Group. *Value in Health*, *18*(6), 906–914. https://doi.org/10.1016/j.jval.2015.05.008

Riedel, F., Galindo, A., Muschalik, N., & Munro, S. (2018). The two TRAPP complexes of metazoans have distinct roles and act on different Rab GTPases. *The Journal of Cell Biology*, *217*(2), 601–617. https://doi.org/10.1083/jcb.201705068

Robinett, C. C., Giansanti, M. G., Gatti, M., & Fuller, M. T. (2009). TRAPPII is required for cleavage furrow ingression and localization of Rab11 in dividing male meiotic cells of Drosophila. *Journal of Cell Science*, *122*(Pt 24), 4526–4534. https://doi.org/10.1242/jcs.054536

Rose, G. D., Gierasch, L. M., & Smith, J. A. (1985). Turns in peptides and proteins. *Advances in Protein Chemistry*, *37*, 1–109. https://doi.org/10.1016/s0065-3233(08)60063-7

Rossi, V., Banfield, D. K., Vacca, M., Dietrich, L. E. P., Ungermann, C., D'Esposito, M., Galli, T., & Filippini, F. (2004). Longins and their longin domains: Regulated SNAREs and multifunctional SNARE regulators. *Trends in Biochemical Sciences*, *29*(12), 682–688. https://doi.org/10.1016/j.tibs.2004.10.002

Sacher, M., Barrowman, J., Schieltz, D., Yates, J. R., & Ferro-Novick, S. (2000). Identification and characterization of five new subunits of TRAPP. *European Journal of Cell Biology*, *79*(2), 71–80. https://doi.org/10.1078/S0171-9335(04)70009-6

Sacher, M., Barrowman, J., Wang, W., Horecka, J., Zhang, Y., Pypaert, M., & Ferro-Novick, S. (2001). TRAPP I implicated in the specificity of tethering in ER-to-Golgi transport. *Molecular Cell*, *7*(2), 433–442. https://doi.org/10.1016/s1097-2765(01)00190-3

Sacher, M., Jiang, Y., Barrowman, J., Scarpa, A., Burston, J., Zhang, L., Schieltz, D., Yates, J. R., Abeliovich, H., & Ferro-Novick, S. (1998). TRAPP, a highly conserved novel complex on the cis-Golgi that mediates vesicle docking and fusion. *The EMBO Journal*, *17*(9), 2494–2503. https://doi.org/10.1093/emboj/17.9.2494

Sacher, M., Shahrzad, N., Kamel, H., & Milev, M. P. (2019). TRAPPopathies: An emerging set of disorders linked to variations in the genes encoding transport protein particle (TRAPP)-associated proteins. *Traffic (Copenhagen, Denmark)*, *20*(1), 5–26. https://doi.org/10.1111/tra.12615

Schieppati, A., Henter, J.-I., Daina, E., & Aperia, A. (2008). Why rare diseases are an important medical and social issue. *The Lancet*, *371*(9629), 2039–2041. https://doi.org/10.1016/S0140-6736(08)60872-7

Schlenker, O., Hendricks, A., Sinning, I., & Wild, K. (2006). The structure of the mammalian signal recognition particle (SRP) receptor as prototype for the interaction of small GTPases with Longin domains. *The Journal of Biological Chemistry*, *281*(13), 8898–8906. https://doi.org/10.1074/jbc.M512415200

Scott, S. V., Hefner-Gravink, A., Morano, K. A., Noda, T., Ohsumi, Y., & Klionsky, D. J. (1996). Cytoplasm-to-vacuole targeting and autophagy employ the same machinery to deliver proteins to the yeast vacuole. *Proceedings of the National Academy of Sciences of the United States of America*, *93*(22), 12304–12308.

Scrivens, P. J., Noueihed, B., Shahrzad, N., Hul, S., Brunet, S., & Sacher, M. (2011). C4orf41 and TTC-15 are mammalian TRAPP components with a role at an early stage in ER-to-Golgi trafficking. *Molecular Biology of the Cell*, *22*(12), 2083–2093. https://doi.org/10.1091/mbc.E10-11-0873

Shintani, T., & Klionsky, D. J. (2004). Cargo Proteins Facilitate the Formation of Transport Vesicles in the Cytoplasm to Vacuole Targeting Pathway *. *Journal of Biological Chemistry*, *279*(29), 29889–29894. https://doi.org/10.1074/jbc.M404399200

Stanga, D., Zhao, Q., Milev, M. P., Saint-Dic, D., Jimenez-Mallebrera, C., & Sacher, M. (2019). TRAPPC11 functions in autophagy by recruiting ATG2B-WIPI4/WDR45 to preautophagosomal membranes. *Traffic (Copenhagen, Denmark)*, *20*(5), 325–345. https://doi.org/10.1111/tra.12640

Stephens, D. J., Lin-Marq, N., Pagano, A., Pepperkok, R., & Paccaud, J. P. (2000). COPI-coated ER-to-Golgi transport complexes segregate from COPII in close proximity to ER exit sites. *Journal of Cell Science*, *113 (Pt 12)*, 2177–2185. https://doi.org/10.1242/jcs.113.12.2177

Sutton, R. B., Fasshauer, D., Jahn, R., & Brunger, A. T. (1998). Crystal structure of a SNARE complex involved in synaptic exocytosis at 2.4 A resolution. *Nature*, *395*(6700), 347–353. https://doi.org/10.1038/26412

Sztul, E., & Lupashin, V. (2006). Role of tethering factors in secretory membrane traffic. *American Journal of Physiology. Cell Physiology*, *290*(1), C11-26. https://doi.org/10.1152/ajpcell.00293.2005

Talarico, R., Aguilera, S., Alexander, T., Amoura, Z., Andersen, J., Arnaud, L., Avcin, T., Marsal Barril, S., Beretta, L., Bombardieri, S., Bortoluzzi, A., Bouillot, C., Bulina, I., Burmester, G. R., Cannizzo, S., Cavagna, L., Chaigne, B., Cornet, A., Corti, P., … Mosca, M. (2022). The added value of a European Reference Network on rare and complex connective tissue and musculoskeletal diseases: Insights after the first 5 years of the ERN ReCONNET. *Clinical and Experimental Rheumatology*, *40 Suppl 134*(5), 3–11. https://doi.org/10.55563/clinexprheumatol/d2qz38

Tan, D., Cai, Y., Wang, J., Zhang, J., Menon, S., Chou, H.-T., Ferro-Novick, S., Reinisch, K. M., & Walz, T. (2013). The EM structure of the TRAPPIII complex leads to the identification of a requirement for COPII vesicles on the macroautophagy pathway. *Proceedings of the National Academy of Sciences*, *110*(48), 19432–19437. https://doi.org/10.1073/pnas.1316356110

Tang, B. L. (2021). Defects in early secretory pathway transport machinery components and neurodevelopmental disorders. *Reviews in the Neurosciences*, *32*(8), 851–869. https://doi.org/10.1515/revneuro-2021-0020

Thomas, L. L., & Fromme, J. C. (2016). GTPase cross talk regulates TRAPPII activation of Rab11 homologues during vesicle biogenesis. *The Journal of Cell Biology*, *215*(4), 499–513. https://doi.org/10.1083/jcb.201608123

Thomas, L. L., Joiner, A. M. N., & Fromme, J. C. (2018). The TRAPPIII complex activates the GTPase Ypt1 (Rab1) in the secretory pathway. *The Journal of Cell Biology*, *217*(1), 283–298. https://doi.org/10.1083/jcb.201705214

Van Bergen, N. J., Guo, Y., Al-Deri, N., Lipatova, Z., Stanga, D., Zhao, S., Murtazina, R., Gyurkovska, V., Pehlivan, D., Mitani, T., Gezdirici, A., Antony, J., Collins, F., Willis, M. J. H., Coban Akdemir, Z. H., Liu, P., Punetha, J., Hunter, J. V., Jhangiani, S. N., … Christodoulou, J. (2020). Deficiencies in vesicular transport mediated by TRAPPC4 are associated with severe syndromic intellectual disability. *Brain: A Journal of Neurology*, *143*(1), 112–130. https://doi.org/10.1093/brain/awz374

Vangipuram, M., Ting, D., Kim, S., Diaz, R., & Schüle, B. (2013). Skin punch biopsy explant culture for derivation of primary human fibroblasts. *Journal of Visualized Experiments: JoVE*, *77*, e3779. https://doi.org/10.3791/3779

Venditti, R., Scanu, T., Santoro, M., Di Tullio, G., Spaar, A., Gaibisso, R., Beznoussenko, G. V., Mironov, A. A., Mironov, A., Zelante, L., Piemontese, M. R., Notarangelo, A., Malhotra, V., Vertel, B. M., Wilson, C., & De Matteis, M. A. (2012). Sedlin controls the ER export of procollagen by regulating the Sar1 cycle. *Science (New York, N.Y.)*, *337*(6102), 1668–1672. https://doi.org/10.1126/science.1224947

Wang, W., Sacher, M., & Ferro-Novick, S. (2000). Trapp Stimulates Guanine Nucleotide Exchange on Ypt1p. *The Journal of Cell Biology*, *151*(2), 289–296.

Westlake, C. J., Baye, L. M., Nachury, M. V., Wright, K. J., Ervin, K. E., Phu, L., Chalouni, C., Beck, J. S., Kirkpatrick, D. S., Slusarski, D. C., Sheffield, V. C., Scheller, R. H., & Jackson, P. K. (2011). Primary cilia membrane assembly is initiated by Rab11 and transport protein particle II (TRAPPII) complex-dependent trafficking of Rabin8 to the centrosome. *Proceedings of the National Academy of Sciences of the United States of America*, *108*(7), 2759–2764. https://doi.org/10.1073/pnas.1018823108

Whyte, J. R. C., & Munro, S. (2002). Vesicle tethering complexes in membrane traffic. *Journal of Cell Science*, *115*(Pt 13), 2627–2637. https://doi.org/10.1242/jcs.115.13.2627

Xu, Y., Zhang, Z., Zhao, Y., Zhao, C., Shi, M., Dong, X., Zhang, J., Tan, L., Zhang, L., & Zhao, Y. (2023). TRAPPC1 is essential for the maintenance and differentiation of common myeloid progenitors in mice. *EMBO Reports*, *24*(2), e55503. https://doi.org/10.15252/embr.202255503

Yang, G., Cintina, I., Pariser, A., Oehrlein, E., Sullivan, J., & Kennedy, A. (2022). The national economic burden of rare disease in the United States in 2019. *Orphanet Journal of Rare Diseases*, *17*(1), 163. https://doi.org/10.1186/s13023-022-02299-5

Yarwood, R., Hellicar, J., Woodman, P. G., & Lowe, M. (2020). Membrane trafficking in health and disease. *Disease Models & Mechanisms*, *13*(4), dmm043448. https://doi.org/10.1242/dmm.043448

Ye, Z., Zhan, H., Mali, P., Dowey, S., Williams, D. M., Jang, Y.-Y., Dang, C. V., Spivak, J. L., Moliterno, A. R., & Cheng, L. (2009). Human-induced pluripotent stem cells from blood cells of healthy donors and patients with acquired blood disorders. *Blood*, *114*(27), 5473–5480. https://doi.org/10.1182/blood-2009-04-217406

Yip, C. K., Berscheminski, J., & Walz, T. (2010). Molecular architecture of the TRAPPII complex and implications for vesicle tethering. *Nature Structural & Molecular Biology*, *17*(11), Article 11. https://doi.org/10.1038/nsmb.1914

Zappa, F., Wilson, C., Di Tullio, G., Santoro, M., Pucci, P., Monti, M., D'Amico, D., Pisonero-Vaquero, S., De Cegli, R., Romano, A., Saleem, M. A., Polishchuk, E., Failli, M., Giaquinto, L., & De Matteis, M. A. (2019). The TRAPP complex mediates secretion arrest induced by stress granule assembly. *The EMBO Journal*, *38*(19), e101704. https://doi.org/10.15252/embj.2019101704

Zerial, M., & McBride, H. (2001). Rab proteins as membrane organizers. *Nature Reviews Molecular Cell Biology*, *2*(2), Article 2. https://doi.org/10.1038/35052055

Zhang, S., Chen, S., Li, W., Guo, X., Zhao, P., Xu, J., Chen, Y., Pan, Q., Liu, X., Zychlinski, D., Lu, H., Tortorella, M. D., Schambach, A., Wang, Y., Pei, D., & Esteban, M. A. (2011). Rescue of ATP7B function in hepatocyte-like cells from Wilson's disease induced pluripotent stem cells using gene therapy or the chaperone drug curcumin. *Human Molecular Genetics*, *20*(16), 3176–3187. https://doi.org/10.1093/hmg/ddr223

Zhao, S., Li, C. M., Luo, X. M., Siu, G. K. Y., Gan, W. J., Zhang, L., Wu, W. K. K., Chan, H. C., & Yu, S. (2017). Mammalian TRAPPIII Complex positively modulates the recruitment of Sec13/31 onto COPII vesicles. *Scientific Reports*, *7*, 43207. https://doi.org/10.1038/srep43207

Zong, M., Wu, X., Chan, C. W. L., Choi, M. Y., Chan, H. C., Tanner, J. A., & Yu, S. (2011). The adaptor function of TRAPPC2 in mammalian TRAPPs explains TRAPPC2-associated SEDT and TRAPPC9-associated congenital intellectual disability. *PloS One*, *6*(8), e23350. https://doi.org/10.1371/journal.pone.0023350